Late Quaternary coastal evolution of the northern Rio Grande do Norte coast, NE Brazil

Dissertation
zur Erlangung des Doktorgrades
der Mathematisch-Naturwissenschaftlichen Fakultät
der Christian-Albrechts-Universität
zu Kiel

vorgelegt von

Luciano Henrique de Oliveira Caldas

Kiel
2002

Referent/in: Prof. Dr. Karl Stattegger

Korreferent/in: Prof. Dr. Helenice Vital

Tag der Mündlichen Prüfung: 12.12.2002

Zum Druck genehmigt: 12.12.2002

Prof. Dr. W. Depmeier
Dekan

ZUSAMMENFASSUNG

Die Küstenentwicklung des späten Quatärs für das Gebiet zwischen Ponta dos Três Irmãos und der Nehrung von Galinhos an der Nordküste des Bundesstaates Rio Grande do Norte, Nordost Brasilien, wurde mit Hilfe sedimentologischer, geophysikalischer, Isotopen- und geochronologischer Untersuchungen rekonstruiert.

Der innere Kontinentalschelf lässt sich in zwei morphologische Zonen untergliedern: die östliche Zone besteht aus submarinen Dünen, die bei einem hohen Sedimentangebot von einer starken Meeresströmung aus Südost als Transportkörper entstehen. Die westliche Zone besteht aus submarinen Sandrücken, die aus einer Kombination von ozeanischen Strömungen aus Nordost und Ost hervorgehen. Ursache für die Bildung dieser großskaligen Sedimentstrukturen ist der Nord-Brasilien Strom. Am Innenschelf gibt es zahlreiche submarine Vorkommen von verfestigen Sedimenten, die etwa parallel zu der derzeitigen Küste in einer Entfernung von etwa 20 km liegen. Diese Sedimentrücken bestehen aus Beachrock und Äolianiten, die ältere Stadien der Überflutung des inneren Schelfs anzeigen.

Die Sedimentation während des Holozäns ist von Meeresspiegelschwankungen, Küstenströmungen und dem Wandern von Küstendünen gesteuert. Sedimente aus der Paläo-Lagune bei São Bento und Caiçara sind auf dem Niveau von 3 Metern unter dem heutigen Meeresspiegel 7000 (Kalender) Jahre alt und zeigen, dass der Meeresspiegel kurz danach seine heutige Position passiert hat. Der holozäne Hochstand wurde mit 1,2 Metern über dem heutigen mittleren Meeresspiegel vor 5900 Jahren erreicht. Danach fiel der Meeresspiegel kontinuierlich auf seine heutige Position. Die Veränderungen der Meeresspiegellage wird durch das Niveau der transgressiven und regressiven Sedimente bei São Bento und dem Recuado Beachrock angezeigt. Darüber hinaus bestätigen die Isotopen-, chemischen und diagenetischen Daten der Beachrock-Zemente aus verschiedenen Vorkommen diese Veränderungen während des Holozän. Das häufige Vorkommen von Evaporit-Mineralen in den Paleo-Lagunensedimenten von São Bento weist darauf hin, dass die Lagune weitgehend vom offenen Meer abgeschlossen war. Die frühere Verbindung zum offenen Meer wurde hauptsächlich durch das nach Westen gerichtete Vorwandern der Dünen geschlossen. Die letzte marine Ingression in die Lagune von São Bento fand vor 3580 Jahre statt. Die Lagune von Galinhos-Galos besteht seit etwa 7000 Jahren, als der Meeresspiegel erstmals seine heutige Positon erreicht hatte. Entlang der Küste bildeten sich transgressive Düneninseln, welche die Entwicklung der landseitigen Lagune gesteuert haben. Die heutige Form der Nehrung von Galinhos wurde während des Meeresspiegelsrückgangs angelegt, als die Kanäle zwischen Lagune und offenem Meer im Bereich der Düneninseln geschlossen wurden und die Dünen auch hier verstärkt nach Westen wandern konnten. Das Schließen der Kanäle hat kurz vor 3330 Jahre vor heute begonnen. Zu dieser Zeit entstanden die ersten Beachrocks, die parallel zur heutigen Küstenlinie und damit senkrecht zu den früheren Kanäle liegen. Heute steuert nur mehr ein Gezeitenkanal am Westende der Nehrung den Ein- und Ausstrom des bereits stark reduzierten Lagunensystems.

Einige Küstenkliffs, die ebenfalls aus Beachrock und Äolianiten bestehen, enthalten Karbonatzemente, die sich von den holozänen Beachrock Vorkommen deutlich unterscheiden. AMS ^{14}C-Datierungen von Schalenresten ergaben Alter von annähernd 45000 Jahren, die somit nahe an der methodischen Grenze liegen. U/Th-Datierungen führten bisher zu keinen verlässlichen Altersangaben, die ältesten Datierungen liegen zwischen 120000 und 130000 Jahren. Dies entspricht dem vorletzten Meeresspiegelhochstand während des Eem (Isotopen-Substadium 5e). Vertikale Unterschiede in der Position des Kontakts zwischen Beachrock und Äolianit wie auch unterschiedliche Diagenese der Zemente lassen auf tektonische Hebungen und Senkungen dieser Ablagerungen schließen. Die Meeresspiegellage zur Zeit der Ablagerung muss ähnlich der heutigen gewesen sein, da größere vertikale Abweichungen die Strandsedimente mehrere Kilometer von der heutigen Küstenlinie land- oder seewärts entfernt abgelagert hätten.

RESUMO

Estudos sedimentológicos, geofísicos, isotópicos e geocronológicos foram efetuados ao longo da costa norte do estado do Rio Grande do Norte, entre a Ponta dos Três Irmãos e o limite oeste do *spit* de Galinhos, para a determinação da evolução costeira durante o Quaternário superior.

A plataforma interna é dividida em duas grandes áreas a partir das feições morfológicas do assoalho oceânico observadas em uma imagem de satélite Landsat. Na porção leste da plataforma interna ocorre principalmente dunas subaquáticas que indicam correntes oceânicas fluindo para noroeste. Na porção oeste ocorre principalmente cordões arenosos subaquáticos que parecem ser controlados por uma combinação de correntes oriundas de nordeste e leste. A Corrente do Brasil Norte e suas componentes parecem ser os principais agentes modeladores dos sedimentos presentes da plataforma interna. Sedimentos litificados encontrados nesta plataforma formam linhas aproximadamente paralelas à costa a uma distância de 18 km e representam provavelmente antigos *beachrocks* e eolianitos que foram depositados e cimentados durante as últimas transgressões e regressões marinhas no Quaternário superior.

A sedimentação durante o Holoceno tem sido controlada principalmente pela variação do nível do mar, correntes ao longo da costa e o padrão do transporte de dunas ao longo da costa. Sedimentos lagunares encontrados na região de Caiçara e São Bento do Norte e posicionados 3 metros abaixo do nível do mar atual foram datados por volta de 7000 Cal anos AP. Estas idades indicam que o nível do mar durante a ultima transgressão passou por sua posição atual neste período. A altura máxima que o nível médio do mar atingiu durante a transgressão holocênica foi 1,2m acima do nível atual por volta de 5900 Cal anos AP. Posteriormente o nível do mar desceu uniformemente até sua posição atual como demonstrado pela altura dos depósitos regressivos próximos as cidade de Caiçara bem como pelos padrões isotópicos e diagenéticos obtidos nos cimentos dos *beachrocks* holocênicos. Grande quantidade de minerais evaporíticos nos sedimentos da paleolaguna de São Bento e Caiçara indica uma sedimentação cíclica com incursão esporádica do oceano nesta laguna. Estas incursões eram controladas principalmente pelo avanço dunar que fechava os canais de ligação entre laguna e mar. A última incursão marinha na paleolaguna de São Bento aconteceu a 3580 Cal anos AP. O sistema lagunar de Galinhos e Galos tem permanecido ativo desde de quando o nível do mar atingiu sua posição atual pela primeira vez no Holoceno por volta de 7000 Cal anos AP. Durante a última transgressão, barreiras transgressivas ao longo da costa formaram sistema ilha-barreiras que propiciaram uma sedimentação típica lagunar na paleo costa. O *Spit* de Galinhos formou-se durante a queda do nível do mar quando o transporte de sedimentos ao longo da costa fechou os canais antigos que ligavam o mar a laguna e o transporte dunar para oeste e sudoeste foi intensificado. Os fechamentos dos canais tiveram início um pouco antes de 3330 Cal anos AP quando os primeiros *beachrocks* paralelos à praia e perpendicular aos antigos canais formaram-se. Atualmente existe apenas um canal de maré na porção oeste do *spit* ligando a laguna ao mar aberto.

Um conjunto de falésias costeiras formadas por Eolianitos e *Beachrocks* apresenta características químicas e diagenéticas totalmente diferentes dos depósitos holocênicos. Idades AMS ^{14}C em conchas de bivalves forneceram idades por volta de 45.000 anos AP perto do limite do método. Datação por urânio-tório não forneceu idades confiáveis, porém as idades mais velhas obtidas por este método (120000 to 130000 anos) são correlacionadas à penúltima transgressão (subestágio isotópico 5e). Diferenças verticais nas alturas dos contatos entre *beachrock* e eolianitos, bem como diferentes padrões diagenéticos encontrados nos cimentos dos *beachrocks* pleistocênicos indicam que um ou mais evento tectônico soergueu e abaixou tais depósitos. O nível do mar quando da deposição dos *beachrocks* pleistocênicos foi idêntico ao atual, pois uma grande variação vertical deste nível em relação ao nível atual acarretaria em deposição de sedimentos de praia posicionados alguns quilômetros em direção ao continente ou na atual plataforma interna.

ABSTRACT

Sedimentological, geophysical, isotopic and geochronological studies were undertaken along the north coast of Rio Grande do Norte state (Brazil), between Ponta dos Três Irmãos and the western limit of the spit of Galinhos to determine the Late Quaternary coastal evolution of this area.

The inner platform presents two main morphological zones: Found on the eastern portion are mainly subaqueous dunes that indicate oceanic currents flowing northwestward. On the western portion exist mainly subaqueous sand ridges that seem to be controlled by a combination of currents coming from northeast and east directions. The North Brazil Current and its branches control the main bedforms on the inner shelf. Lithified sediments found on the inner platform form lines approximately parallel to the current coast at a distance of 18 kilometers and occur as former beachrocks and aeolianites that were deposited and cemented during inner shelf flooding in the Late Quaternary.

The sedimentation during the Holocene has been controlled mainly by the variation of the sea level, longshore currents and the advance of active dunes along the coast. Basal lagoonal sediments found in a paleo-lagoon close to São Bento and Caiçara 3 meters below the modern sea level were dated at 7000 Cal yr BP. Passing its current position shortly afterwards it reached the Holocene highstand 1.2m above the current mean level at 5900 Cal years BP and dropped afterwards to its present position. These sea level changes are shown by the height of transgressive and regressive deposits close to São Bento and Recuado Beachrock. This is further substantiated by isotopic, chemical and diagenetic signatures of the beachrock cements from various deposits. Great amounts of evaporite minerals in the lagoonal sediments close to São Bento indicate a semi-closed lagoon with sporadic ocean incursion controlled mainly by the advance of active dunes that closed such connections between lagoon and open sea. The last sea incursion in the paleo-lagoon occurred 3580 Cal yr BP. The lagoonal system of Galinhos and Galos has remained active since the sea level reached the current position for the first time shortly after 7000 Cal yr BP. During the Holocene transgressive phase, transgressive barriers along the coast formed barrier-islands that induced typical lagoonal sedimentation landward. The actual shape of the Galinhos' spit was formed during the sea level drop when the transport of sediments along the coast closed the old channels that linked the sea to the lagoon. The closing of the channels begun a little before 3330 Cal years BP when the first beachrocks parallel to the beach and perpendicular to the old channels, were formed, and westward aeolian transport by moving dunes was intensified. Today there is only one tidal channel at the western end of the spit linking the already strongly reduced lagoon and the open sea.

Carbonate cements of coastal cliffs, formed by aeolianites and beachrocks, present chemical and diagenetic characteristics different to Holocene deposits. AMS ^{14}C ages of bivalve shells supplied ages approximately 45000 years BP, close to the limit of the method. Dating using uranium-thorium did not supply reliable ages. The oldest are 120000 to 130000 years and refer to the penultimate transgression (isotope substage 5e). Vertical differences in the heights of the contacts between beachrock and aeolianites, as well as different diagenetic patterns found in the cements of the Pleistocene beachrocks, indicate that one or more tectonic events lifted and subsided such deposits. The former sea level when the Pleistocene sediments were deposited was identical to the current sea level, because a great vertical variation of former level in relation to the current level would deposit beach sediments some kilometers landward or on the inner shelf.

ACKNOWLEDGEMENTS

I would like to express my sincere thanks to all who, direct or indirectly, have contributed to the completion of this thesis. In particular, I thank Prof. K. Stattegger and Dr. Helenice Vital who allowed me to carry out my Ph.D. research here in Kiel. Prof. K. Stattegger and his family are also sincerely thanked for their openness and attention with my wife and me during our stay here in Kiel.

I thank the Brazilian National Research Council (CNPq) for the full-time scholarship throughout my studies in Kiel and also for airline tickets for the fieldwork in Brazil. I also thank the *Deutsche Akademischer Austauchdienst* (DAAD) for the six-months of German language course at the Goethe Institute Bremen, and particularly Helga Wahre who always helped the Brazilian students here in Germany.

I gratefully acknowledge the following persons for help in this research: Dr. H. Erlenkeuser who measured our isotopic data and introduced me to the fantastic "world" of the stable isotopes; Dr. D. Ackermand and B Mader from *Abteilung Mineralogie* that provided invaluable assistance with electron micro-probe analyses; Dr. Samtleben and U. Schuldt for the beautiful photos of bivalve shells with SEM and suggestions; Dr. Jan Scholten for the U-Th chronology of the bivalve shells and fruitful discussions; Prof. Pieter Grootes and Dr. Frank Bruhn from *Leibniz* Laboratory for the radiocarbon dating, productive discussions and suggestions; W. Reimers for the thin-sections; "Frau" Faber for always helping me as I got to know my way around the laboratory ("was wäre ich ohne Dich!!!). The "Hiwis" Karin Rinke and Marion Menning helped with laboratory work and SEM analyses.

All the people of the first floor of the Institute of Geosciences for their hospitality during my stay in the institute, especially B. Rinnbauer, Prof. P. Stoffers, H. Kawamura, S. Steinke, T. Hanebuth, C. Bühring, C. Stielow and H. Crnjar.

I am particularly grateful to the German colleagues who worked together with us and have made the research on the coast of the Rio Grande do Norte possible. Special thanks goes to P. Miketta, K. Rotzoll, V. Röber, S. Hustedt, C. Einig, F. Paschelke, K. Riedel and A. Schimanski. I also wish to thank Helmut Beese for keeping the geophysical devices running and Klaus Schwarzer for the use of the laboratory of sedimentology.

For the critical reading of the chapter 4, suggestions, freedom and sympathy, I owe my grateful thanks to Joanna Rotnicka. I express also my special appreciation to Nadia Weitz for her English corrections.

I thank the staff of the Departamento de Geologia from Universidade Federal do Rio Grande do Norte (UFRN)–Brazil involved in the project, especially Hilário Bezerra, Venerando Amaro, Maria Helena Macêdo, Walter Eugênio de Medeiros and Emanuel Jardim de Sá. I am thankful for the help of Werner Tabosa, Josibel Oliveira, Flavia Taone, Zuleide Lima, Marcelo Chaves, Ingrede Guedes, Carlos Cesar, Iracema Silveira and Perycles Raniere during the field and laboratory works in Brazil.

Field and laboratory analyses were funded by the German Research Agency DFG in a joint project between "Universität Christian-Albrechts zu Kiel" and "Universidade Federal do Rio Grande do Norte" - Brazil (UFRN), which has been coordinated by Prof. Karl Stattegger and Prof. Dr. Helenice Vital. The Universidade Federal do Rio Grande do Norte also provided laboratory and infrastructure facilities to conduct fieldwork and basic sedimentological analyses.

Finally, I want to express my deepest gratitude to my dear wife Joseane and my family in Brazil for their support, affection, understanding and encouragement. Without their support and love I could have never been successful.

CONTENTS

1 - Introduction

1.1 - General introduction

In 1998, the program of post-graduation of Geodynamic and Geophysic of the University Federal do Rio Grande do Norte (UFRN) and German researchers from the Institute of Geosciences of the University Christian-Albrechts zu Kiel began to research the north coastal zone of the Rio Grande do Norte (RN). This research included in PROBRAL Program (CAPES/DAAD – 98/072) with the project name "*Fortalecimento de um grupo multidisciplinar em dinâmica externa: dinâmica sedimentar e evolução costeira do litoral do Rio Grande do Norte (Área piloto: Região da Foz do Rio Açu)*" and DFG-Project STA 401/7-*2 Holozäne Küstenentwicklung und heutige Küstendynamik in Rio Grande do Norte (NE-Brasilien).*

The Quaternary coastal geology of the north costal zone of the RN is poorly investigated and up to recently only few publications about it are available. Existing results of previous authors are focused on punctual onshore interpretations and locally limited to offshore survey. Srivastava & Corsino 1984, Nogueira *et al*. 1990 and Moreira 1994 working in the coast of Touros discussed the origin of some coastal outcrops. These authors concluded that these outcrops are correlated to those of the Guamaré Formation and that they were deposited in a coastal environment. Silva (1991) working in the Açu river delta proposed a Holocene stratigraphy and evolution for this area. Other authors by use of ^{14}C dating in beachrocks shells (Bezerra *et al*. 1998 and Caldas 1996) and morphotectonic analyses (Fonseca 1996 and Fonseca 1997), attributed a tectonic control for the north coastal geometry as well as for the coastal Holocene sedimentation. Testa & Bonsence (1998) and Costa-Neto (1997) focused their works on hydrodynamic processes and bedform structures at the inner platform of Macau and Touros, respectively. Based on remote sensing Vianna & Solewicz (1988) described physiographic features of the Touros platform floor, while Testa & Bonsence (1999) mapped carbonatic formations and siliciclastic bedforms at the shelf area of Touros using remote sensing and diving operations. Barreto *et al*. (2001) pointed out some considerations about sea level curves for the area between Ponta dos Três Irmãos (PTI) and São Bento do Norte, while Suguio *et al*. (2001) and Barreto *et al*. (2000b) proposed Pleistocene coastal deposits in this area. Within the project between Brazil-Germany some authors have began to enlarge the discussion about the coastal evolution of the area from integrated onshore and offshore studies (Tabosa 2000, Einig 2000, Paschelke 2000, Hustedt 2000, Riedel 2000, Röber 2001, Rotzoll 2001 and Caldas *et al.* 2001).

The investigation of the north coast of the RN includes geophysical, sedimentological, geochronological and geochemical studies in order to obtain quantitative and qualitative data. This data will be used to decipher the late Quaternary coastal geology of this area. The main objectives of this dissertation are:

- AMS ^{14}C and uranium series dating as well as vibro-core descriptions in order to propose a stratigraphic framework for the study area
- Reconstruction of the last post-glacial transgression for the area
- Characterization of the inner platform morphology and hydrography from geophysical surveys and remote sensing data
- Paleogeographic characterization of the coast
- Holocene coastal evolution

1.2 - Work area

The investigation area is located on the north coast of the federal state of Rio Grande do Norte, which is situated in the northeast region of Brazil (Fig. 1.1). The area is about 140km northwest of the state capital Natal and 40 km east of Macau. The area stretches from 35°50'W to 36°20'W and from 4°55'S to 5°10'S between Ponta dos Três Irmãos and Guamaré city and covering a region from the coast to the shelf edge.

The coastal zone of this area is an open, wave dominated, meso-tidal coast. It is associated with an inner zone of the continental shelf that is shallow (maximum 25m depth) and has an average width of 18km. The continental shelf and coastal zones are strongly influenced by oceanic and wind driven currents from N and E-NE directions, which promote local erosion as well as deposition in the shore zone. A big lagoonal channel system can be recognized on the backside of the sand spit of Galinhos. Some closed lagoons occur near to São Bento do Norte and Caiçara. In the beach zone beachrocks occur numerously along the actual foreshore zone and in the backshore zone. Dune fields increase to the hinterland while dunes close to the shore are quickly overgrown and subjected to permanent reorganization.

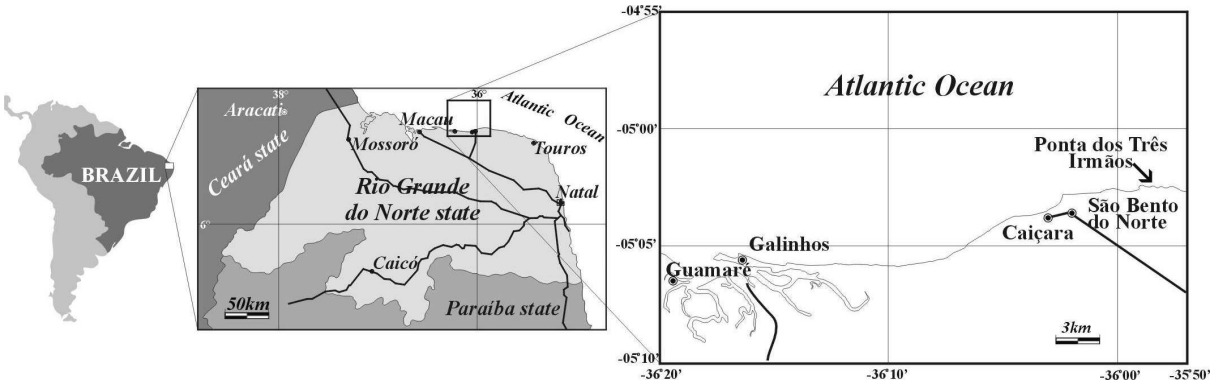

Figure 1.1 - Localization of the area of study.

1.3 - Geological setting

The investigation area is located in the eastern part of the Potiguar basin (Fig. 1.2) that covers one area of 48000 km^2 of which 26000 km^2 is offshore (limited by the 2000 m isobath) and 21500 km2 is onshore.

The Potiguar basin is located in the Borborema Province, which was characterized by Jardim de Sá (1984) as being composed by various supracrustal belts. According to Neves (1987), the Potiguar Basin represents a continental rift in the onshore portion and a pull-apart basin in the offshore portion. The Potiguar basin is part of the NE Brazilian Rift System together with the Recôncavo, Tucano, Jatobá, Rio do Peixe and Sergipe-Alagoas basins (Matos 1994).

1.3.1 - Pre-Quaternary geology

Up to recent there is no consensus about the origin of the Potiguar rift. The two most accepted models are differentiated by the stress orientations and mechanisms that took place during the rift origin. According Françolin & Szatmari (1987) a compressive phase occurred during the Santonian-Campanian while Matos (1992) did not recognize it.

Françolin & Szatmari (1987) proposed that the first manifestations of the separation between South-America and Africa occurred in the late Jurassic with E-W divergent movements. These movements produced a mega fracture in the range of a few thousand kilometers that

started in the south of the continent and progressively extended to the north. As a result of this movement, took place in the Borborema Province compression in the south and a distention in the north. During the Neocomian the entire Borborema Province was subjected an E-W compression and a N-S distention, which promoted numerous fault reactivations permitting the creation of the actual onshore portion. Concomitant to this tectonic, the NE-NW late-Proterozoic faults were reactivated and the Potiguar Rift took place.

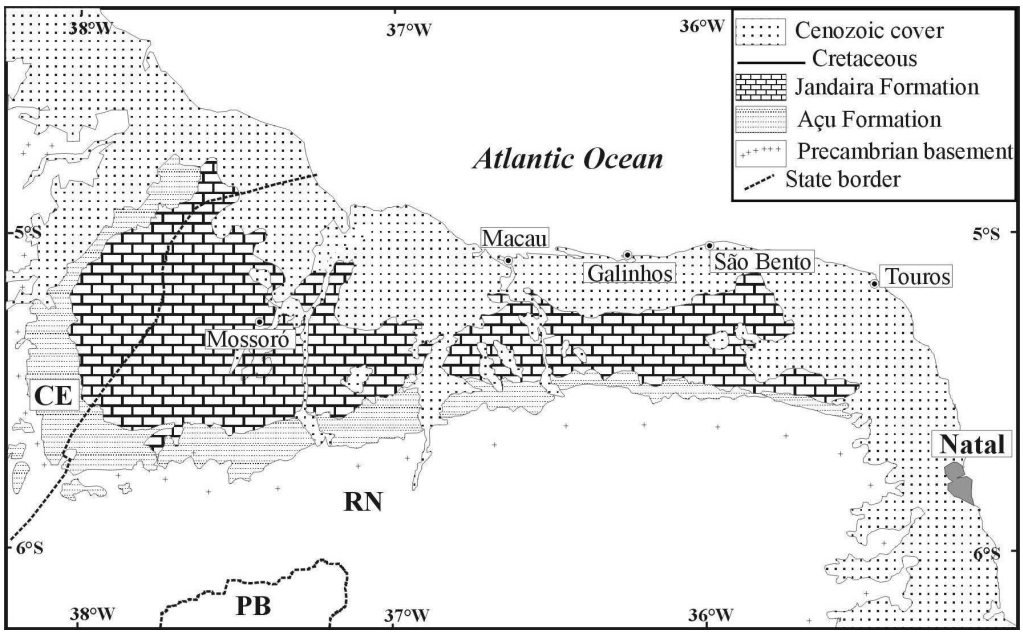

Figure 1.2 - Geological map of the Potiguar Basin (Matos 1992).

According to Bertani *et al*. (1990) the sedimentation into the basin was controlled mainly by three tectonic stages: *rift*, *transitional* and *drift* (Fig. 1.3).

The *rifting* phase was characterized by mainly fluvial, lacustrine and deltaic fan sedimentation that composes the Rift Sequence of (Asmus & Guazelli 1981). The Rift Sequence was later designated by Souza (1982) as the Continental Sequence, which is composed of Pendência Formation.

The *transitional* phase occurred during Aptian, when the Borborema Province experienced a N-S distension and the onshore sedimentation ended. According to Bertani *et al*. (1990), in this time horsts were reactivated culminating with a large regional discordance and the beginning of the offshore sedimentation. In this phase the proto-oceanic sequence (Asmuz & Guazelli 1981) subsequently called transitional by Souza (1982) was deposited (Fig 1.3). It is represented for Alagamar Formation, which is composed of deltaic sandstones merged by lagoonal shales and mudstones that indicate the beginning of marine influence in the basin.

The *drift* phase took place when the divergent E-W movements between South American and African plates during the Albian permitted the ocean ingression, producing transgression and later marine regression into the Potiguar Basin.

Asmus & Guazelli (1981) described sediments within the transgressive marine sequence and regressive marine sequence, while Souza (1982) grouped the transgressive and regressive phases and named them as the Drift Sequence. The Albian-Turonian transgressive sequence is composed of conglomerates, sandstones and mudstones (Açu Formation) deposited in the alluvial fan, braided and meandering fluvial environment, and the estuarine-deltaic environment. The Açu Formation is intercalated in the subsurface of the basin with limestones of the Ponta do Mel Formation and also with siltstones and sandstones of the

Ubarana Formation. On the top of the sequence Turonian-Campanian carbonates of the Jandaíra Formation occur. It is composed of calcarenites deposited on the tidal flat, lagoon, shallow shelf and open marine environments.

Following the deposition of the fluvio-marine transgressive sequence, the regressive sequence was deposited as a function of the continental shelf tilting towards the ocean (Ponte *et al.* 1978) during the Campanian (Souza 1982). The regressive sequence is composed of Ubarana, Tibau and Guamaré Formations.

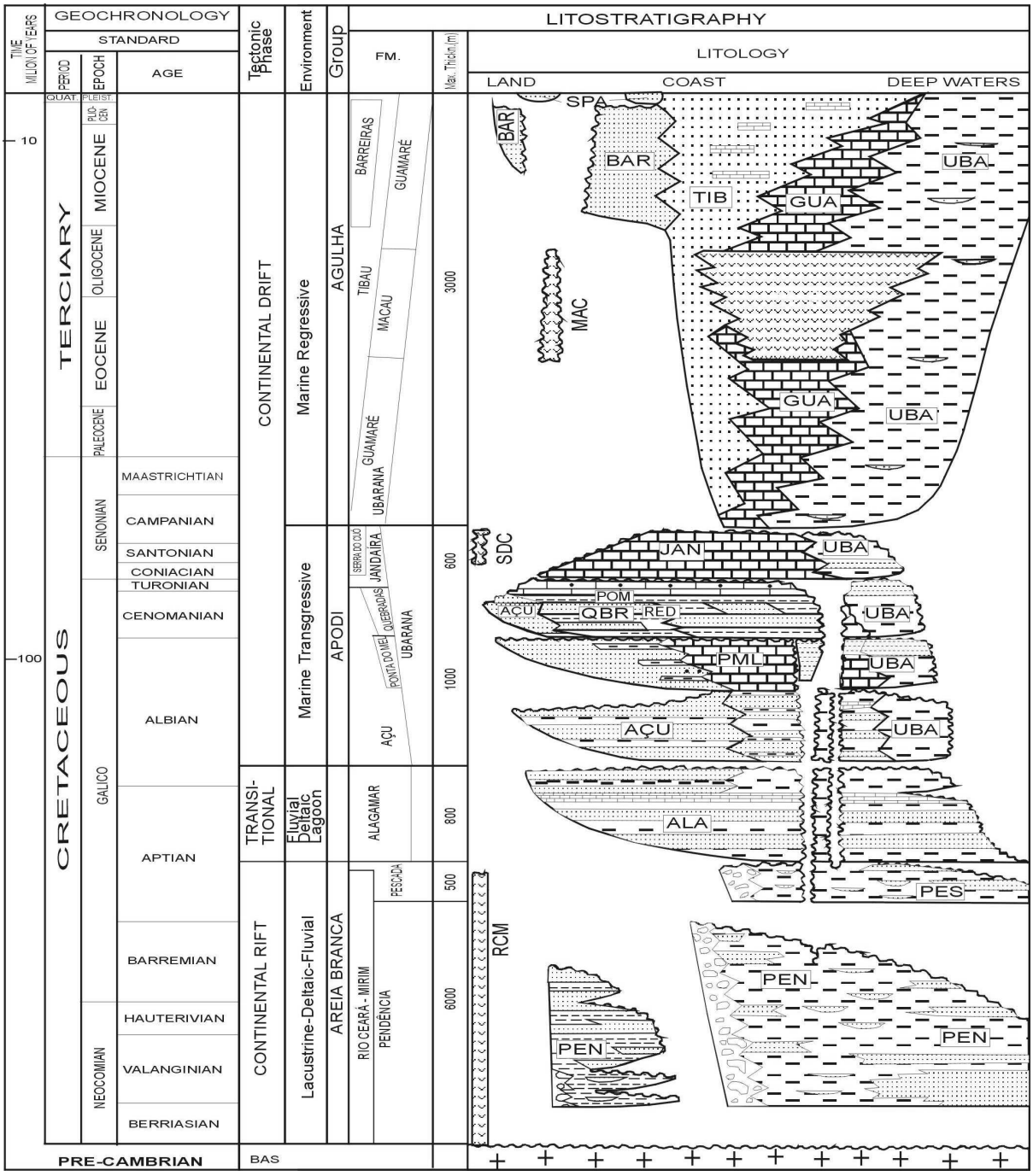

Figure 1.3 - Potiguar Basin stratigraphic column (modified from Araripe & Feijó 1994).

The Macau volcanism (Mayer 1974) was placed in a submarine and subaerial environment during Oligocene-Miocene times. From the Miocene the deposition of the

Barreiras Formation started, which is composed for fluvial and alluvial fan deposits. Quaternary marine and fluvial deposits resume the basin sedimentation. The Quaternary geology will be described in detail in the next section.

1.3.2 - Quaternary Geology

The coastal geology of the Quaternary period can be understood concisely as being a product of the variations in the sea level during this period. Unfortunately absolute ages of the first sea level variations occurring in the beginning of Pleistocene are not available due to the lack of markers.

Studies of the sea level in Brazil show that immense part of the Brazilian coast had been submerged during the Holocene (Van Andel & Laborel 1964; Fairbridge 1976; Suguio *et al*. 1980; Suguio *et al*. 1985, Angulo & Lessa 1997; Angulo *et al*. 1999; Barreto *et al*. 2000a; Lima-Filho *et al*. 2000). However as these authors show, the sea level amplitudes were different for each area studied of the Brazilian coast. Mörner *et al*. (1999) suggested that for the coast between Belém (Pará State) and São Luís (Maranhão State) the sea level between 5100-4400 BP was very close to the present, different to the proposed sea level curve of Salvador (Suguio *et al*. 1985).

Martin *et al*. (1993) proposed a paleogeographic evolutionary model based on eustatic and paleoclimatic mechanisms for the Brazilian coastal plains (Fig. 1.4) located between Macaé and Maceió (see Fig. 1.7). They admitted that two or more stages of this model could be omitted in the explanation of the evolutionary history of other Brazilian coastal plains

The deposition of the Barreiras Formation (Fig. 1.4a) probably took place during the Pliocene, where the climate was semi-arid with sporadic rains of considerably magnitude. Following the Barreiras sedimentation, the maximum antepenultimate transgression possibly already began in Pleistocene. This transgression partially eroded the sediments of the Barreiras Formation (Fig. 1.4b) producing a cliff line. The semi-arid climate during the subsequent regressive phase of the antepenultimate transgression maximum made the sedimentation of new continental deposits composed by alluvial fans at the bottom of Barreiras Formations cliffs possible (Fig1.4c). The maximum of the penultimate transgression occurred approximately 123000 years before present, generating almost total erosion of the continental deposits of the previous stages. The drowning of the fluvial valleys produced lagoons and estuaries. A second erosive phase of the Barreiras cliff lines occurred (Fig. 1.4d). The subsequent regression made the deposition of Pleistocene terraces formed by prograding beach ridge plains possible (Fig. 1.4e). The invasion of the Pleistocene terraces by the sea, during the last transgression, started approximately 7000 years B.P., reaching its maximum around 5100 years B.P. The drowning of the coastal plains made the development of the barriers-island system possible. Behind the barrier-island, lagoons formed (Fig. 1.4f). The lagoons formed during the previous stages were buried by intralagoonal deltas (Fig. 1.4g). Concomitant, the lagoon slowly became a fresh water lake with development of swamp and peat. The falling relative sea level over the last 5100 years has produced extensive beach ridge plans from the original barrier-island (Fig. 1.4h).

In the Rio Grande do Norte coast some of these stages can be recognized but only few works dealt with the Holocene stratigraphy and coastal evolution. Silva (1991) is one of the few authors who proposed a complete Holocene coastal stratigraphy and sedimentary coastal evolution for one area in the coast of the RN. From vibro-cores and radiocarbon dating in the Açu river delta deposits (near to Macau – Fig. 1.2), the author suggested that the main factors controlling the Holocene sedimentation in this area are the antecedent topography, recent tectonic movements and Holocene sea level fluctuations. The relative transgression of the Holocene sea level for this area above modern sea level, according to Silva (1991), started before 7200±100 years BP with its maximum occurring approximately 5020±120 years B.P.

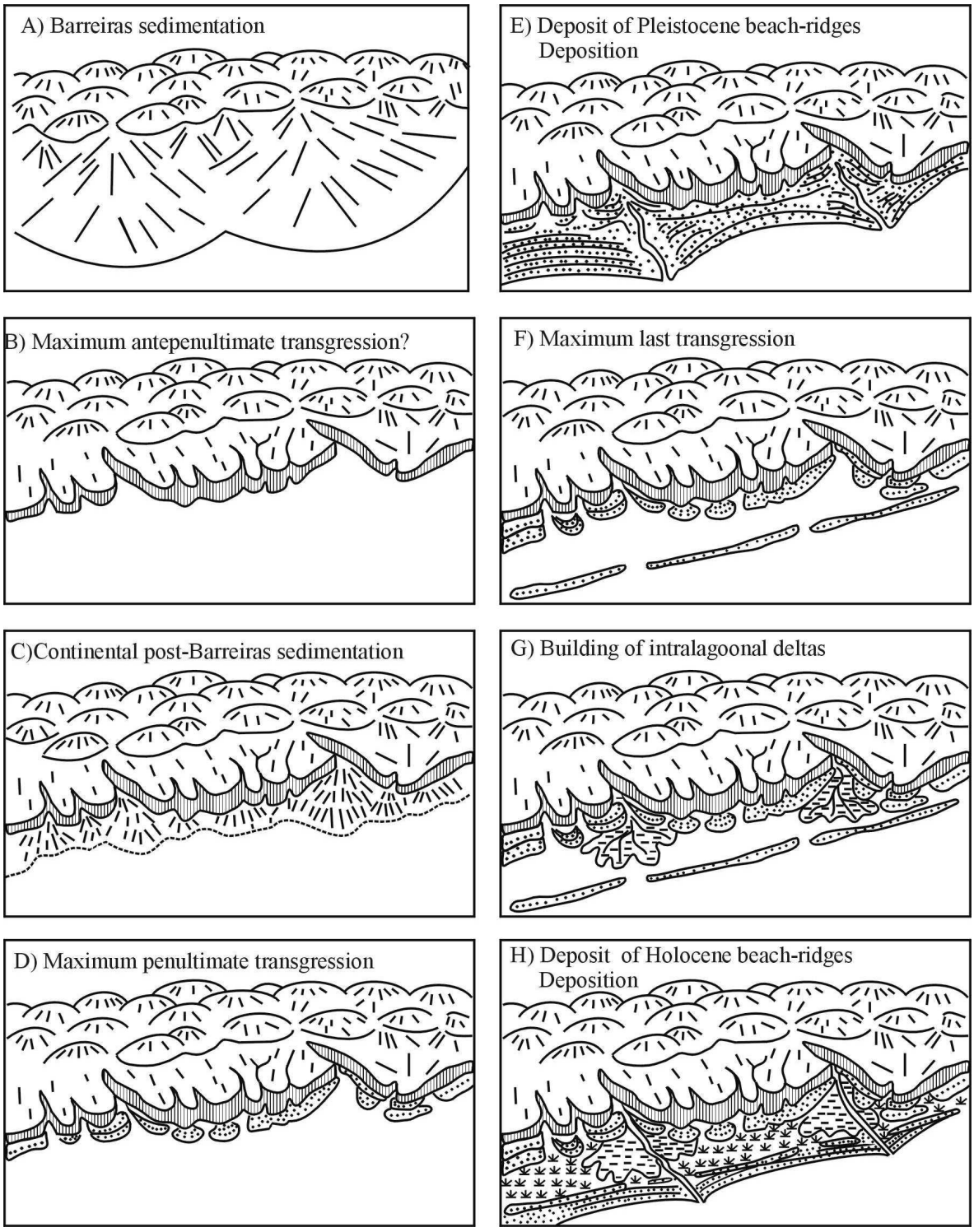

Figure 1.4 - Evolutionary stages of the coastal sedimentation from eustatic and paleoclimatic mechanisms since the end of the Tertiary period until present (Martin *et al.* 1993).

The Holocene highstand coincides with the findings of Martin *et al*. (1993) (Fig. 1.4f). Additionally Silva found radiocarbon age of 30190±370 years B.P. that was attributed to Pleistocene paleo-spits and could be correlated to the Pleistocene penultimate regression (Fig. 1.4e) of Martin *et al.* (1993) since this age is close to the method limit.

1.4 - Climate

The climate of the area is considered tropical, hot and semi-arid (Nimer 1989), and it is subjected to the conditions of the intertropical convergence zone. The dry period of 7 to 8 months, lasts from June to January (Fig. 1.5), while the rainy period of 3 to 4 months, lasts from February to May. The mean air temperature is approximately 26.8° C, with minimum temperatures of 25°C occurring at the end of winter (July) and maximum of 28.6°C in February during the summer.

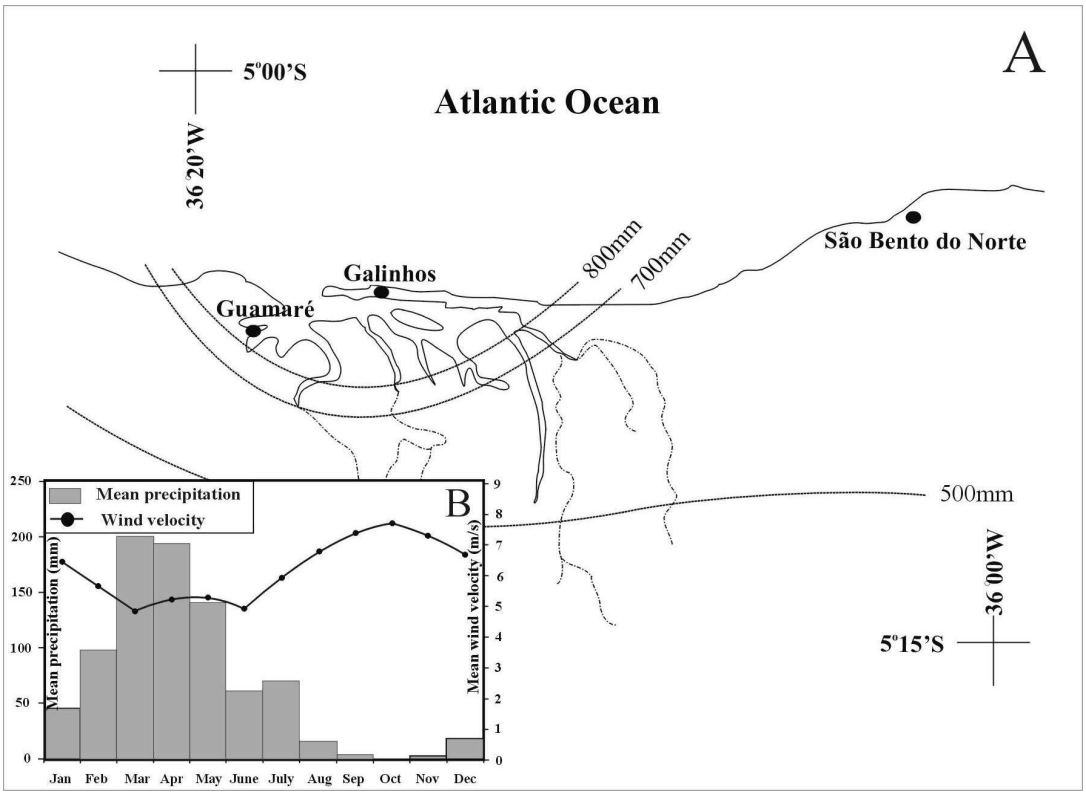

Figure 1.5 - (a) Precipitation in the area of Galinhos and (b) mean precipitation in contrast with mean wind velocity in Guamaré city between 1963 and 1990 (After Cestaro 1994).

The mean insolation is 7.1h/day (NATROTEC 1995) and the annual mean humidity approximately 71% reaching its maximum in March (Cestaro 1994). The mean annual precipitation is approximately 854mm in Guamaré city but the variability is high: 2238mm in 1985 and 164mm in 1979.

1.4.1 - Wind

According Dominguez *et al*. (1992), the south Atlantic anticyclone produces trade winds, which blow toward the equator. The seasonal migration of the Atlantic high-pressure cell together with the thermal heating of the continent force the trade winds to tangent the Brazilian coast. The wind direction presents two patterns in the north coast of the Rio Grande do Norte: from southeast between March-July and stronger from east-northeast between August-January (Fig. 1.6). During the day the thermal heating causes a convection over the continent that leads to an increase of wind velocity around noon and deflects the wind in the study area to more easterly directions. The mean wind velocity in March is 4.8m/s while in

October is 7.7m/s (Cestaro 1994). The relation between dune migration and meteorological parameters can be obtained from these data. The dune migration on the north coast is restricted to the dry period when the stronger NE winds occur. Therefore the dune morphology shows a predominant NE-SW direction (Fig. 1.6).

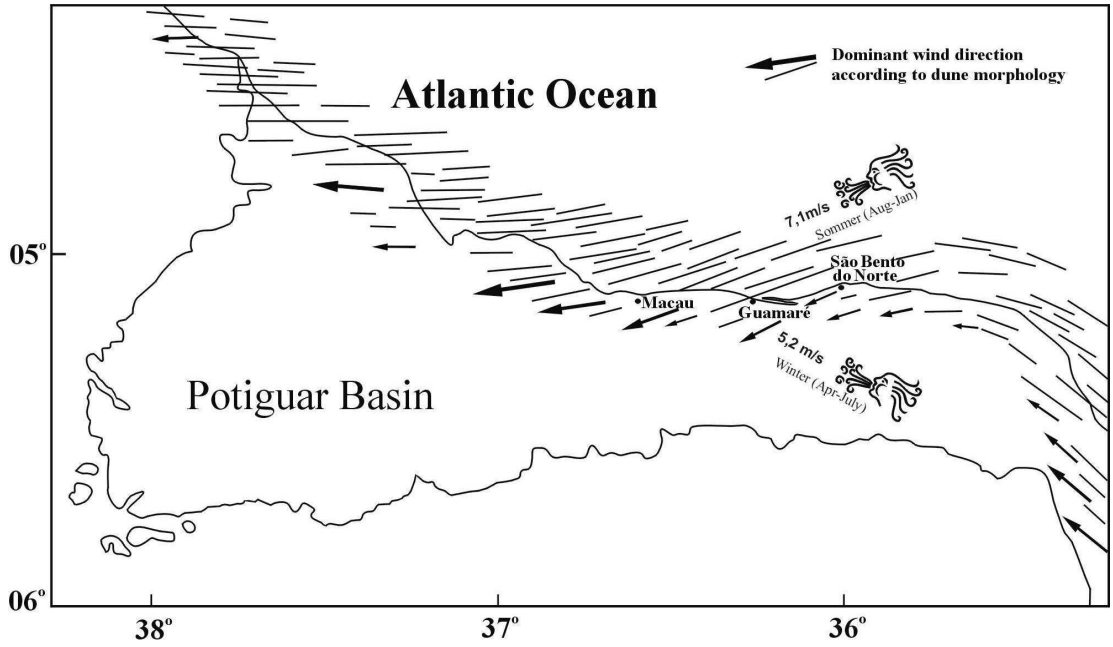

Figure 1.6 - Dominant wind direction as indicated by the dune morphology and associated wind velocity for Guamaré city (Adapted from Fortes 1987 and Cestaro 1994).

1.5 - Hydrography

1.5.1 - Rivers

Rivers of predominantly medium to small sizes with preferential orientation varying from NW-N-NE, characterize the hydrography of the area. The rivers are intermittent and they drain into lakes (paleolagoons) or tidal flats. There are some lakes in the area, and according Oliveira *et al.* (1990) they are formed by the damming of rivers by coastal dunes, as well as the outcropping of the water table. Fortes (1987) characterized some of these lakes as tidal flat.

1.5.2 - Waves and currents

The waves in the area are produced basically by wind action (see section 1.4.1). Unfortunately only few measurements for this coast are available. Measurements performed during one year in the coast of Macau show that mean waves heights for this area is approximately 0.75m (DHN 1974). For the São Bento coast Tabosa (2000) measured wave height values of 1.35m (maximum) and 0.20m (minimum) while Silveira (2002) describe wave heights around 0.8m during winter and 0.5m during the summer for the cost of Guamaré. The waves approach the coast with a NNE to ENE direction (Tabosa 2000 and Silveira 2002).

The current pattern at the inner shelf is controlled predominately by the North Brazilian Current (NBC), which is a branch of the South Equatorial Current (SEC) (Fig. 1.7). The submarine banks with an E-W direction at the inner shelf floor are oriented in function of

NBC. Longshore currents are produced by the ENE waves refraction in the EW coast (Gorini *et al.* 1982). The migration of the sand spits to the west is another indicator of the predominant longshore current that flows to the west.

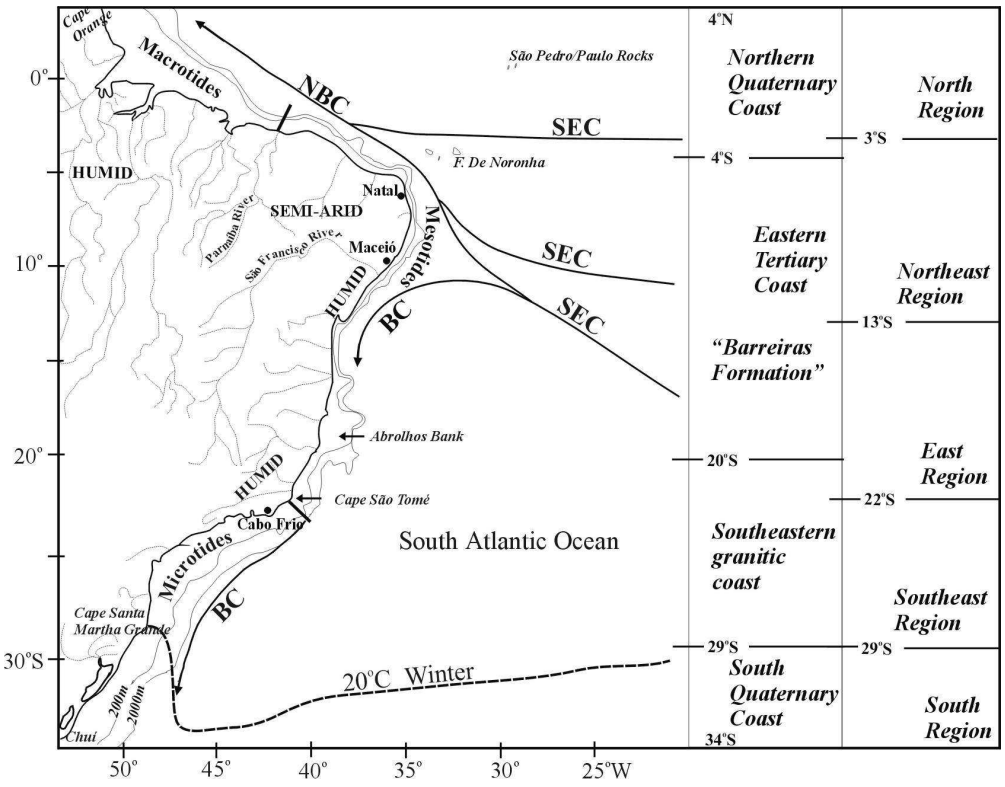

Figure 1.7 - Current system along the Brazilian coast. The South Equatorial Current (SEC) splits into Brazil Current (BC) and North Brazil Current (NBC). The hydraulic regime of north coast of the Rio Grande do Norte is influenced by NBC (after Knoppers *et al*. 1999).

1.5.3 - Tides

The area of study presents a semidiurnal mesotidal regime with the maximum spring tide reaching 3m and minimum of 0,8m during neap tides (Riedel 2000). The tidal measurements performed in the harbor of Macau showed that the amplitudes of spring and neap tide are 2.55m and 1.27m, respectively (DHN 1974).

1.6 - Organization of the this study

The structure of this work can be seen in the Figure 1.8. The work was divided in three main stages: a) Cartography and bibliographic research, b) collection and handling of the field data and c) integration of the data.

This dissertation is divided into 7 chapters. The chapter 1 (*Introduction*) gives a general overview about the geology of the area and its physiographic features. The objectives of this study are also presented in the chapter 1. *Materials and methods* are described in chapter 2. Chapter 3, *Inner shelf and coastal zone: morphological features and Morphodynamics,* deals with the interpretation of the remote sensing data together geophysical surveying at the inner shelf. Chapter 4, H*olocene sediments and stratigraphy*

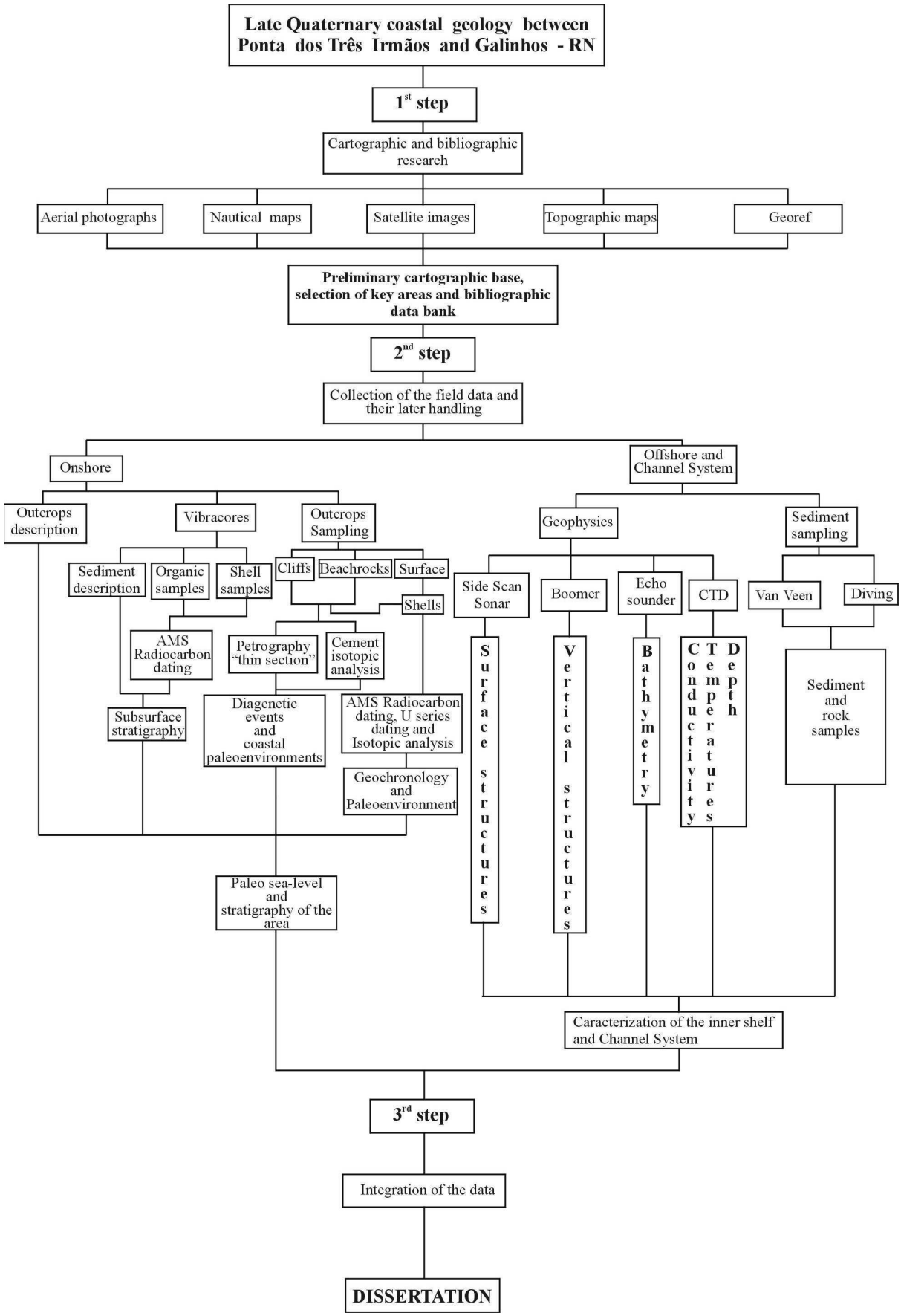

Figure 1.8 - Flow chart of the work.

discusses about Holocene coastal sedimentation in the study area. Chapter 5, *Holocene sea level changes: evidences from beachrocks and Paleo-lagoons*, is focused on Holocene sea level changes at the study area. Chapter 6, *Late Pleistocene and Holocene coastal evolution*, gives a vision on the paleogeography of the area during the last Pleistocene and Holocene transgression-regression. Chapter 7 presents the conclusions and perspectives of this study.

2 - Materials and Methods

2.1 - Materials

2.1.1 - Satellite images

The remote sensing products were used to get an overview of medium-large scale features of the study area. The remote sensing database consists of two oblique aerial photographs from 1942 with 1:20.000 scale, seven aerial photographs from 1950 with 1:40.000 scale, four aerial photographs from 1967 with 1:70.000 scale and one satellite image Landsat 7ETM+ at 10:00 AM from the 12th of June 2000 during low water level. The satellite image was processed using the ER-Mapper 6.2 and Arc View in the Remote Sensing Laboratory (Geology Department) of the Federal University of the Rio Grande do Norte (Brazil). One nautical map (DHN 1974-Marinha do Brasil – Fortaleza a PTI) and two topographic maps (Ministério do Exército 1985 - Folha SB.24-X-D-III Jandaíra and Folha SB.25-V-C-IMI-900 Pureza) were also used.

2.1.2 - Vibro-cores

In order to obtain a reliable stratigraphic framework for the region, ten vibro-cores were taken in the study area. All cores were obtained utilizing aluminum barrels with a length of 6m and width of 0,70mm.

Seven cores were located in the tidal plan of Galinhos and Galos (VCGAL-1, VCGAL-2, VCGAL-3, VCGAL-6, VCGAL-7, VCGAL-8 and VCGAL-9). The cores VCGAL-1 and VCGAL-2 were positioned near the island between Galinhos and Galos, directly in a swamp and at the edge of a mangrove area, respectively. The core VCGAL-3 was located between the mangroves and Pisa Sal River's margin. The core VCGAL-6 was taken at the limit between the sand beach and the tidal channel close to the Galos city. The cores VCGAL-7 and VCGAL-8 were placed in the tidal flat south of Galinhos: one to the east and one to the west of the Catanduva river mouth. The core VCGAL-9 was taken in the tidal flat at the western end of the island between Galos and Galinhos. Two vibro-cores were situated in the swamp landward of Caiçara and São Bento do Norte (LCSBN-1 and LCSBN-2). One vibro-core was located in the Cabelo River bed (VCLC-1) beside the road that connects São Bento do Norte/Caiçara to Galinhos/Galos. A general sampling and analytical procedure is shown in Figure 2.1.

Descriptions of five water-wells from RN state's water company (CAERN) located in Caiçara do Norte were also used.

2.1.3 - Beachrocks, coastal outcrops and surface samples

The analysis of the coastal outcrops provide elements for the depositional paleoenvironment reconstruction for the area and they, together with the vibro-core, are the principal data supplier for the temporal and spatial interpretation of the coastal deposition. All data were used to propose a stratigraphic framework for the area. In this way coastal outcrops in form of coastal cliffs (e.g. Ponta dos Três Irmãos) and beachrocks located in the intertidal and onshore zones were described in detail, as well as sampled for later laboratory analyses.

Bivalves were used to obtain the age of coastal deposits found in the area. The stable isotopic pattern of the shells could be correlated to the paleoenvironment of the area. The bivalves were obtained principally from beachrocks and vibracores of the study area. In order to obtain reliable data, appropriated bivalves were selected *in situ* during their sampling in the

coastal outcrops. Only the well-preserved bivalves with some original shell-color (no visible superficial alterations) were collected.

Surface sediment sampling of both the tidal plan of Galinhos and the inner shelf were conducted to measure the sediment properties and grain size distribution in the working area.

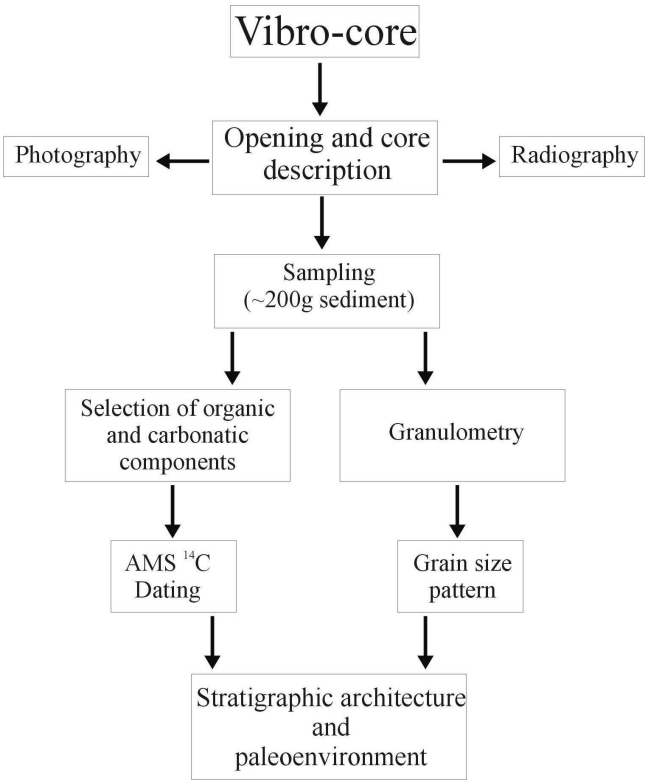

Figure 2.1 – Flow chart showing depicting stages for the vibro-core

2.2 - Methods

2.2.1 - Stable isotope – $\delta^{13}C$ and $\delta^{18}O$ analysis

Fossil bivalve shells and carbonates cements from beachrocks and other coastal deposits were selected for isotopic measurements.

Following the strategy from Erlenkeuser & Wefer (1981), to decipher the shell growth history that is intimately correlated to the short-term paleoenvironment changes Hendry *et al*. (2001), carbonates of well preserved bivalve shells were sampled to know their stable isotope pattern. From two well-preserved shells, carbonate sub-samples were taken in a transect normal to the growth rings of the shells.

Isotopic measurements were also carried out on aragonite shells that presented some signal of recrystallization. The isotope values allow the mapping of the secondary mineralogy (e.g. calcite) of the original aragonite bivalve shell.

The isotopic pattern of the beachrock cements was also obtained since the isotopic trace of carbonate sediments can be used to know the processes evolved during their formation and post-depositional stabilization (Veizer 1983).

The isotopic measurements were performed at the Leibniz Laboratory, Kiel, with a Finnigan mass spectrometer MAT 251. The system precision reaches 0.04‰ for $\delta^{13}C$ and 0.08‰ for $\delta^{18}O$ relative to the PDB standard.

2.2.2 - *X*-ray radiography and *X*-ray diffraction

X-ray radiographs were performed in the vibro-core sediments to make the fine internal structures of sedimentary origin in lagoonal deposits more visible. A 2cm thick slice of sediment was taken and fixed on the x-ray table. The slice remained 10 seconds under X-ray action (44kV).

X-ray diffraction on bivalve shells was used to determine whether they contained recrystallization or not. The alteration of aragonitic shells is readily detected by X-ray diffraction because the product is usually calcite (Stodart & Cann 1965; Hopley 1986 and Bezerra *et al*. 2000).

2.2.3 - AMS ^{14}C dating

The radiocarbon dating method is widely used in coastal studies where biogenic materials are commonly available. Such materials like shells make the determination of coastal deposit ages that could be correlated to the former sea levels possible. In the last decades the use of radiocarbon dating in coastal studies has allowed significant progress in the understanding of this region in time and space.

Precise AMS-radiocarbon dating of both terrestrial organics from several vibro-cores and mollusk shells of coastal deposits permitted to comprehend the environmental changes in time and space.

A careful selection and a detailed pretreatment on the bivalve shells allowed us to eliminate and to control the problems related to the contamination.

The AMS radiocarbon ages were determined with a 3MV HVEE Tandetron 4130 AMS system at the Leibniz Labor, Kiel. The standard procedures are described in Nadeau *et al*. (1997) and Schleicher *et al*. (1998). The system presents an average zero background of 0.3%

All AMS^{14}C carbonate ages were not corrected for a standard mean ocean reservoir effect. Radiocarbon ages of carbonate and organic samples were converted to calendar ages using version 4.1.2 of CALIB radiocarbon software (Stuiver & Reimer 1993) that has been updated with recent calibration data sets (Stuiver *et al*. 1998). All calibrated ages were rounded up or down to the nearest multiple of ten.

2.2.4 - U-Series disequilibrium (^{230}Th-^{238}U and ^{232}Th-^{234}U) dating

The U-series disequilibrium dating methods have been most useful in the study of sediments and calcium carbonate deposited in the oceans and lakes during the Pleistocene epoch (Faure 1986). In this way some ^{14}C AMS dated coastal deposits, which provided radiocarbon ages older than Holocene were dated with U-series disequilibrium dating methods. Selection and detailed pretreatment of thin sections of rock samples containing fragments of the shells was undertaken to identify the most appropriate shelly material for U-Th dating. Pretreatment included the investigation of the mineralogy and crystal structure via an electronic scanning microscope.

The U/Th was measured by a double focusing sector field ICP-MS (Micromass Plasma Trace 2) in combination with a desolvating nebulizer (Cetac MCN6000, modified with self-aspirating 100µl/l-PFA nebulizer and PFA spraychamber). For the determination of ^{232}Th, ^{230}Th, ^{234}U and ^{238}U by means of TIM, bivalve shells were spiked with ^{229Th} and ^{233}U. Samples were dissolved in a mixture of HNO_3/HCL/HF and then processed using standard chemical techniques as described in Edwards *et al*. (1986). Chemical procedures in the laboratory of the Institute of Geosciences (Kiel) were performed in cleanrooms with double distilled reagents.

2.2.5 - Electron microprobe (EMP)

The chemical composition of the beachrocks cements can be used to recognize the coastal zone where they were precipitated. According to Alexanderson (1972), Coudray & Montaggioni (1986) the high-Mg content (12 to 18mol‰) in the beachrock cements suggests an intertidal zone for precipitation whereas low-Mg contents (less than 2 mol‰) indicate meteorically water-influenced precipitation zones.

The chemical compositions of some Pleistocene and Holocene beachrock cements were determined using the electron microprobe. Pre-described and $\delta^{13}C/\delta^{18}O$ measured beachrocks cements were selected for chemical determinations.

The chemical elements analyzed were: Mg and Sr.

The EMP at Mineralogy Division, University Kiel, is a Cameca, Camebax-Microbeam, with four wavelength-dispersive spectrometers. Operating conditions were 15kV accelerating voltage and 15nA beam current, which allows a beam diameter smaller than 10 µm.

2.2.6 - Geophysical survey

2.2.6.1 - Echo sounder and Side Scan Sonar

Bathymetry data of the area seaward of Galinhos were gained from 13 echo sounder profiles. The profile lengths vary from 3 to 6 km from preferential SSW (210° Az) to NNE (30° Az) directions. The echo sounder consists of a regarding unit and an emitter/receiver in the water. The device operated with frequency of 200Khz and was powered by two car batteries (24V).

All data were printed on paper and the profile positions were obtained using GPS (GARMIN GPS48).

The surface structures were surveyed by several tracks of side scan sonar. The profiles were taken offshore of the village of Galinhos and Galos parallel to the direction SSW (210°) to NNE (30°) as well as to ESE (120°). The system consists of a record device and a side scan transducer. The transducer is simply towed behind the vessel. An acoustic signal with a frequency of 200kHz was emitted, back scattered by the sea floor and received by the same device. Positions (GPS), water depth, date and time (UTC) were annotated every 3 minutes.

The echo sounder and side scan sonar together make up the "Hydrotec" which was manufactured by the Odom Hydrographic Systems Inc (USA).

2.2.6.2 - CTD and currents measurements

Data of conductivity, temperature, depth (CTD) and currents measurements of 9 stations located north of the spit between Galinhos and Galos were obtained. Furthermore data from 13 current stations for the area between Ponta dos Três Irmãos and Caiçara are available (Tabosa 2000 and Riedel 2000).

The data near Galinhos were obtained by using a CTD/current instrument manufactured by AANDERA INSTRUMENTS, Norway. Those obtained near São Bento were obtained with a Mini Current Meter (Model SD-30) from Sensordata, Norway.

The first one is composed by a "Doppler current sensor 3500" that measures the water temperature, current velocity and current direction. A "C/T/D Sensor 3231" that is linked to the "Doppler Current Sensor 3500" measured the conductivity and depth.

The Mini Current Meter is composed of a paddle wheel rotor that measures the average current speed. A magnetic compass inside the electronic unit measures the directions,

which in turn is calculated by a microprocessor as a mean current direction (0-360^{o}). A sensor on top of the device measures temperature (^{o}C).

Three measurements were carried out in the water column near Galinhos. The sampling interval at each depth was 10min and every 30s an average value was recorded.

The measured data were processed and displayed a board with the "Datalogger 3660".

The data close to Galinhos was collected in November 2000 while those from São Bento were collected in November 1999.

2.2.6.3 – Boomer

The sedimentary vertical structure of the channel system sediments of Galinhos could be visualized using seismic reflection. The boomer system, a towed electromagnetic source that transmits sound energy towards the sea/channel bottom, was used.

The system composes of power supply, streamer, sound source and a recorder.

The power supply receives regular main voltages (220V) from a generator and converts this constant voltage to a higher voltage (up to 4000V) required to energize the sound source. The signal energy used during the research was set up to 300 Joule and later 150 Joule.

The streamer is composed by 8 hydrophones that receive the reflected acoustic signals and transform them to electrical signals.

The sound source comes from a sudden separation of an aluminum plate from a flat copper coil embedded in a hard epoxy resin (Jones 1999). When the capacitor in the power supply is discharged through the coil, eddy currents are induced in the aluminum plate causing a rapid repulsion the creation of a cavitation volume in the water (Jones, 1999).

The signals received by the hydrophones are amplified, filtered and stored using a laptop with the NWC program. A high pass filter (4302 Dual 24db/Octave filter) was used to eliminate frequencies lower than 0.315 kHz to improves the quality and structure observed while recording.

About 80 km of boomer transects were performed.

3 - Inner shelf and coastal zone: Morphological features and dynamics

3.1 - Introduction

The morphological features located in the northern coastal zone and its inner shelf of Rio Grande do Norte state (NE Brazil) are described and correlated morphodynamics are discussed.

The study area is an open, wave dominated, meso-tidal coast. The associated inner shelf is shallow (maximum 20m depth) and has an average width of 18 km (Fig. 3.1).

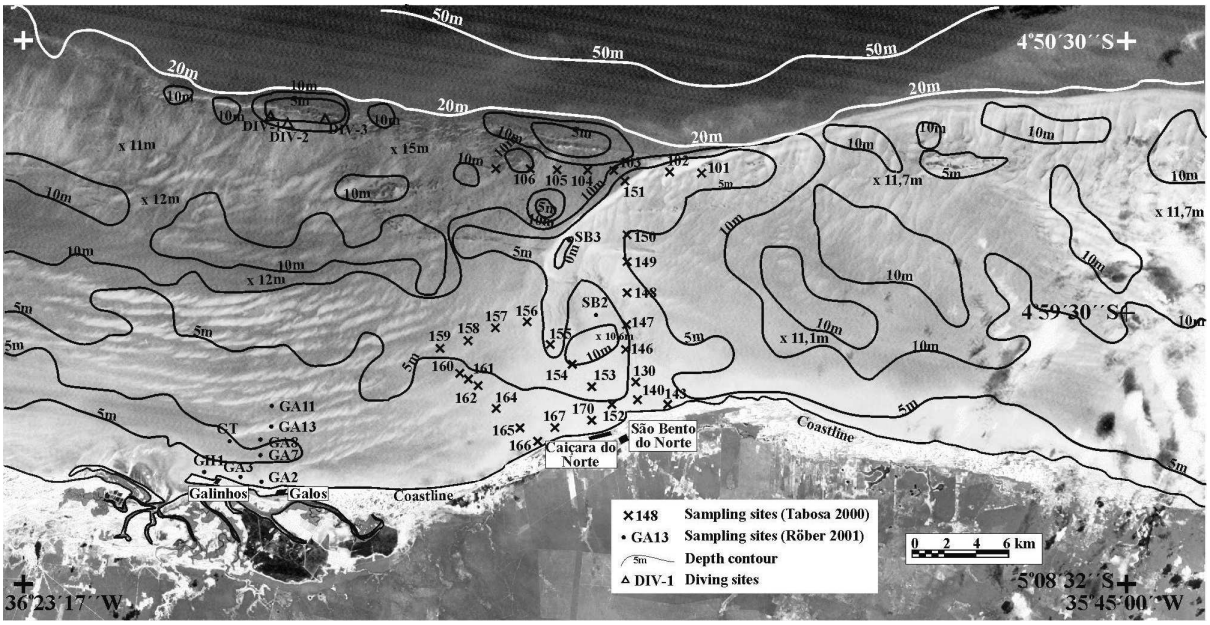

Figure 3.1 - Satellite image (Landsat 7ETM+, Band 1, from June 2000) of the coastal zone and inner shelf of the central north coast of Rio Grande do Norte State, NE Brazil. Sampling sites are marked by crosses (Tabosa 2000) and by dots (Röber 2001). Bathymetric data from DHN (1974).

Research work facilities concerning inner shelf flow dynamics and correlated larger-medium bedforms and coastal zone have largely improved since remote-sensing products (e.g., satellite images and aerial photographs) are available (see Vianna & Solewicz 1988; Vianna *et al*. 1993; Testa & Bosence 1998; Testa & Bosence 1999). Unfortunately, many inner shelves present a high volume of suspended sediments, which impede the penetration of light through the water mass in such a way that no sharp image of the inner shelf bedforms can be obtained. In this case, geophysical coastal surveys (e.g., Side Scan Sonar) must be conducted and the general image of the bottom of the inner shelf will depend on the quality and quantity of the acquired geophysical data. Generally, side scan sonar is very useful to detect medium to small-scale features while remote-sensing products gives a general overview (images are spatial resolution dependent). The combined use of many tools (geophysical surveys, sampling and remote sensing products) will produce more reliable data and subsequently better interpretations.

This chapter focuses on describing and interpreting the inner shelf sediments and their associated bedforms. The work is partially based on a large-scale Landsat 7ETM+ from June 2000 that allow the recognition and pre-delimitation of the main morphological features of the inner shelf bottom. Additionally bathymetry surveys, punctual current measurements,

diving observations, side scan sonar recordings and samples of the bedforms enables the correlation of these morphological features to their sedimentological compositions and morphodynamics.

Of the coastal zone, the principal morphological elements are described and individualized from a satellite image, aerial photographs and field descriptions.

3.2 - The inner shelf and coastal region: image interpretation and surface sediment characteristics

In the last decades some authors have started to study the Brazilian continental shelf. Summerhayes *et al*. (1975) and Martins & Coutinho (1981) focused their works on shelf physiography and sedimentological cover characterization of the coast between Salvador and Fortaleza. On the east-northeastern Brazilian shelf some works stressed regional ocean currents and their material transport (Stramma *et al*. 1990; Silveira *et al*. 1994; Knoppers *et al*. 1999). Tintelnot (1996) and Arz *et al*. (1999) discussed late Quaternary stratigraphy and climatic changes for the shelf between João Pessoa and Fortaleza.

The regional character of these studies has improved the large-scale knowledge and characterization of the 7300 km (MMA 1996) long Brazilian shelf, but more local studies important to understanding how the last post-glacial sea level changes took place are still scarce. Perhaps many answers about it can be obtained in such shelf areas, where whole Holocene sea level changes are printed. The bedform patterns and their lateral relationships visualized in the Landsat image seem to be unique. The understanding of their build up and related morphodynamics will improve to understand the Quaternary flooding history of the shelf.

Recently some authors began to study the inner shelf zones more locally (Testa & Bosence 1999, Testa & Bosence 1998, Costa-Neto 1997 and Tabosa 2000).

In the studied inner shelf a variety of bedforms can be described. The criteria used to describe these larger scale bedforms are principally their shapes (images are spatial resolution dependent), sedimentary texture and composition (Ashley 1990). Additionally diving, current measurements, side scan sonar survey and bathymetry profiles were undertaken in order to improve the satellite image interpretation.

The sampling sites were chosen in order to cover all morphological features that are represented by different shades of gray on the Landsat image (Fig. 3.1).

From Landsat image interpretation six morphological zones can be identified (Fig. 3.2).

3.2.1 - The Coastal Zone (CZ)

The coastal zone of the study area presents a variety of morphological features and coastal deposits. Siliciclastic beaches and adjacent dune fields compound the main deposits (Fig. 3.3a). The beaches are mainly composed of medium to very coarse sand with bioclastics (<5%) associated. The length of the siliciclastic coastal dunes varies from a few meters (5-20m) to a few kilometers (1-10km), while the heights range between 4 to 50m. The dune fields present an E-W oriented transport direction on the eastern coast, deviating to NE-SW on the western portion.

The beachrocks (Fig. 3.3b) occur nearly always along the actual beach in the foreshore zone, and also in the backshore zone. All beachrocks consist of siliciclastic sand often containing bioclastics. The grain size varies from medium sand to medium gravel and $CaCO_3$ cements all clastic components.

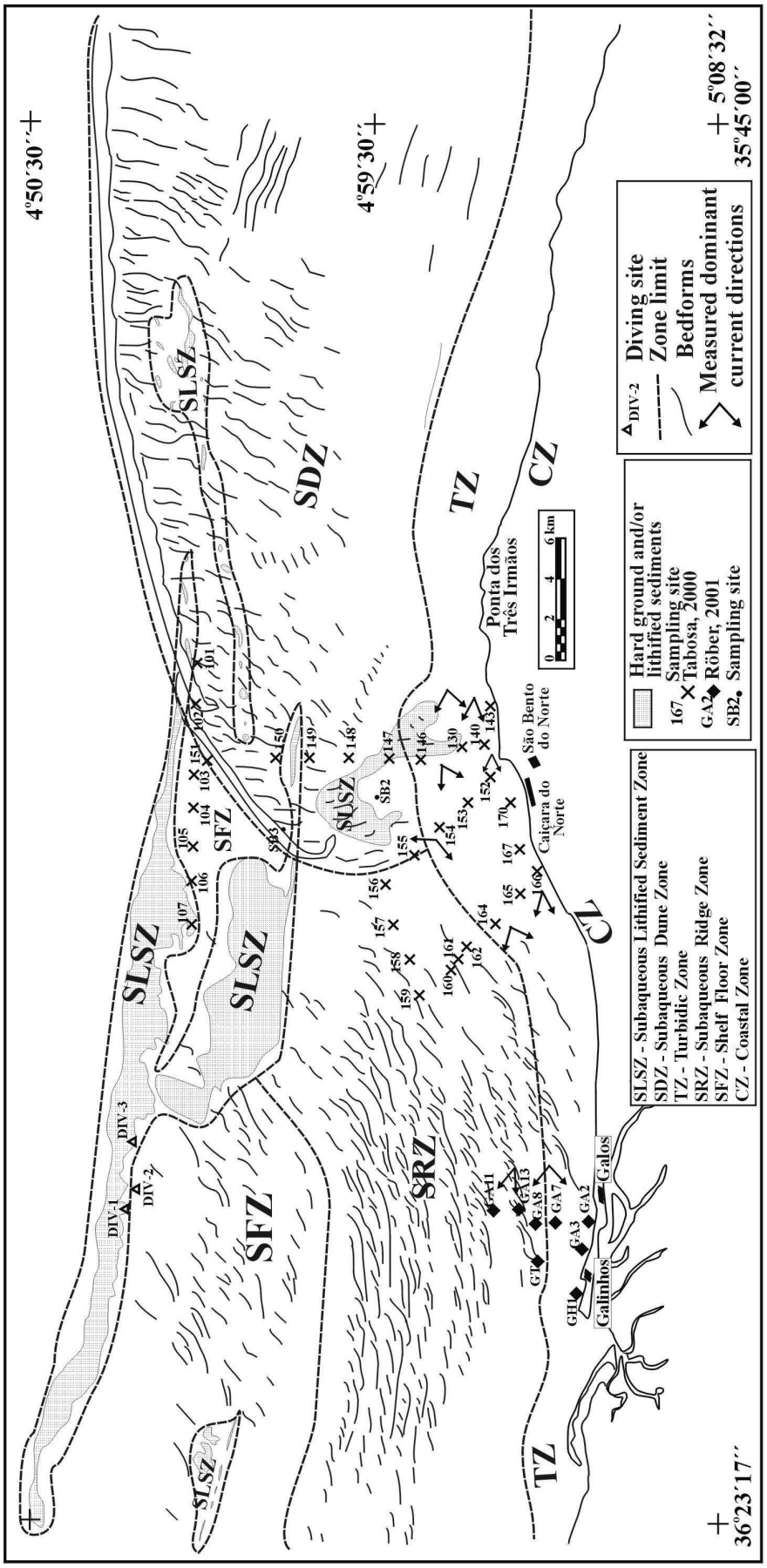

Figure 3.2 - Large scale map of the morphological features and sedimentary zones on the inner shelf based on a Landsat 7 ETM+ band 1 image, from June 2000.

Sandstones forming active cliffs (Fig. 3.3c) are found mostly east of São Bento. The Ponta dos Três Irmãos (PTI) is the best representative outcrop of this sandstone. This rock most probably consists of aeolianite resting on by upper foreshore deposits.

The eolianite consists of fine to very fine siliciclastic sand (<80%) containing often more than 15% of bioclastics (mostly green algae). At some points some trough-cross-bedding-stratification with a tangential base could be recognized in the eolianite. The sandstone at the cliff base shows the same grain size pattern and composition of the adjacent beach. Swash-cross stratification was observed. The sandstone found at PTI is similar to that described by Srivastava & Corsino (1984) at the coast of Touros city.

Some flat areas (Fig. 3.3d and 3.3e) located landward of the beaches that are without connection to the open sea and that experience flooding during the rainy season are found close to the São Bento city. The sediments found at these flat areas vary from silt/clay to very fine sand. Fossil shells found in living position and forming banks several meters long (center of Figure 3.3d) are positioned on the surface of the flat areas. It is thought that these flat areas represent former tidal flats. The flat area is separated from the sea by a set of sand ridges, which are covered by dunes (Fig. 3.3f).

Longshore drift has produced a long sand spit where the cities of Galinhos and Galos are located (Fig. 3.3e). Consequentially, a larger tidal flat has developed landward of the spit.

3.2.2 - The Turbidic Zone (TZ)

The turbidic zone is 3 to 6 km wide (Fig. 3.2) and represents the area directly parallel to the shoreline with depths reaching 5m. The TZ is subjected to intense sediment suspension and its water is nearly always turbid.

The surface sediments of this zone are characterized dominantly by siliciclastic sand and mud (Fig. 3.4). The grain size varies from silt to medium sand appearing in the Landsat image as plumes of suspended sediment moving to west.

The carbonate content in the sediments collected in this zone reaches a maximum of 26% (Fig. 3.5, point 154) but values lower than 10% are more common.

3.2.3 - Subaqueous Dune Zone (SDZ)

In the eastern part of the inner shelf (Fig. 3.2) large subaqueous dunes form a tongue-shaped dune field approximately 30km long and 16km wide. The dune field covers almost the entirely inner shelf. The large subaqueous dunes in the Landsat image are 500 to 2000m long, N-NE oriented linear crests and are limited in the north by a 34km long hook-shaped subaqueous bank (Fig. 3.2). The sampled sediments show that the dunes are composed basically by sand with a grain size varying from fine sand to very coarse sand (Fig. 3.4). Gravel content less than 7% and mud content less than 4% was also found in the subaqueous dune zone. The hook-shaped sand bank sampled at position 102 and SB3, shows the same grain size pattern of the SDZ. Some supposed sand ribbons occur in the east of the SDZ. Unfortunately there are no available samples of these bodies, although they can be compared to those sand ribbons described by Testa & Bosence (1999) in the Touros inner shelf. The carbonate content found in the sediments of the SDZ increases moving northwards. Values closer to 50% of carbonate are found at points 101 and 102 (Fig. 3.5).

Figure 3.3 - Morphological features present in the coastal zone. (A) Siliciclastic sand beach at the Galinhos spit backed by active aeolian dunes; (B) Cemented sand beach [beachrock] positioned in the intertidal zone near to São Bento; (C) Sandstone as active cliffs at the Ponta dos Três Irmãos; (D) Paleo tidal flat SW from São Bento with shell bank; (E) Oblique aerial photograph facing the sand spit with the village of Galinhos and the channel system in the background (SW). (F) Aerial photograph from 1950 showing the paleo tidal flat (PTF) SW from São Bento and sand ridges between São Bento and Caiçara.

3.2.4 - Subaqueous Lithified Sediment Zone (SLSZ)

The SLSZ occurs closer to the margin of the inner shelf at a distance of 19 kilometers of the coastline and it is oriented basically parallel to the actual coastal zone (Fig. 3.2). The SLSZ comprises underwater rocky outcrops elevating 0.5 to 3.0m above the sea floor (Fig. 3.6) and hard grounds that probably do not form underwater cliffs. Both form dark gray strips in the Landsat image.

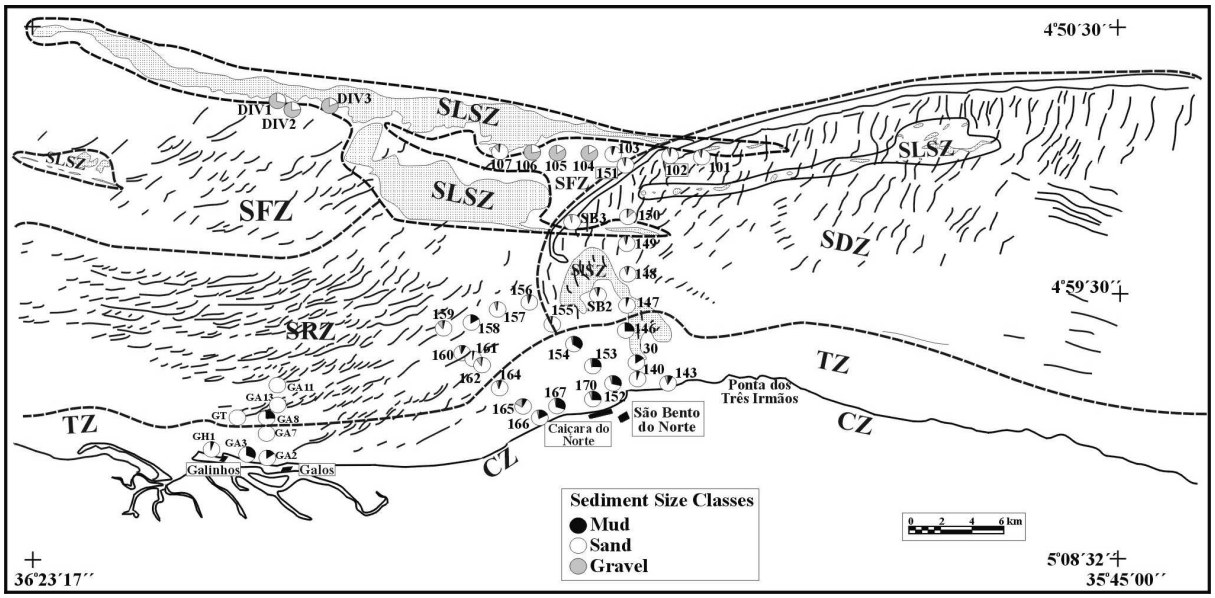

Figure 3.4 - Pie charts of the sampled sites showing the relative percentages of mud, sand and gravel within different morphological zones.

The rocks are carbonate-cemented sand similar to that beachrock and eolianite relicts of the last sea level transgressions and regressions. Sedimentary structures like cross bedding can be visualized in some outcrops (see Fig. 3.6 on the right hand side) although often a dense encrusting of biota on sandstone occurs. In the eastern part of the inner shelf the SLSZ seems to be covered by the subaqueous sand dunes while in the western part of the inner shelf it is more observable due to the lack of sand. The carbonate content of the SLSZ is variable and it can reach 30%. In the Figure 3.5 the pie charts show the carbonate content on the floor of the SLSZ.

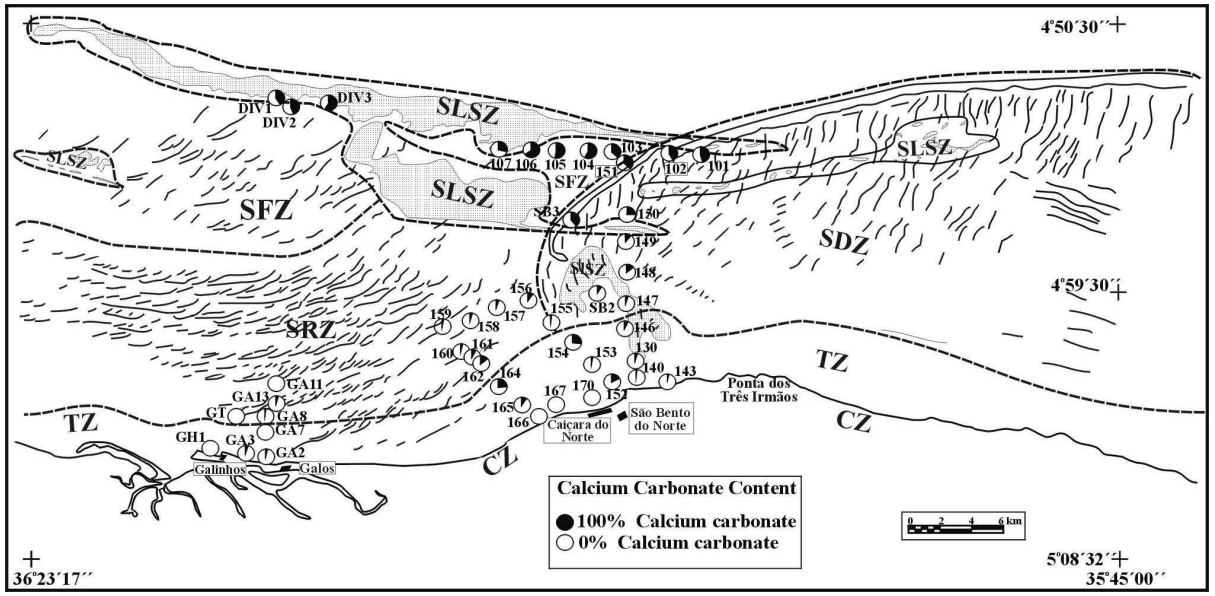

Figure 3.5 - Pie charts illustrating the carbonate content in each sample. Note that the carbonate-rich areas increase moving offshore.

Figure 3.6 - Rocky outcrop at DIV1.

3.2.5 - Subaqueous ridge zone (SRZ)

The SRZ is present in the western part of the study area (figs. 3.1 and 3.2). It consists of sub-parallel ridges oriented NE-SW in the east of the zone. Further offshore and westward these ridges have an E-NW orientation. The outer ridges are curved while the inner ridges are straight. The ridges closer to the shore are about 12km long while those located further offshore are about 18km long. The ridges area measured to be 300-500m wide and approximately 1 to 1,5km apart from another. In the Landsat image the sand ridges seem to consist of several short sigmoidal banks attached to each other (Fig. 3.1). Sediments collected at the ridges show that they consist basically of sand with the grain size varying for medium to fine sand (Fig. 3.4). It can be observed too, that the more fine grains tend to occur in deeper water between the sand ridges. The carbonate content in the SRZ (Fig. 3.5) is rather low at approximately 2-4%. It is noteworthy that to the east, carbonate content increases slightly, possibly due to the close proximity of the carbonate-richer sediments of the SDZ.

3.2.6 - Sea Floor Zone (SFZ)

The SFZ in the Landsat image cannot be compared with the other zones. It shows a relatively dark gray color with some light patches certainly representing sand bodies (Fig. 3.1 and 3.2). Diving operations and the samples at the points DIV1 and DIV2 show that the SFZ consists basically of rhodoliths (coralline red algae) (see the foreground of Fig. 3.6), which were also found by Costa-Neto (1997) in the extension of the SFZ to west and by Testa & Bosence (1999) in the inner platform of Touros. This zone presents a higher content of carbonate in the sediments, reaching more than 50%.

3.3 - Bathymetry, Side Scan Sonar and current measurements

3.3.1 - Bathymetry

The bathymetry of the area north of Galinhos spit was investigated with 25km of echo sounder profiles (Fig. 3.7) in order to cross the subaqueous sand ridges in the offshore zone. Side scan sonar tracks also in the area north of Galinhos spit (Fig. 3.7) were studied to obtain data of surface structures. Current measurements were performed off the coast of São Bento (Tabosa 2000 and Riedel 2000) and north of the Galinhos spit (Röber 2001) (Fig. 3.2).

The bathymetric profiles 1 and 4 do not show any large ridge morphology because they are too short. The other bathymetric profiles cover part of sand ridge 1 and the northerly sand ridge 2 (Fig. 3.7). The high-frequency oscillations on the missives do not represent any morphological features but are responses to the rolling of the vessel due to the wave action. Therefore small-scale features could not be detected. Apart from profile 11 all other bathymetric profiles end close to the shore and the plots demonstrate a drop of the sea floor of 4m towards to the shoreline in a relatively short distance. The lack of nearshore bars could be a possible cause of this channel-like structure.

In the profiles of transects 8, 9 and 12 bar-shaped elevations of 1m were recognized close to the shoreline but denser bathymetric data is necessary to propose a more reliable interpretation.

The transects 2, 5, 6, 8, 9 and 10 cross the sand ridge 1 at an angle of 75°. The water depth at the crest of this ridge varies from 1.5m to 4m and in the Landsat image the ridges are represented for the light strips. The letters A to I in the Figure 3.7 represent the stretches where the bathymetric profiles crossed the sand ridges 1 and 2.

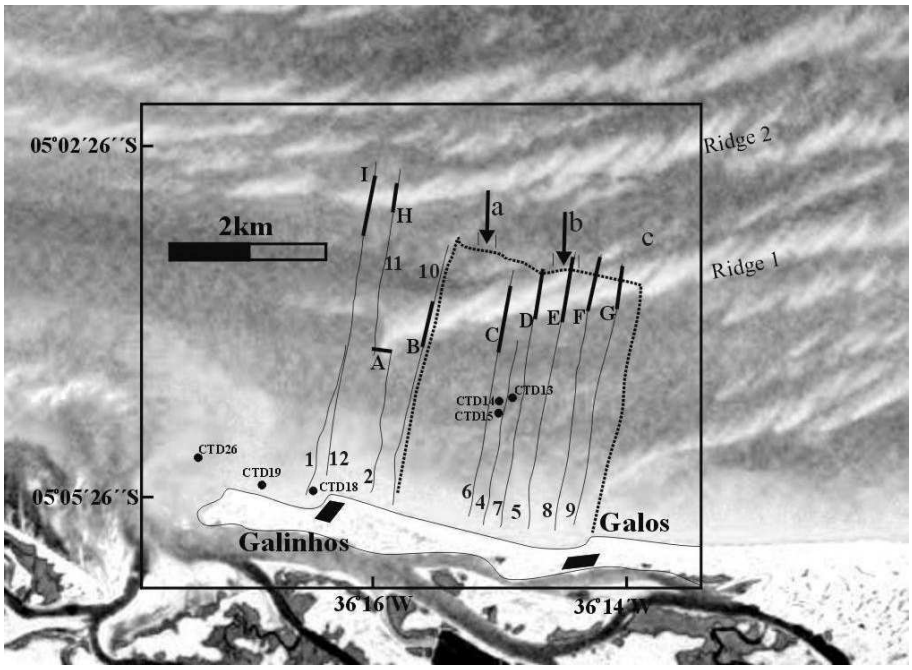

Figure 3.7 - Bathymetric profiles (solid lines) and the side-scan sonar track (dotted line) overlaid with a Landsat 7ETM+ scene north of Galinhos and Galos. The bold line stretches with letters correspond to the examined topographic sectors. The arrows indicate the examined side scan sonar sections. The dots indicate the current measurements.

The geometry of sand ridge 1 could be investigated from 7 bathymetric profiles. As can be seen in the Landsat image, sand ridge 1 is composed of a group of smaller elongated sigmoid-shaped sand bodies that together form a SW-NE oriented sand ridge. These features could be detected in the bathymetric profiles. Each feature seems to broaden moving from ENE to WSW, with widths varying between 400 and 1000m.

The variability of the ridge slope inclination, geometry and length is significant. Missives of transect 5, 7, 8, 9 and 10 show pronounced asymmetries with steeper onshore-directed slopes and less inclined in the offshore directions (Fig. 3.8).

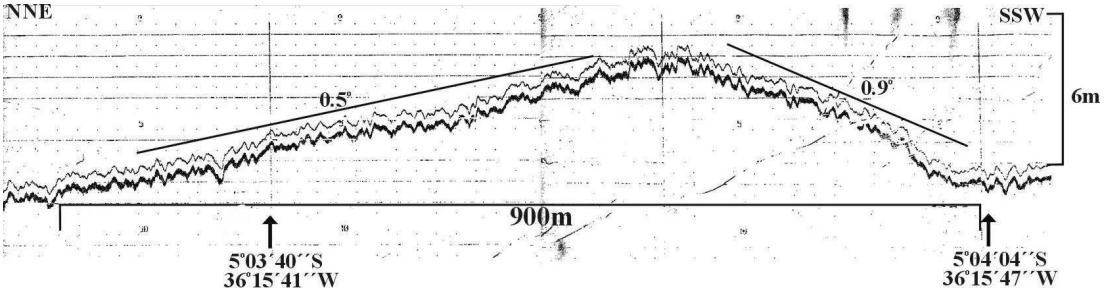

Figure 3.8 - Geometry of sand ridge 1 in the transect 10 (sector B). Note the flank asymmetry: the landward side (SSW) is almost twice as steep as the seaward side (NNE).

The transect 9, sector G was taken further eastward (Fig. 3.7), but from the profile one can see that the geometries of the flanks are similar to those located further westward. Sector G shows that the landward flank has an inclination of 6.5° while the seaward flank has an inclination of 3.4° (Fig. 3.9).

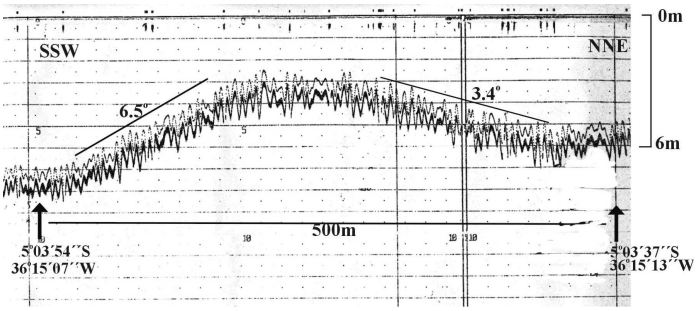

Figure 3.9 - Flank asymmetry of sand ridge 1 visualized by the echo sounder transect 9, sector G. Note that the inclination on the SSW side is lager than that of the NNE side.

At the southwestern end of the sand ridge 1, sector A was oriented in an east-west direction at this position sand ridge 1 has an abrupt end (Fig. 3.10). This sand ridge has a maximum height of 5.7m.

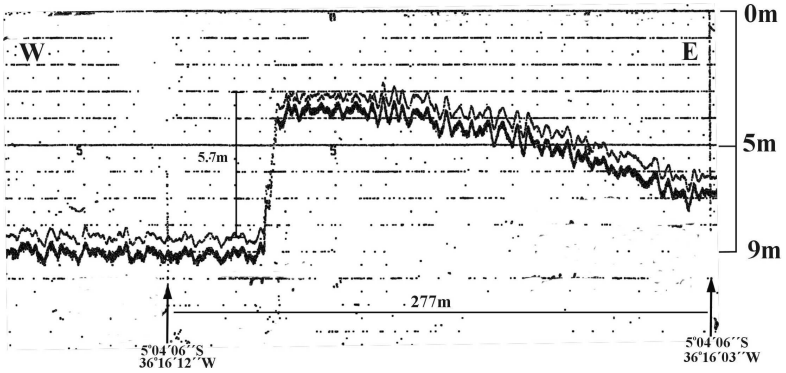

Figure 3.10 - Steep edge of sand ridge 1 at its southwestern portion. The inclination at this position is 34°.

The geometry of the sigmoidal pattern observed in the Landsat image could also be detected in the echo sounder profile. Sector D and sector E show this feature that is caused when two smaller sand bodies blend with each other (Fig. 3.11). Transect 7 shows this feature in the southwestern part of the smaller sand bodies (Fig 3.7).

In the sector D (Fig. 3.11) the flank asymmetry shows the same pattern seen in the other ridge 1 areas. The landward flank (facing SSW) is stepper than the flank seaward (NNE). This sector crosses the southwestern limit of two smaller sand bodies. It can be observed that these two sand bodies are amalgamated forming a "M-shaped" cross section. In the sector E once again illustrates this "M-shaped" topography (Fig. 3.12).

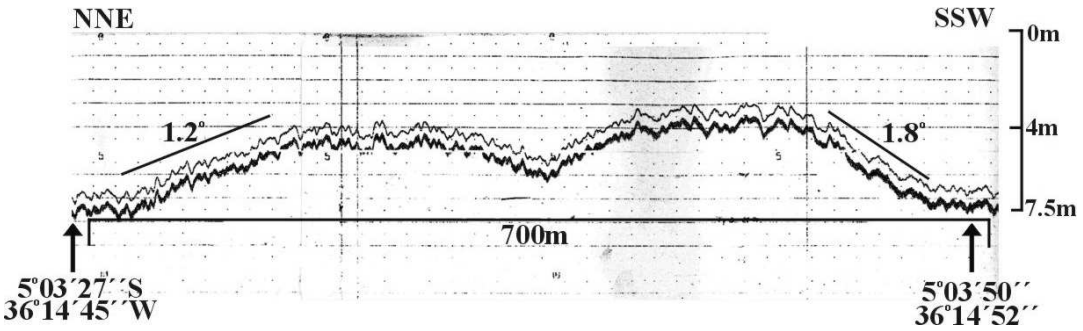

Figure 3.11 - Sector D showing the "M-shaped" form of sand ridge 1 in the southwestern area. This feature is developed when two smaller sand bodies blend with each other forming the sigmoidal pattern.

In the profile of sector E (Fig. 3.12) it can be observed that the two sand bodies amalgamated in the sector D are in this case separated by a 220m long trough. It can be observed too that the sand body positioned landward (SSW) is wider than that located seaward (NNE). The geometry of the flanks show the same pattern seen in the other transects. While the seaward side presents an inclination of 0.75°, the landward side is inclined at 1.4°.

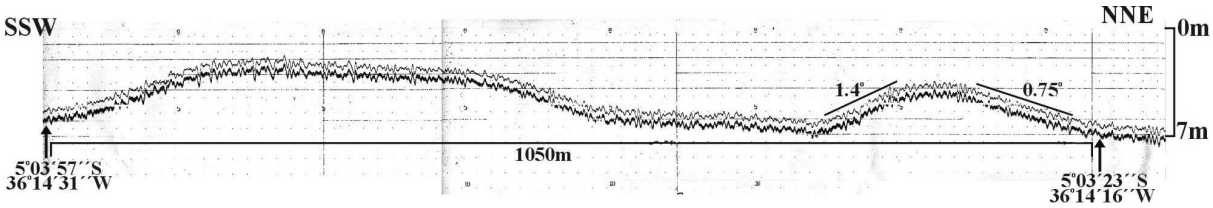

Figure 3.12 - Sector E showing two separated sand bodies. These two sand bodies are that already amalgamated sand bodies shown in the sector D.

Sectors H and I could illustrate the geometry of sand ridge 2. The sand ridge 2 seems to have the same sigmoidal pattern as seen in sand ridge 1, but its direction tends to E-W direction. At its highest point, the sand ridge crest is 3.5m below the water level where the overall water-depth is 8.5m (Fig. 3.13).

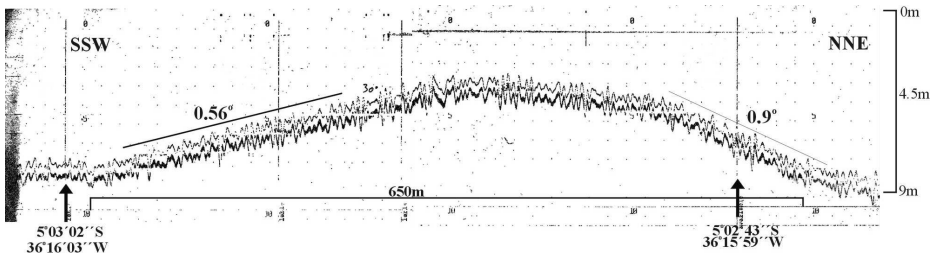

Figure 3.13 - Geometry of sand ridge 2 (sector H). The asymmetry is contrary to ridge 1, as the seaward flank is steeper than the landward flank.

3.3.2 - Side Scan Sonar

Side scan sonar recordings gave additional information on the surface morphology of sand ridge 1 (Fig. 3.7). The arrow "a"in the Figure 3.7 is represented as a sonograph in the Figure 3.14.

In the Figure 3.14 it can be observed bedforms sub-parallel with the track direction, i.e. they are directed in a WNW-ESE direction. Tendency towards northeasterly and towards a northwesterly direction is also observed. The distance between crests is between 20 and 35 cm. The crests heights cannot be deduced from the printout. The geometry of these bedforms is similar to the oscillation ripples described in the general geological literature. It is plausible that these small ripples recorded by side scan sonar system belong to wave-induced oscillation ripples. Therefore wind-induced waves from a northeasterly direction could produce such bedforms, which are in accordance with the wind pattern of the north coast of Rio Grande do Norte State (see Figure 1.6).

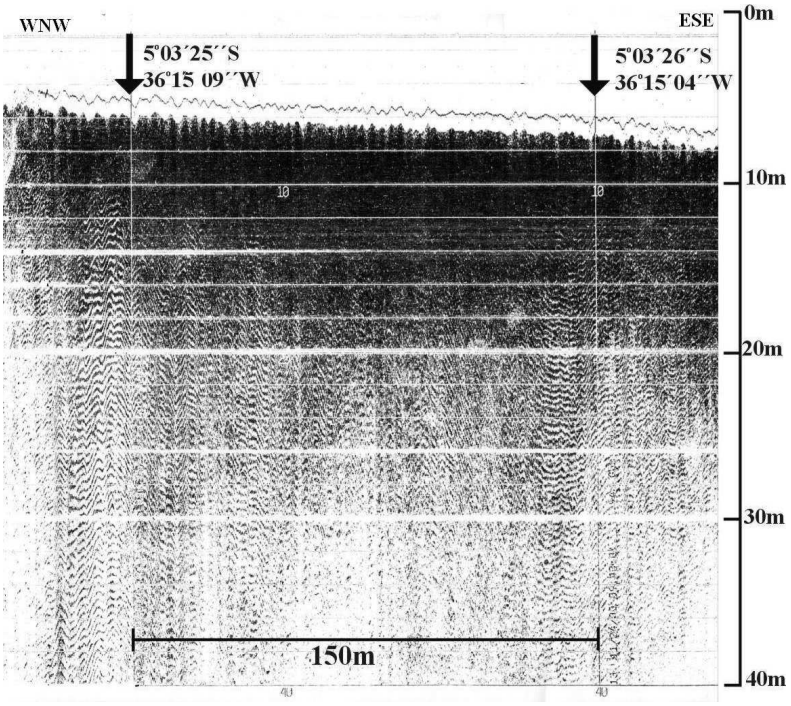

Figure 3.14 - Sonograph showing bedforms found through track "a". For location, see fig.3.7.

In the Figure 3.15 from the side scan sonar the surface of part of sand ridge 1 is shown. Since wind speeds and waves were small during recording, the undulating depth line on the missive is due to the topography present on the surface of sand ridge 1 (Fig. 3.15).

Two bedform patterns can be observed in the sonograph of sand ridge 1. The first is probably related to large current ripples that are present as successive depressions and crests with heights differing between 0.5 and 1 m while the separating distance lies between 15 and 25m. The second pattern is related to small ripples with crest distances reaching between 20 and 35cm.

The ripple index L/H (length/height) ≥ 15 shows that the first bedform belongs to the category of current ripples (Reineck & Singh 1973). These ripples are oriented perpendicular to the track direction and sub-parallel to the sand ridge 1. This pattern would suggest a mean current direction from southeast or northwest.

The small ripples are oriented mostly perpendicular to the current ripples. The average distance between the crests is about 40 cm and they are oriented in a SSW direction. Unfortunately their heights cannot be deduced from the printout, but these bedform structures are very similar to the wave induced oscillation ripples seen in the Figure 3.15.

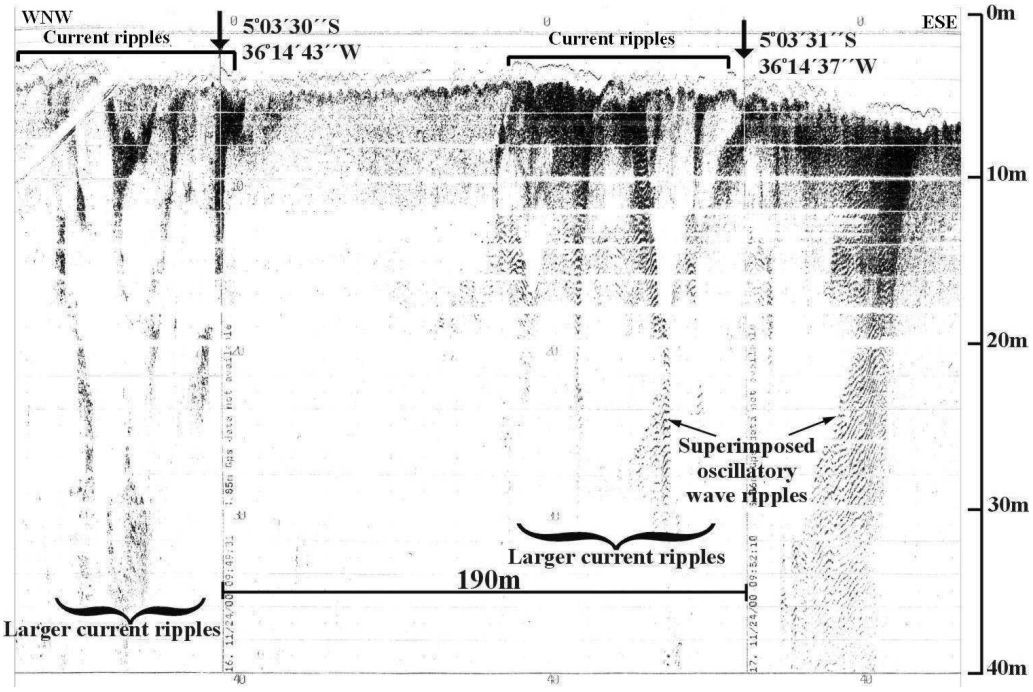

Figure 3.15 - Sonograph showing bedforms present on sand ridge 1 (track "b" in the Figure 3.7).

3.3.3 - Current measurements

The current measurements were performed in November 2000 at three stations located offshore (CTD13, 14 and 15), and at three stations (CTD18, 19 and 26) along the shore between Galinhos and the free end of the spit (Fig. 3.7). Current data from Tabosa (2000) and Riedel (2000) for the coast of São Bento for November 1999 were used as well. The offshore measurements were taken during ebb tide at moderate wind conditions (8-10 m/s). The data obtained along the shore was gained during ebb tide as well as during flood tide. During this ebb phase, strong winds of approximately 10 m/s and rough seas occurred. The flood period was characterized by weak winds of less than 5m/s and small waves.

All current measurements offshore indicate large variations of velocity and direction. These variations are probably due to the oscillation movements of wind-induced waves. Figure 3.16 illustrates the current measurements taken at station CTD15. At this station the upper water column seems to be dominated more by oscillation movements than the water near to the bottom, which is more restricted. The current directions measured at CTD15 show that at the bottom of the water column, a northwesterly direction dominates while the surface currents have northwesterly and southerly directions. The flow orientation from N to S found at the three stations offshore may lead to the assumption that these currents are tidally influenced. The current velocities measured at CTD15 a maximum of 17.5cm/s and a minimum of 4 cm/s.

The currents at station CTD13 are oriented in a NNE direction whereas station CTD14 shows a mean direction of SE. The mean velocities of the two stations vary slightly on the surface between 7 and 9.3 cm/s. Variance in the velocity closer to the bottom is lower and measure between 7 cm/s and 8 cm/s.

The currents measured along the shore during flood phase display rather uniform current directions (CTD 19 and 26). The CTD 19 shows a component to WNW which is probably due to the wind- and wave-induced longshore current. It does not reflect the N-S

tidal-dependent flood phase. At the CTD26 a strong inflow of 25 cm/s from the NE into the channel system is significant. At CTD18 the current directions change between ENE-SSE and seems to adopt a vortex system. Einig (2000) described this current pattern and suggested that the westward flow might be forced to enter into Galinhos cove and the development of an eddy system would cause an easterly current.

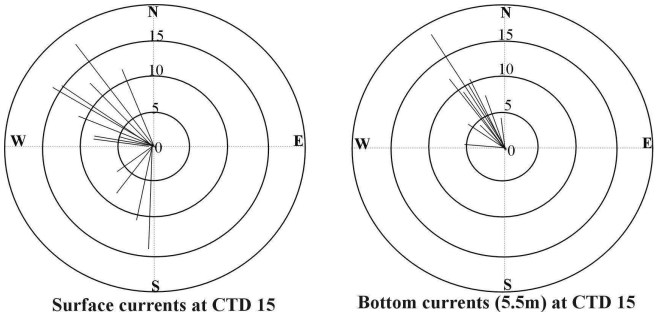

Figure 3.16 - Variations of current velocity and directions at station CTD15. Each circle represents an increase in current velocity of 5cm/s and the average velocity over 30 seconds. It is noteworthy that the bottom currents are more restricted in magnitude and direction.

The currents measured at CTD26 during ebb tide are clearly dominated by the ebb current occurring in the channel system. The northeasterly outflow of about 30 cm/s can also be observed in the Landsat image (See Fig. 3.7). At stations CTD 19 and 18 no dominant current can be detected.

The currents measured by Tabosa (2000) and Riedel (2000) in the coast of São Bento demonstrate a clear tendency towards northwesterly and towards southwesterly directions with a periodical southerly direction. According to Tabosa (2000) and Riedel (2000) 31.5% of all superficial currents converges whereas 34.5% of all bottom currents converge, and this convergence takes place at the coast. These two authors found values up to 40 cm/s for superficial currents and 10 cm/s for bottom currents.

3.4 - Discussions and conclusions

The north coast of Rio Grande do Norte and its related inner shelf shows a large variety of morphological features that demonstrate how this area has been subjected to the combined action of wind, currents, tidal and sea level oscillations. Pre-existing topography probably related to Mesozoic-Cenozoic vertical tectonism (Vital *et al*. 2002a) can also play an important role in the coastal evolution.

The onshore portion has different morphological features. Sandstone-forming active cliffs, possibly compared to those described by Srivastava & Corsino (1984), together with active dunes on the coast form the highest topographical features. Up to now there is no consensus as to how old and as to what the role was of this coastal sandstone in the late Quaternary (?) evolution of the area. Holocene beachrocks (Bezerra *et al*. 1998 and Caldas *et al*. 2001) occur principally in the intertidal zone, although they are also present in other coastal sub-environments like backshore and nearshore zone. The process of formation and geological time of formation of both aeolianite and beachrock of this area is not yet fully understood. Certainly these deposits can be used as a good a sea level indicator (Badyukov 1986, Hopley 1986, Cooper 1991, Kindler & Bain 1993) and in this way they could represent different sea level stillstands during the late Quaternary. The knowledge of ancient tidal flats, the current positions of existing flats combined with historic sea level oscillation, may show

how the area has been subjected to coastal dynamics. Stratigraphic studies of the tidal flats deposits could elucidate this question as well as give data to construct a paleogeographic overview of the area.

From a Landsat image, it can be observed that the inner shelf for this area demonstrates a clear division. In the eastern region of the inner shelf there is more intense sediment movement mostly by subaqueous sand dunes whereas in the western region movement is restricted by elongated sand ridges. The North Brazil Current (NBC) that was first described by Metcalf & Stalcup (1967) seems to play an important role in Holocene sedimentation and flow dynamics of the inner shelf currents (Fig. 3.17). This current originates at 10°S at the NE-coast of Brazil and flows parallel to the eastern coast eventually turning west approximately 5° south and continues to follow the continental margin (Silveira *et al.* 1994). In addition Silveira *et al.* (1994) found that the NBC continues northwards to join the northern branch of the Central South Equatorial Current (CSEC) at approximately 5°S (Fig. 3.17) resulting in a northwestward flow of about 37 Sv (1 Sv = 10^6 m^3 s^{-1}), with a velocity core centred at 100-200m depth. Richardson & Walsh (1986) using ship drift concluded that from the NBC strong shelf-parallel and longshore currents are generated.

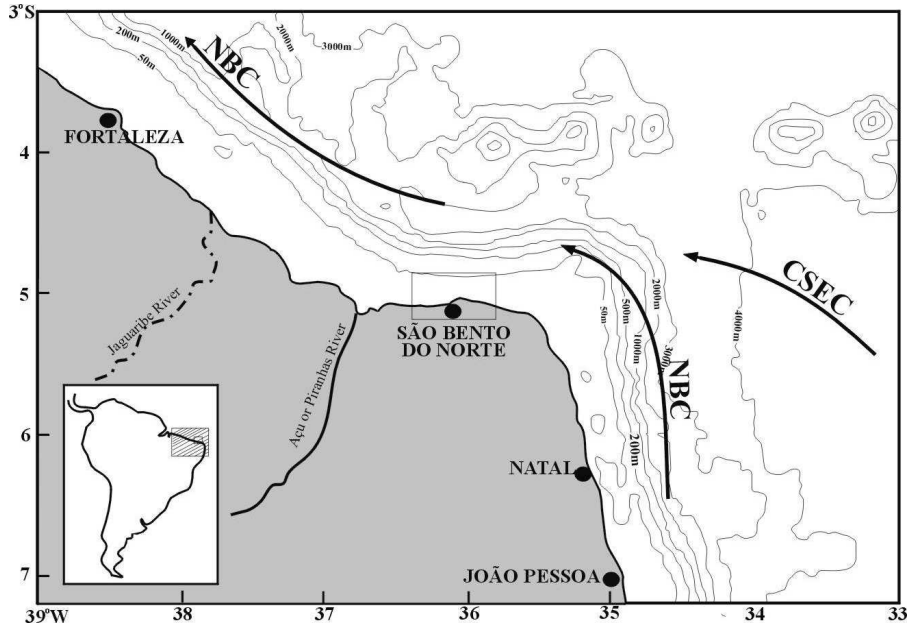

Figure 3.17 - Map with schematic illustration of the surface circulation pattern off NE-Brazil. Abbreviated terms: NBC = North Brazil Current, CSEC = Central South Equatorial Current. Modified from Arz *et al.* (1999), Silveira *et al.* (1994) and Stramma *et al.* (1990).

Comparing the Landsat image (Fig. 3.1) and the schematic illustration (Fig. 3.17), it is possible to conclude that the tongue-shaped subaqueous dune field in the SDZ is a direct result of a branch of the NBC cornering the landmass along the inner shelf (Fig. 3.1). If the sediments on the eastern part would continue to be transported to NW as the dune crests suggest, they would be deposited on the continental slope. It is not the case. A 34km long sand bank limits the SDZ on the north-northwestern part of the inner shelf where the water is deeper. Although there are no current measurements for this area, it is believed that the stronger NBC deflects the inner shelf predominant current (ISPC) trough velocity differences, inducing the build up of the long sand bank. The ISPC may be a branch of the NBC acting on the inner shelf.

Certainly most of the bottom sediments present on the eastern part of the inner shelf has been transported by the NBC and ISPC since the Holocene transgression. These sediments have been most probably transported from S-SE part of the northeastern coast where the main sediment supplies occur (Summerhayes *et al*. 1975; Martins & Coutinho 1981; Testa & Boscence 1998 and Hustedt 2000). It is also believed that older sediments during the last transgression in this part of the shelf were reworked during the flooding of the shelf, which according Arz *et al*. (1999) began at 11000 years ago.

The sand bank curvature to the SW marks the limit between the eastern SDZ, richer in bottom sediments, and the western SRZ and SFZ with less sediment quantity. It is possible that this curvature is being maintained by a southwesterly branch of the NBC (Fig. 3.18). The mechanisms that induce this current deviation are not yet clear. The wind pattern may play an important role. If the dominant wind pattern for this area (Fig. 1.6) is compared with the Landsat image, the curvature of the sand bank follows the landward tendency of the wind.

Generally water depths are less in the eastern region of the inner shelf than those of the western region (Fig. 3.1). Two possible explanations exist: a) the former shelf basement or shelf bottom topography (a result of tectonics?) could drive this difference and/or (b) the sedimentary rate in the eastern area is higher than in the western area. There is a basement horst structure called Touros' high (Bertani *et al*. 1990; Cremonini *et al*. 1996) located between Touros and Galinhos that could produce topographic differences on the shelf surface. These bottom irregularities would facilitate or induce the entry of such currents toward the continent. The surface of the western limit of the Touros' high almost matches the curvature of the sand bank towards the continent.

On the western part of the inner shelf the pattern and geometry of the sand bodies differ to those located on the eastern side. Sand ridges with lengths of up to 20km, width of a few hundred meters, heights reaching 5m and distances between ridges reaching 1.5 km are the main morphological features. Such sand bodies have been found in many modern continental shelves and different theories concerning their genesis have been proposed during the last 30 years (Swift 1975, Figueiredo 1980, Mcbride *et al*. 1991, Snedden & Dalrymple 1999, Snedden & Bergman 1999 and Snedden *et al*. 1999).

The sigmoidal pattern for the sand ridges was also described by Swift (1975) and regards the combination of several current components as being the main factor responsible for the development of such structures. Figueiredo (1980) working on the inner shelf of Rio Grande do Sul (south Brazil) concluded that current velocities greater than $20cms^{-1}$ is sufficient to erode and to transport bottom sediments on the shelf, thus forming sand ridges. The findings of this study show that at least two main bottom currents act to shape the sand ridge 1 (Fig. 3.7). The main geometry of the sand ridge 1 shows that a dominant current probably from the northeast builds the sand bodies, producing a steep flank towards the continent and gentle flank toward sea. This dominant southwestward flowing current may be identified as the NBC (Fig. 3.18) but current measurements offshore show velocities of 6 to 7cm/s from a northeasterly direction.

Side scan sonar results show that the sea floor is covered by sand ridges which been presumably formed by a branch of the NBC. Superimposed on these sand ridges are larger current ripples striking almost perpendicular to the waves ripples and parallel to the main sand body and W to E oriented oscillatory wave ripples (Fig. 3.18b). These larger current ripples could be formed by bottom currents flowing from the east-southeast (Coastal Parallel Current, Fig. 3.18a). Such currents flow with velocities between 15 to 17 cm/s. The wave action only modifies those features found on the sand bodies but, as Swift & Field (1981) suggested, it does not lead to any large-scale changes.

Although such consideration may be considered, the formation of bedforms is certainly not so simple. Oceanic, tidal and wind driven components may act together on the

build up of such structures. Only with the help of systematical and long-term measurements will be such question fully answered.

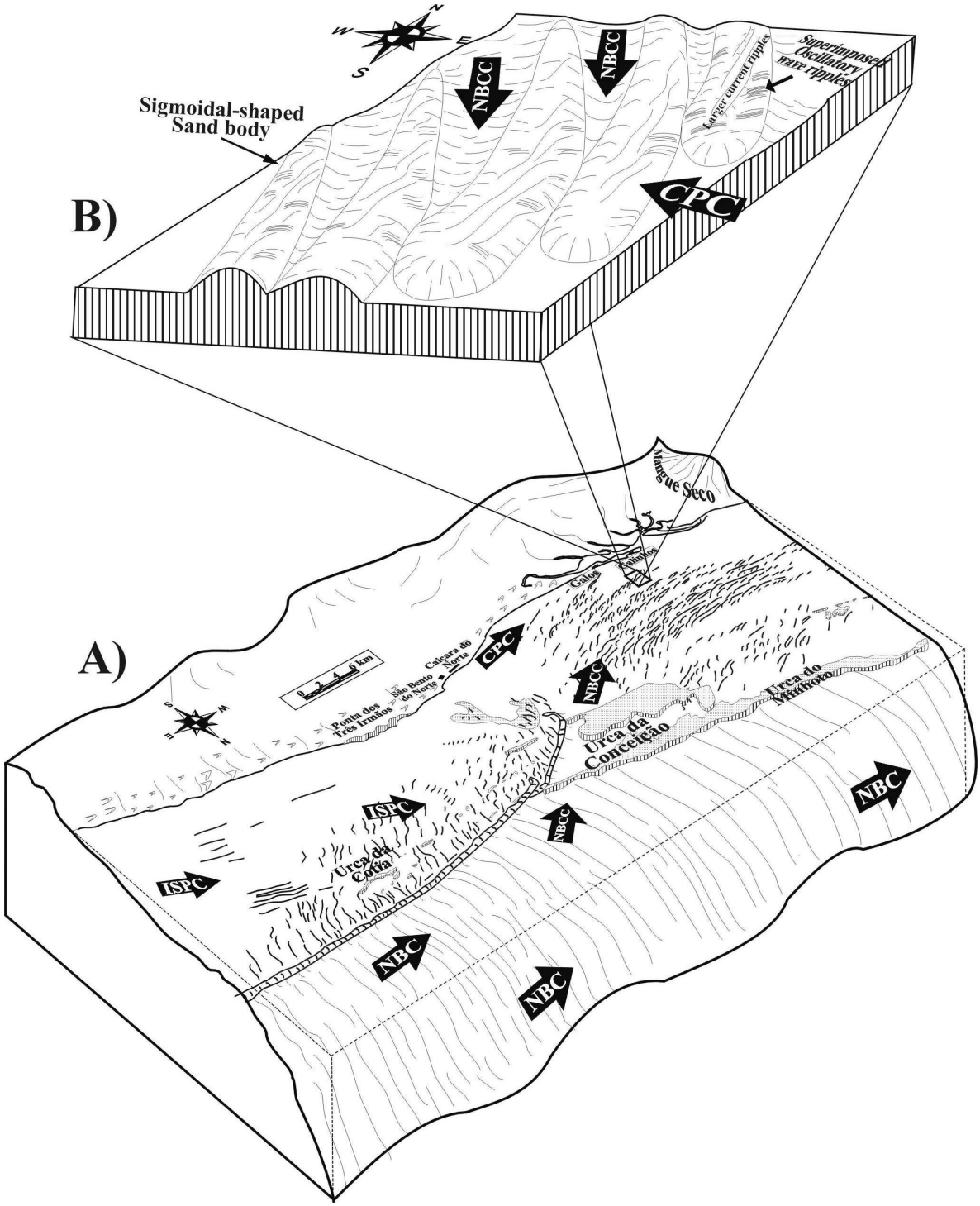

Figure 3.18 - (A) 3D sketch of the northern shelf of the Rio Grande do Norte state and (B) zoom out of the sand ridge 1 composed of smaller sigmoidal-shaped sand bodies The arrows in both sketches indicate probably dominant current pattern acting in this area. Abbreviated terms: ISPC = Inner Shelf Predominant Current, NBC = North Brazil Current, CPC = Coastal Parallel Current, NBCC = North Brazil Component Current. Geographical localities obtained from DHN(1974).

4 - Holocene sediments and stratigraphy

4.1 - Introduction

The Holocene coastal stratigraphy of the study area will be discussed in this chapter. The analysis and interpretation of sedimentologic characteristics of 10 vibro-cores and 5 water-wells (Fig. 4.1) permitted the identification of different facies, which are correlated to the environment of deposition of the sediments.

The lithologic information from the 5 water wells near to Caiçara is based on the driller's technical logs of CAERN (State water Company).

In order to position the cores relative to the present mean sea level, topographic profiles were measured on the coast of Caiçara (Fig. 4.2). The elevation of the cores performed by CAERN and those vibro-cores from Galinhos are related to the surface.

The stratigraphy of beachrocks and their potential as sea level indicators is treated separately in chapter 5.

4.2 - Sediment cores

The vibro-core unit used is a self-constructed portable gear. A gasoline engine with a metal pipe in motion is fixed by a clamp to a 7,5 cm wide and 6 m long aluminum tube. The vibration of the metal is transferred over the bar to the aluminum tube, which is forced into the sediment. Recovery of the core after drilling involves a chain pulley mounted on a tripod.

Each vibro-core was carefully labeled in the field recording the site location, as well the position of the upper and lower extent of the cores. The tubes were transported to University of Rio Grande do Norte (Natal) where further analyses were conducted. All the cores were cut into segments of 33cm and pressed out of the tube. Longitudinal slices from the central part of the core were cut out for radiographic measurements. One half of the core was photographed in daylight and stored, and the other half was used for description and sampling.

Descriptions of the cores were done using a magnifying glass. Grain size, sediment texture, color and composition were first estimated visually by comparison with charts presented in Tucker (1996), Tucker (1988) and Rock-Color Chart of the Rock-Color Chart Committee (1984).

The cores were further sampled in selected points for further standard grain-size analysis (Sieve) and AMS ^{14}C dating.

4.3 - Radiocarbon dating

The radiocarbon ages are listed in Table Nr. 4.1. Four samples of the vibro-core LCSBN-2 and one sample of the vibro-core LCSBN-1 were selected for AMS ^{14}C dating. In the vibro- core LCSBN-1 only one sample composed of wood was dated. In the vibro-core LCSBN-2 two samples of bivalves shells and two of organic rests (leaves and wood remains) were dated. For those vibro-cores near to Galinhos, six samples of organic remnants were chosen for dating.

Shells and wood radiocarbon ages cannot be directly compared because shell samples generally require an "environmental correction" for ocean reservoir effect (Woodroffe & Grime 1999). A correction of approximately -400 years is generally applicable because the marine carbonate is +400 years too old. However the shell isotopic signatures do not show typical marine values (Table Nr. 4.1) therefore an ocean reservoir correction would not make sense. The $\delta^{13}C$ obtained for these shells show a tendency to negative values (Table Nr. 4.1), which according Mook & Van de Plassche (1986), suggests the presence of freshwater

(lagoon) in the environment where the shells lived. Shell from typically marine origin presents $\delta^{13}C$ values close to 0‰ σ positive. All radiocarbon ages presented here were first corrected for isotopic fractionation based on the $^{13}C/^{12}C$ ratio measured by AMS-system simultaneously with the $^{14}C/^{12}C$ ratio. The ages were then calibrated using Dataset 2, and combination of dataset 1 and 3 of CALIB rev4.3 (Stuiver *et al*. 1998) (for more detail see section 5.4 of the Chapter 5).

It is also important to keep in mind that the radiocarbon ages from the shells represent the time of death of the organism and not the time of its deposition. Thus individual shells as well as organic rests may have been reworked several times before being deposited in coastal deposits. Therefore such dates sometimes may not agree with their position in a vertical sequence.

Table 4.1 - AMS radiocarbon data of the vibro-cores samples

Laboratory Number*	Sampling sites	Material (%MC)	$\delta^{13}C$ AMS (‰)	Age (^{14}C yr BP)	1σ [yr] # +/-	Calibrated age† [Cal yr BP]	1σ ranges‡ [Cal yr BP]
KIA14743	LCSBN-2	Shell (68%)	-3.08±0.15	3575	30	3580	3630-3550
KIA13957	LCSBN-2	Leaves	-26.33±0.2	6125	40	6990	7150-6910
KIA13958	LCSBN-2	Wood remains	-27.19±0.13	6035	35	6880; 6880; 6870 6820; 6810	6910-6800
KIA16093	LCSBN-2	Shell (68%)	-3.09±0.41	6355	45	6950	7000-6890
KIA13956	LCSBN-1	Wood	-25.91±0.14	6522	44	7430	7480-7330
KIA13950	VCGAL-1	Wood remains	-24.30±0.11	2554	31	2740	2750-2510
KIA13951	VCGAL-2	Wood remains	-27.83±0.10	2513	32	2710; 2630; 2620	2730-2500
KIA13952	VCGAL-2	Charcoal	-27.77±0.13	2707	27	2780	2850-2770
KIA13953	VCGAL-3	Wood remains	-28.98±0.11	4070	31	4570; 4560; 4530	4780-4450
KIA13954	VCGAL-3	Wood remains	-24.08±0.12	2176	26	2150	2300-2120
KIA13955	VCGAL-7	Wood remains	-25.87±0.09	1323	25	1270	1290-1240

*Leibniz Laboratory – Kiel, Germany
%MC =Percentage of Marine Carbon
Probability of conventional age
‡1σ enclosing 68,3% of area of probability distribution
† Calibrated applying CALIB rev4.3 (Dataset 2 and combination of datasets 1 and 3): Stuiver *et al*., Radiocarbon 40:1041-1983, 1998

4.4 - Description of the cores and their facies association

The cores and water-wells located near to São Bento/Caiçara were grouped in one set and those located close to Galinhos in another one (Fig. 4.1), as the large horizontal distance between them do not allow a good correlation of all cores and water-wells. The vibro-core VCLC-1 was not used for the same reasons.

4.4.1 - São Bento area

The analysis of the aerial photograph of the area of São Bento and Caiçara (Figs. 4.1 and 4.2) shows that in this area three main types of deposits can be individualized: dune

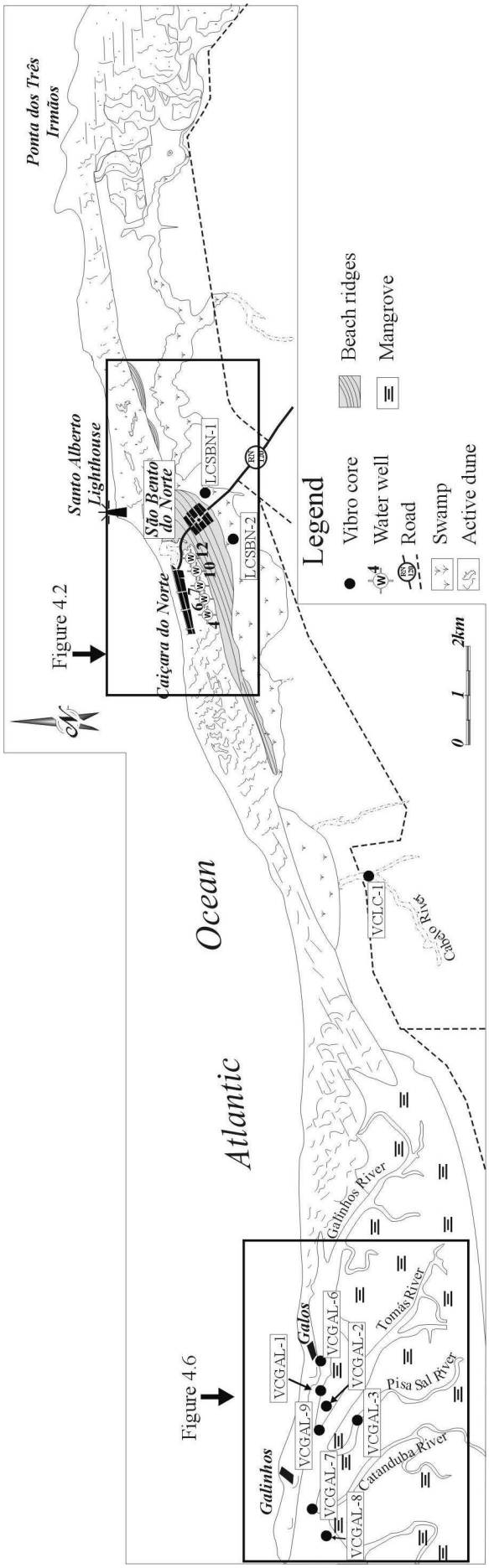

Figure 4.1 - The coast between Ponta dos Três Irmãos e Galinhos with the location of the vibro-cores and water-wells.

deposits, beach ridges and paleo-tidal flat. The vibro-core and water-wells data should allow a better understanding of the vertical relationship between these deposits. Therefore two vibro-cores (LCSBN-1 and LCSBN-2) were taken in the swamp area adjacent to the beach ridge deposit (Fig. 4.1 and 4.2a) and an integrated description with the water-well logs was done.

The topographic profile (Fig. 4.2b) shows the flat area of the tidal flat, gentle seaward slope of the beach ridges and the highest points marked by active dunes.

It is interesting to comment that the topographic profile was obtained in November 2000 and it fits well with the aerial photograph from 1950. Only between points "C" and "D" in Figure 4.2a can some modifications be observed. These differences may due to the dune migration from northeast that in 1950 had not yet reached this area (gray color between "C" and "D" aerial photograph).

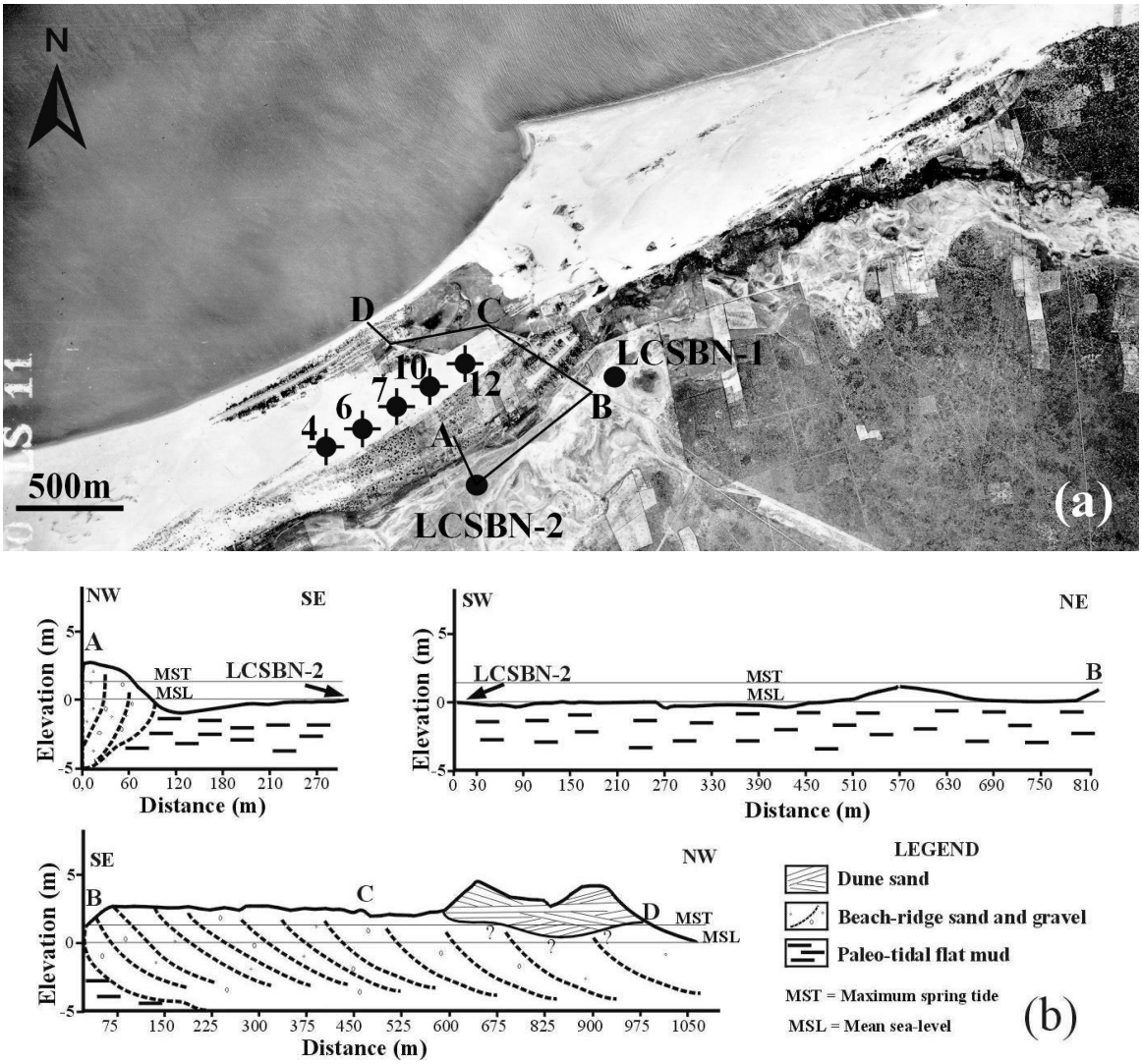

Figure 4.2 – (a) Aerial photograph from 1950 showing the vibro-core sites (black dots) and water -wells (semi-crossed dots). (b) Topographic profiles with sedimentary environment.

4.4.1.1 - Water-wells

The lithologic interpretation of the water-well cores (Fig. 4.3) suggests that the upper part of the sediments is composed mainly of aeolian sediments. The sediment is composed of medium to very fine white sand and although no information about the sedimentary structure

is available, it can be assumed that this upper part of the cores represents dune sand because these cores were taken on the dune.

Cores 4, 6 and 7 show gravel with very coarse sand and shell fragments underlying the upper dune sand unit. This gravel-sand layer can be interpreted as a beach deposit of the sand ridges seen in Figure 4.1 and 4.2b. Basal mud sediments occur directly beneath the upper dune sand deposit in cores 10 and 12. Underlying all upper units, this deposit is consisting of grayish mud sediment identified as paleolagoonal (tidal flat).

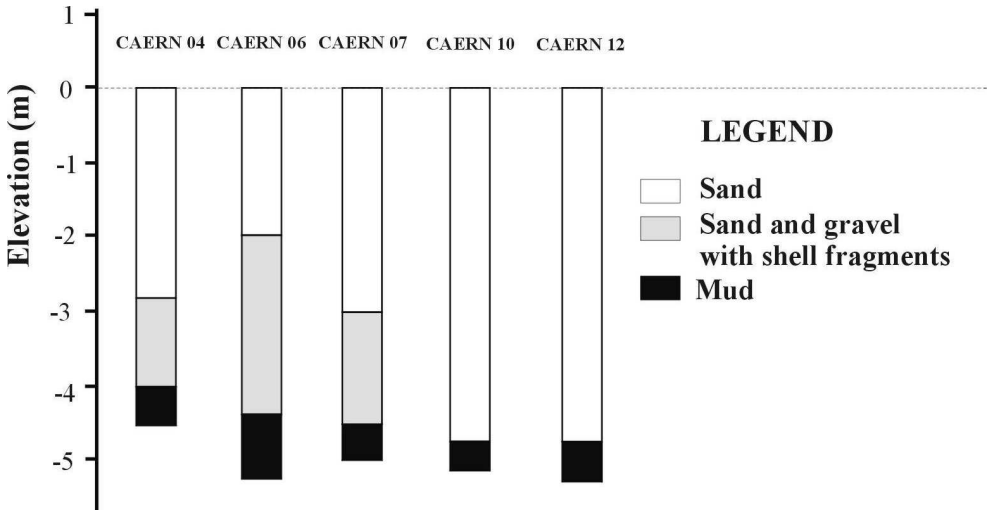

Figure 4.3 - Interpretation of the water-well cores.

4.4.1.2 - Vibro-cores

Figure 4.4 shows the grain size variation and sedimentary structures observed in vibro-cores taken in the paleo-tidal flat, which surface corresponds approximately to the present mean sea level (Fig 4.2b). The sediments are mainly mud with some sand at the bottom of the cores. The sedimentary structures vary from plane-parallel laminations at the top to subhorizontal sets of plane-parallel lamination at the base. A higher amount of organic matter (roots and leaves) was found in the mud sections. Crystals of halite and gypsum were found mainly at the top of the cores but also at the base in the core LCSBN-2.

The detailed description of the sedimentary structures, texture, composition and distance from the shoreline allows for two main facies to be distinguished.

1) *Tidal flat deposits* (Facies A): Deposition in the intertidal flat is dominated by vertical accretion. In the cores, this deposit is composed of greenish-black (5G2/1) mud with organic layers, halite and gypsum crystals, root and shell fragments and leaves (probably from mangrove trees). Some shells in living position (Fig. 4.5) form banks on the paleo-tidal surface. The *facies* A is more extensive in vibro-core LCSBN-2, where it attains 2.9m in thickness. In the vibro-core LCSBN-1 the *facies* A has a 0.7m thickness and downwards it occurs as intercalations with sands that composes the *facies* B. The basal contact with sediments of *facies* B is abrupt and defined by an increase of grain size and change in color from greenish-black to medium gray (N5).

2) *Washover deposits* (Facies B): Washover deposits are built up through overwashing of the sand barrier. In the cores, it comprises of moderately sorted medium to coarse gray sand. The sedimentary structure is a plane parallel lamination dipping at 5^{o} to 7^{o} towards the continent (150^{o} to 180^{o} Az). In the vibro-core LCSBN-1 its maximum thickness reaches 0.8m at the base while in the vibro-core LCSBN-2 it reaches 0.17m at the base.

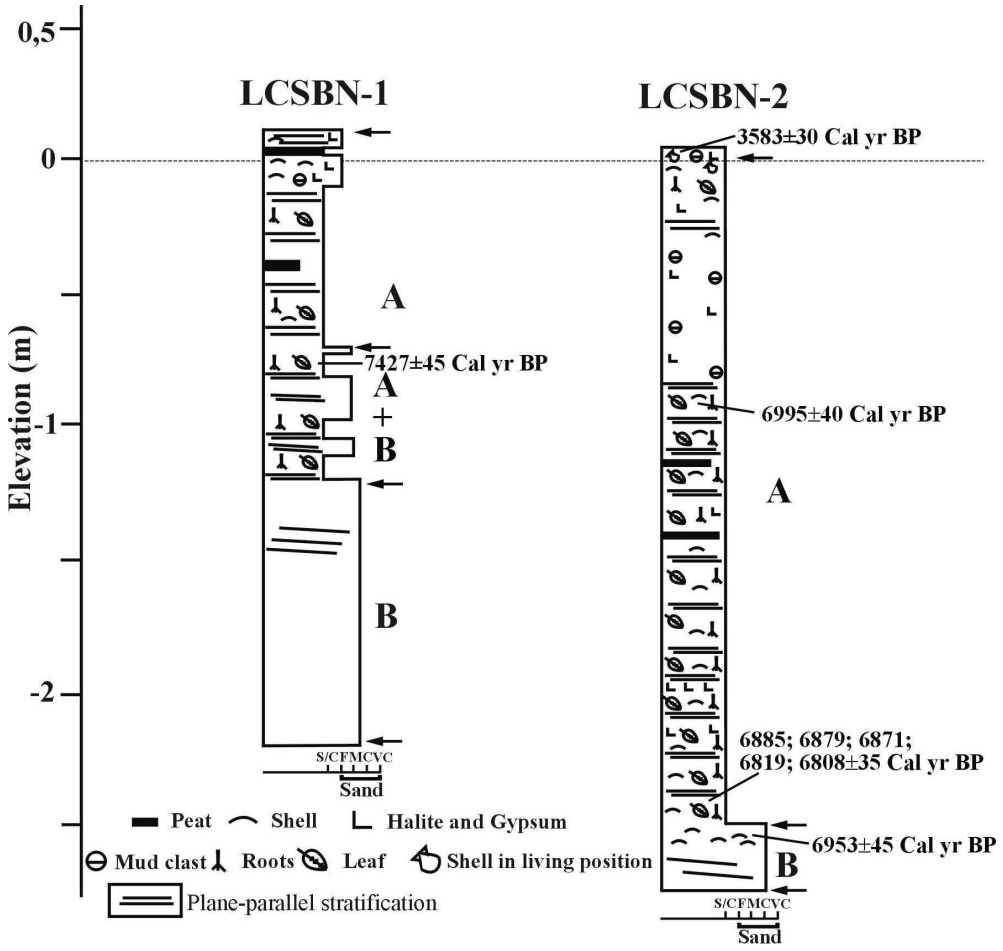

Figure 4.4 - Sedimentary facies (represented by letters between arrows found on the right hand side of the column), grain size variation, sedimentary structures and AMS radiocarbon ages for the vibro-cores taken in the paleo-tidal flat close to São Bento and Caiçara (see location in Fig. 4.1 and 4.2a). Facies: A = Tidal flat and B = Washover. Zero elevation corresponds to the current mean sea level.

Figure 4.5 - Bivalve shell in living position on the paleo-tidal flat close to the vibro-core LCSBN-2.

4.4.2 - Galinhos area

The upper sediments of the tidal flat and channel systems located southward of the sandy spit of Galinhos and Galos were partially investigated by seven vibro-cores (Fig. 4.1 and 4.6). The cores were taken during low tide in November/December 2000. From the aerial photograph (Fig. 4.6) it can be seen that the tidal channel system and its associated tidal flat with mangrove trees is protected from open sea. The picture shows that longshore currents from the east have built the Galinhos' spit and the build up of sediments in the channel system is controlled mostly by point bar accumulations. There are no geomorphological evidences that the channel system and its surrounds had been subjected to open sea action.

Figure 4.7 shows the vibro-cores with their sedimentary characteristics, facies associations and radiocarbon ages. The sediments are mainly composed of mud interbedded with fine sand both showing parallel lamination as the principal sedimentary structure. The sedimentary structures vary from plane-parallel laminations in the finest sediments to cross bedding in the coarsest. Organic matter (rest of wood, leaves and peat) as well as mud clasts and shells in living position occur mainly in the fine sections. Three main facies could be individualized from core description and sedimentary analysis: tidal flat deposits, tidal channel point bar deposit and tidal channel deposit.

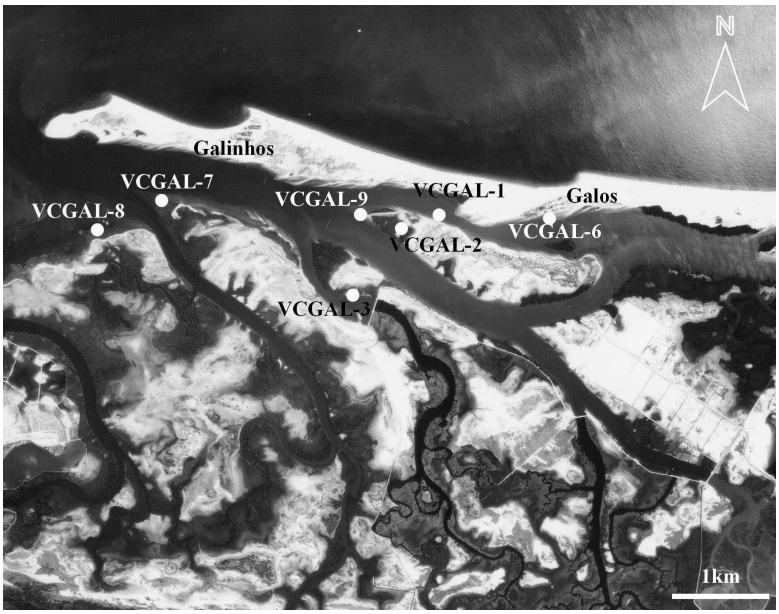

Figure 4.6 - Aerial photograph of 1988 showing the vibro-core sites (white dots) in the tidal flat and channel system between Galinhos and Galos.

4.4.2.1 - Vibro-cores

1) *Tidal flat deposits* (Facies A): this facies is dominantly composed of dark greenish gray (5GY 6/1) mud with olive black (5Y 2/1) organic layers. Greenish gray (5GY 6/1) very fine sand occurs as intercalations in the mud. In this facies some shells in living position as well as mud clasts and shell fragments were found (vibro-core 3). Only in vibro-core VCGAL-6 that contains massive channel deposit facies A is missing.

2) *Tidal channel point bar deposits* (Facies D): Tidal channel point bars produce lateral accretion deposits accompanying migration of the channel toward the outer bank. In the vibro-cores from Galinhos and Galos the facies D is represented as laminated mud and sand distinguished by a subtle contrast in grain size. The base of this unit is usually composed

of greenish gray (5GY 6/1) medium to coarse sand that changes gradually to dark greenish gray (5GY 4/1) or olive black (5Y 2/1) mud. It is also observed that the mud-clasts occur within sand and mud beds. Cross bedding is common in the coarsest units.

3) *Tidal channel deposits* (Facies E): This unit is restricted to vibro-core VCGAL-6. It is composed of poorly sorted, medium to coarse sand showing a slight tendency to fining upwards. The color varies from yellowish-gray (5Y 7/2) to moderate yellow (5Y 7/6). Cross bedding dipping between 15^{o} to 30^{o} is marked by bioclasts. Mud clasts are observed in the finest unit.

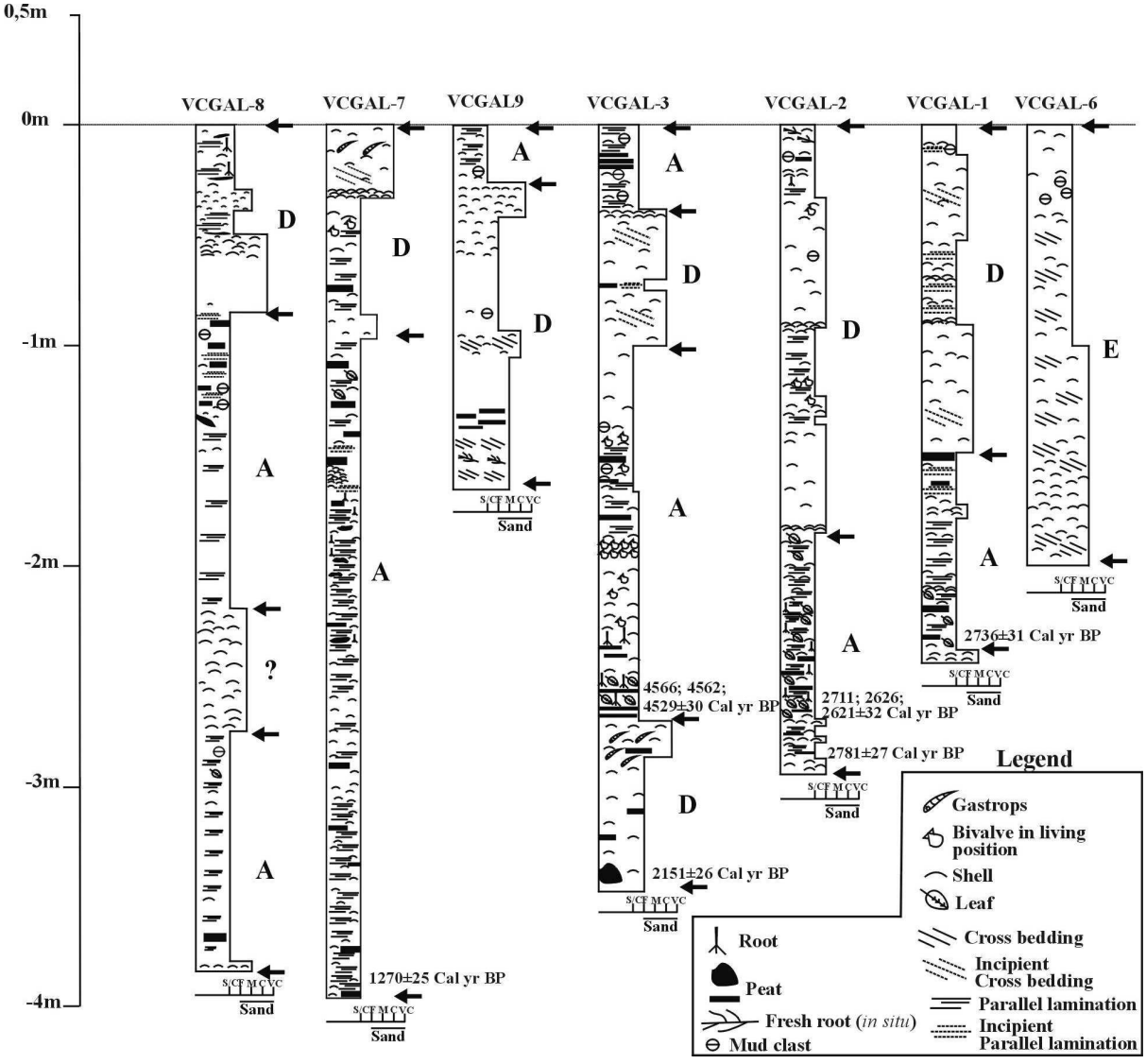

Figure 4.7 - Sedimentary facies (represented by letters between arrows found on the right hand side of the column), grain size variation, sedimentary structures and AMS radiocarbon ages for the vibro-cores taken in the channel system and tidal flat close to Galinhos and Galos (see location in Fig. 4.1 and 4.6). Facies: A = Tidal flat; D = Tidal channel point-bar; E = Tidal channel.

4.5 - The sediments and their ages

4.5.1 - São Bento area

The radiocarbon ages obtained for paleo-tidal flat sediments of São Bento and Caiçara are Holocene. The oldest age was found in the middle part of vibro-core LCSBN-1 reaching 7430±44 Cal yr BP whereas the youngest reaches 3580±30 Cal yr BP in the top of the vibro-core LCSBN-2 (Fig. 4.4). In the latter vibro-core an age of 6950±45 Cal yr BP at 2.7m depth was determined for a bivalve shell in good state of conservation (the bivalve shell was intact showing original color and no signal of recrystallization) which suggests that this bivalve probably died and its shell was deposited shortly afterwards together with the base sediment. The calibration of the sample (possibly wood remain) located in the mud sequence at 2.4m (3 cm over the age obtained at the base sand) provided five ages. The oldest is 6880±35 Cal yr BP while the youngest is 6810±35 Cal yr BP. If these ages are compared with those positioned higher up, an accumulation rate of 3 cm during 68 years at least should be proposed (if 1σ error is not taken into account).

The age of leaves in the middle of the core LCSBN-2 (-0.9m) reaches 6990±40 Cal yr BP, at least 110 years older than that positioned at -2.4m, indicating that they are not *in situ*. Although this age does not represent the sediment age at the time of its deposition, it may be assumed that a typical lagoonal environment existed in this period because the obtained age probably belong to plants, more specifically mangrove leaves, of the former lagoon. On the top of the tidal flat sequence a bivalve shell in living position (Fig. 4.5) gives an age of 3580±30 Cal yr BP indicating a lagoonal environment at this age. It is interesting to observe that the organic matter in the vibro-core LCSBN-2 disappears exactly at –0.9m and appears again at –0.3m to continue to the top. This could suggest pulses of lagoonal influence with limited connection to the open sea. The sediments are rich in evaporitic minerals (halite and gypsum) from -0.9m to the top confirming the regime of a semi-closed lagoon. The last marine ingression occurred approximately 3580±30 Cal yr BP when the last typical lagoonal environment existed.

In the core LCSBN-1 only one sample of wood was dated. It was positioned at -0.7m and gives an age of 7430±44 Cal yr BP. This age is the oldest found in the paleo-tidal flat of São Bento and Caiçara and confirms the presence of a lagoonal environment during this time.

Identical ages were found by Silva (1991) in the transgressive basal sequence of the Açu River Delta (~100 km westward). It may be supposed that the sedimentation on the former tidal-flat of São Bento and Caiçara was intense during the Holocene transgression, which according Suguio *et al*. (1985) reached the east Brazilian coast shortly before 7000yr BP. Although there are no ages for the beach ridges parallel to the present coastline, those located seaward represent certainly regressive sequences that has been deposited concomitant with the sea level drop after its maximum at 5200 yr BP (Suguio *et al*. 1985).

4.5.2 - Galinhos area

In general, all ages found for Galinhos' area were younger than those from São Bento and Caiçara. Although all ages were obtained from organic samples that naturally are less resistant to reworking and redeposition, it seems that all ages are reliable with an exception of one sample that was probably reworked and afterwards redeposited. The age of the peat material at the base of the vibro-coreVCGAL-3 was 2150±26 Cal yr BP (Fig. 4.7). The next organic sample further up, with a position of –2.7m, has calibrated ages of 4570±31 Cal yr BP, 4560±31 Cal yr BP and 4530±31 Cal yr BP. One of the two samples must have been reworked and redeposited. To know which of the determined ages is reliable, a third dated sample must be used for comparison. As this is not available, these ages can be compared

with those of the other neighbor vibro-cores. From Figure 4.7, it can be seen that almost all samples located at the base of the cores, present average ages situated between 2100 to 2800 Cal yr BP, with the exception of the sample located at the base of the vibro-core VCGAL-7 that has an age of 1270±25 Cal yr BP. Therefore it can be concluded that the calibrated ages positioned at –2.7m represent reworked organic material probably from deeper sections.

The younger ages found in the upper 4m and the higher sedimentation rate in the lagoon of Galinhos when compared with São Bento show that the Galinhos' lagoonal system has been active since the last sea level highstand.

4.6 - Discussions and conclusions

4.6.1 - São Bento and Caiçara area

Figure 4.8 shows a cross-section normal to the shoreline along the paleo-tidal flat and beach ridges near São Bento and Caiçara. The cross-section was constructed from vibro-cores, water-wells and topographical data. It can be seen that a Holocene transgressive sequence was deposited probably during the maximum of the last Holocene transgression. The presence of typical transgressive deposits (marine sand – washover deposits) intercalated with lagoonal mud suggests such a transgression, although radiocarbon ages are not available. The regressive sequence is clearly represented by the sand ridges, which started deposition shortly after the maximum Holocene sea level highstand and continued deposition until present day. According to the topographic profile (Fig. 4.2b) the Holocene sea level highstand that is represented by the uppermost part of the proposed transgressive sequence should have not been higher than approximately 2.8m above present mean sea level (PMSL) or 1.3m above the present maximum spring tide. In fact, the paleo-tidal flat surface lies almost at the same altitude as the PMSL (Fig. 4.8) and the top of the proposed transgressive sequence does not reach more than 3m above PMSL. The fact that such coastal evolution has taken place in a region without large active river mouths has attracted attention. This type of coastal evolution has been described for other areas on the Brazilian coast where big rivers occur and the sediment availability is enormous (Dominguez *et al*. 1987, Dominguez *et al*. 1992, Martin *et al*. 1993 and Lessa *et al*. 2000). These authors have demonstrated that the main source of sediment for the progradation was provided by wave-induced longshore drift of sediments and the river-borne sediments only play a secondary role during progradation of the coastline. The data presented here agree with those from the above authors. The São Bento and Caiçara coast regressive barrier is located in a semi-arid region associated only with small intermittent rivers. The source of the sediment that builds up the regressive sequence is the inner shelf upon which terrigenous sand occurs in large quantities (see Chapter 3).

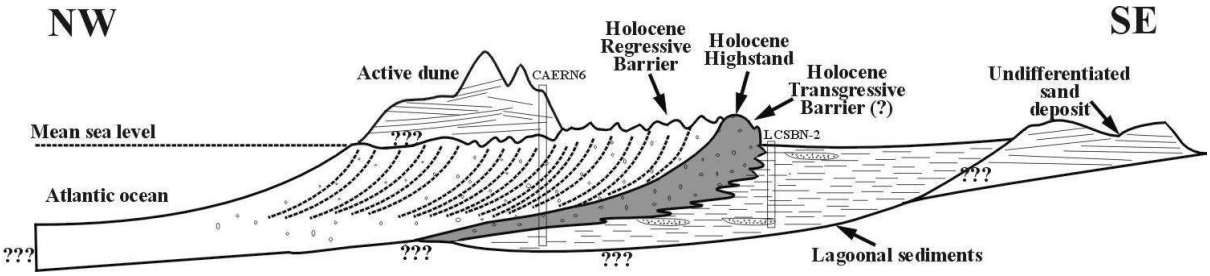

Figure 4.8 - Stratigraphic cross-section normal to the São Bento and Caiçara coastal plan.

It is interesting to note that Dominguez *et al*. (1992) suggested that following the Holocene sea level drop usually the lagoons became emergent and the beach-ridge plains prograded creating a regressive sand sheet. In the case of this study, the sea level drop did not

promote the emergence of the lagoon. It was or is a consequence of both longshore drift of nearshore sediments and dune migration parallel to the beach that obstructed the connection between the sea and the lagoon (see Fig 4.2). Morais (1998) cited a good example of such dune migration, when a dune advancing from the northeast buried Caiçara in 1912. The paleo-tidal surface lies at the same level as the PMSL and it is protected by the marine ingression mainly by such actual active dunes. The occurrence of evaporate minerals in different levels in the vibro-cores demonstrates that such obstruction was cyclic producing environment of semi-closed lagoon. The last marine ingression occurred at 3580±30 Cal yr BP and subsequently the lagoon has become inactive.

4.6.2 - Galinhos area

The evolution of the lagoonal system of Galinhos seems to be quite different to the São Bento and Caiçara area. The ages determined in the Galinhos' vibro-cores show that the sediments are much more younger than those from São Bento at approximately same elevation relative to sea level. The sedimentation rate was also higher in the lagoon of Galinhos than in São Bento. The vibro-core data show a typical sedimentation in an active lagoonal system where lateral and vertical accretion are controlled mainly by tide and tidal channels, respectively. In fact, the facies associations described for the upper 4m of sediment confirms the induced tide and channel sedimentation.

The lagoonal system of Galinhos has been active since the last Holocene highstand. The large sand spit that protects the lagoon system from the sea seems to play an important role in the lagoonal evolution. In the aerial photograph (Fig. 4.6) no geomorphological feature can be identified in the lagoon that indicates an open marine influence. Although such features could be obliterated by lagoonal evolution itself, normally some relict deposits of marine ingression should be visible. This lack of open marine conditions support the hypothesis that the Galinhos' spit was earlier a barrier-island system protecting the backbarrier area towards the shoreline. The landward transgression of such a barrier-island may be controlled by geological parameters such as substrate slope, nearshore sediment budget and accommodation space as may have been the case with the Galinhos' spit. The absence of geomorphological features indicating an earlier open marine ingression in the lagoonal system and the absence of regressive deposits may explain the current position of the Galinhos' spit, which is assumed to have remained at the position it had during the last Holocene highstand. As will be demonstrated in the following chapters, boomer profiles parallel to the Galinhos spit will demonstrate that at least three tidal inlets through this spit once connected the open sea to the lagoon. Although no absolute ages are available for this evolutionary stage, it can be assumed that it took place concomitant to the Holocene sea level transgression. During the subsequent sea level drop, sediments drifting via the local longshore currents closed such inlets and the actual spit took shape.

5 - Holocene sea level changes: Evidences from beachrocks and Paleo-lagoons

5.1 - Introduction

The study of sea level is enormously improved when accurate paleo sea level indicators are available. To date many coastal deposits and marine organisms are directly or indirectly used to infer former sea levels. Amongst some existing sea level indicators formed by coastal deposits one of the most reliable is beachrock. Although some authors believe that beachrocks are more reliable sea level indicators in microtidal coasts (e.g. Hopley 1986, Cooper 1991, Kindler & Bain 1993, Ramsay 1995, Omoto 2001 and Ramsay & Cooper 2002), their use in sea level studies in mesotidal coasts should not be underrated. A careful sedimentological description of beachrocks in mesotidal coasts and further comparison with modern beaches has permitted the vertical positioning of sea levels (see Bigarella 1975, Oliveira *et al*. 1990, Bezerra *et al*. 1998). Furthermore, the recognition and description of the diagenetic products found in beachrocks can be useful to determine the sea level history of a coastal area (Longman 1980, Coudray & Montaggioni 1986, Vollbrecht & Meischner 1993) and together with radiocarbon dating and chemical analyses provide enough elements and data to position former sea levels in time and space in a coastal area.

In the area of study beachrock is one the most important coastal deposits occurring mainly in the intertidal zone along the entire coast. The description of sedimentary structures, recognition of diagenetic products, chemical analyses and radiocarbon dating of the beachrocks and other coastal deposits allow some considerations to be made about sea level changes for this area during Holocene time.

5.2 - The Brazilian coast and Holocene sea level changes

The sea level studies in Brazil started in the 60's when Van Andel & Laborel (1964) and Delibrias & Laborel (1969) published the first attempts to establish the regional Holocene sea level changes based on radiocarbon datings of paleo sea level indicators. According to Delibrias & Laborel (1969) the sea level reached its present position 6000 years BP and then started to rise reaching to 3m above the present mean sea level at 4500 years BP. From this time the level fell gradually to its present level. Fairbridge (1976) by the use of shell middens from the south and southeastern coasts, proposed a similar sea level variation to Delibras & Laborel (1969), although he recognized five periods of transgression with amplitudes varying between 1 and 5m. The following sea level studies have been undertaken in more restricted areas and some Holocene sea level curves have been proposed for different sites along the Brazilian coast (Fig. 5.1). Suguio *et al*. (1985) were the first to propose systematical, well-constructed Holocene sea level curves for the Brazilian coast. The Salvador Curve (Fig. 5.1a) is their best example. The Salvador Curve (Fig. 5.1a) shows that the sea level starts the transgressive phase above the present sea level shortly before 7000 years BP and reached 5m above present approximately 5100 years BP. Furthermore two intervals of negative oscillation at 4000 and 2700 years BP were proposed.

After the work from Suguio *et al*. (1985) the discussion involving Holocene sea level changes has mainly been focused on whether or not of secondary Holocene sea level oscillation occurred (see Angulo *et al*. 1999 and Angulo & Lessa 1997) as proposed by Suguio et al. (1985). Figure 5.1b shows the sea level curve proposed by Angulo & Lessa (1997) for the Brazilian Coast. It was based on 93 dated vermetid samples (incrusting aragonitic gastropod) and according to Angulo & Lessa (1997) no secondary oscillation was detected after the Holocene highstand. These findings agree with the Holocene sea level

trends for other coastal regions of the southern hemisphere, where a smooth decline of the sea level may be observed since the Holocene highstand (Isla 1989 and Pirazzoli 1991).

For the work area and surrounds there exists no constructed Holocene sea level curve from paleo sea level indicators and only some diagrams gained from glacio-hydro-isostatic models have been published. Peltier (1988) used a numerical model associated with some sea level data and three different melting chronologies to predict emerged beaches on continental shorelines. Figure 5.1d shows the sea level curves for Recife area (~370 km southeast from the work area) obtained from: (a) melting chronology of the ICE-2; (b) a 5000 year delay of the Antarctic component of melting and (c) 7000 year delay of the Antarctic component of melting. According to Peltier's model three Holocene sea level maxima occurred at 6800 years BP with 3m and 1.6m, at 5500 years BP with less than 0.5m above the mean present sea level. Bezerra *et al*. 1998 cite a curve for the Touros site based on and constructed from Peltier's model (Fig. 5.1c). The Touros coast is located some 100km east of this study work area. The proposed curve predicts a Holocene highstand reaching 2.3m above the current mean sea level 5100 cal yr BP. No secondary sea-level-oscillations were proposed.

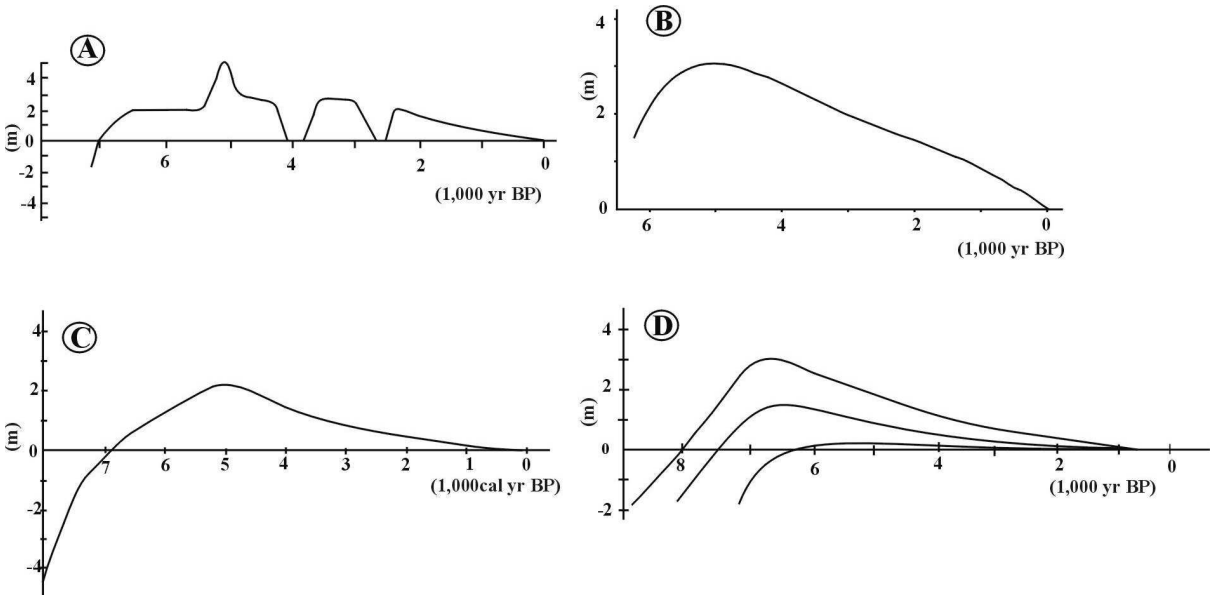

Figure 5.1 – Sea level curves proposed for the Brazilian coast: (A) Suguio *et al*. 1985; (B) Angulo & Lessa 1997; (C) Peltier 1997 (Cited in Bezerra *et al*. 1998); (D) Peltier 1988.

5.3 - The beachrocks

Beachrock is carbonate-cemented beach sediment dipping seaward, found and formed mainly in the intertidal zone of tropical beaches although it does occur in the sublittoral zone and subtropical coasts. In the study area the beachrocks (Fig. 5.2) exhibit a great range of dimensions and shapes. The beachrocks here are denominated informally according to their geographic locality and using further denomination from Bezerra *et al*. (1998). The São Bento Beachrock is the longest, stretching 2.3km along the beach, while the Cabelo Beachrock is the shortest with a length of 0.3km (Fig. 5.2). The beachrock bodies range in thickness from 0.4m to 2m and in width from 3 to 17m and occur mainly parallel to the present shoreline with exception of Recuado Beachrock (Fig. 5.2). The beachrock bodies are subhorizontally oriented dipping gently seaward (<8^{o}). Their surfaces are irregular and often organic encrusting of algae and marine organisms is present. All Holocene beachrocks from the study

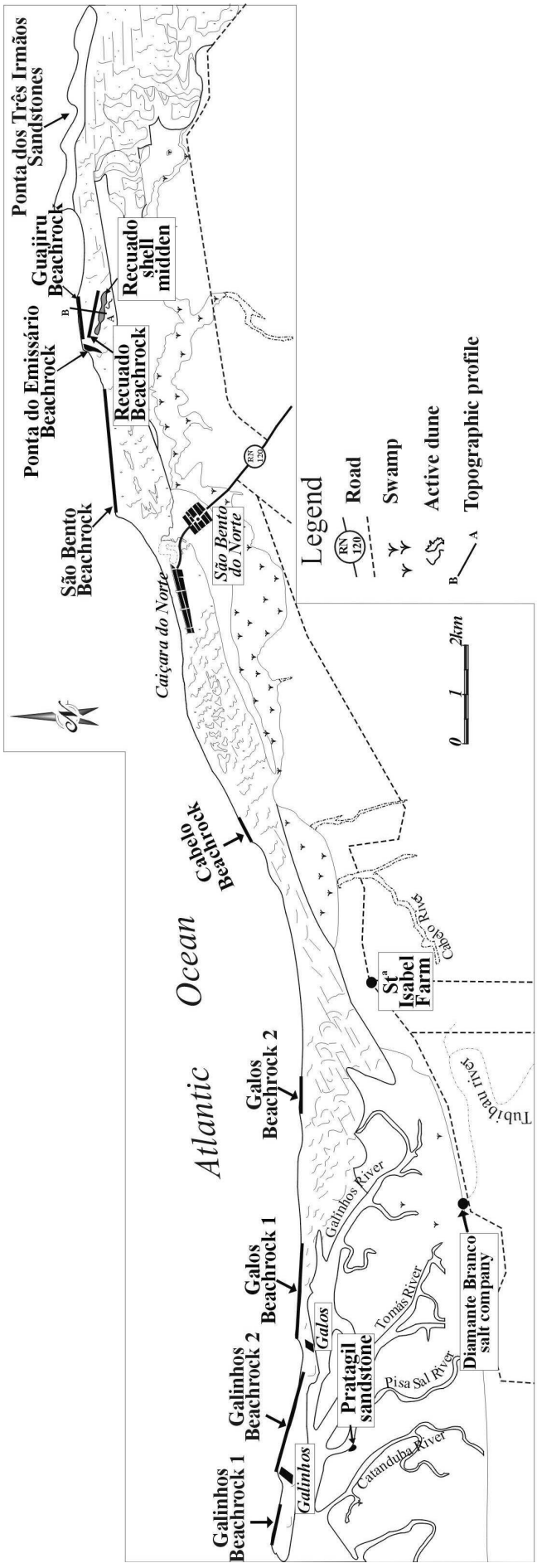

Figure 5.2 - Beachrock location in the study area.

area are positioned in the intertidal zone with the exception of Recuado Beachrock that lies entirely in the backshore zone east of São Bento and Caiçara (Fig. 5.2).

The beachrocks have a gray color and the grain sizes vary from very fine sand to pebbles forming poorly sorted sediment. The grain morphology varies from subangular to subrounded with grain contacts being mostly punctual. The beachrocks are composed basically of terrigenous components with quartz being the main constituent (20-45%) followed by feldspar, limonite and quartzite as rock fragments. Zircon, opaques and tourmaline occur as trace minerals. The bioclastic constituents can reach up to 30% and are mainly red algae and bivalves. It is also observed that gastropod, coral, foraminifer (*Miliolid, Textulariid and Nummulite*), echinoderm spins, bryozoans and green algae (*Halimeda*) are present. It is interesting to observe that the beachrock compositions are almost always analogous to the modern sand of the adjacent beaches.

Following the strategy of Bezerra *et al*. (1998) the sedimentary structures present in the beachrocks were compared with modern beaches to identify their paleogeography. Moreover elevation measurements of the beachrocks were carried out in order to position them in relation to the present mean sea level (MSL) and maximum spring tide sea level (MSSL). All horizontal positions were gained by the global positioning system (GPS), and corrected by using tide-tables, supplied by the Brazilian Navy, of the local standard ports, Natal and Macau. These procedures are recommended by Admiralty (1996). The zero level used was the Brazilian "Corrego Alegre" National Datum.

The Figure 5.3 was based on field observations (Fig. 5.4) and it shows a typical beach profile mainly characterized by swash-cross-stratification in the foreshore zone and trough-cross-stratification in the shoreface zone. Observed in Figure 5.4 is that the foreshore deposits dip seaward (right side of the photo) while the washover deposits dip gently landward (left side of the photo).

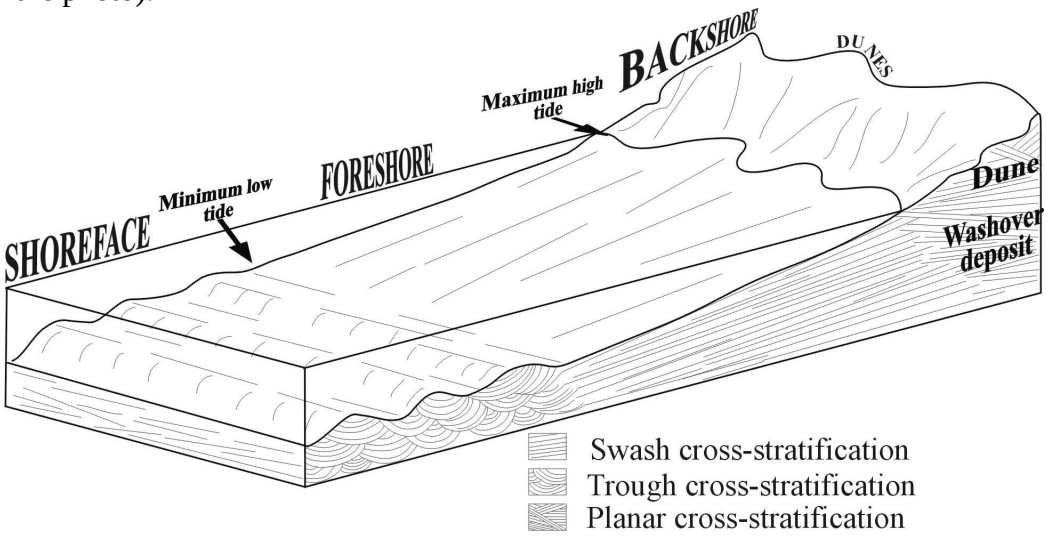

Figure 5.3 - Typical sedimentary structures found in a mesotidal modern beach.

The differences between shoreface and foreshore deposits are basically marked by the grain sizes and sedimentary structures. The shoreface deposits are characterized by coarse to conglomeratic quartz sand often with bioclastics. The most common sedimentary structure is the trough-cross-stratification that is a result of migration of sinuous crested bedforms during transportation. Observations show that the palaeocurrents are directed in a westward direction although some trough-cross-stratifications are induced by an important N-S component.

The foreshore sands are slightly finer than those of shoreface, varying from coarse to medium sand. Tabular beds and sheets with thickness of 0.1 to 0.4m compose the seaward dipping swash-cross-stratification that is the main sedimentary structure. According to

Bezerra *et al*. (1998) the middle to lower foreshore deposit can be used as a sea level indicator with a precision of ± 1.0m while the upper shoreface deposits that correspond to the minimum low tide level (Fig. 5.3) can be used as a sea level indicator with a precision of ± 0.5m.

Figure 5.4 - Upper foreshore and backshore deposits on the beach located between Ponta do Emissário Beachrock and São Bento Beachrock (For location see Figure 5.3)

Figure 5.5 shows the two most common sedimentary structures found in the beachrocks of the study area. The description of cross-sections of each beachrock help to position them and their samples (bioclastics to later ^{14}C dating) in relation to the maximum spring tide sea level and mean sea level.

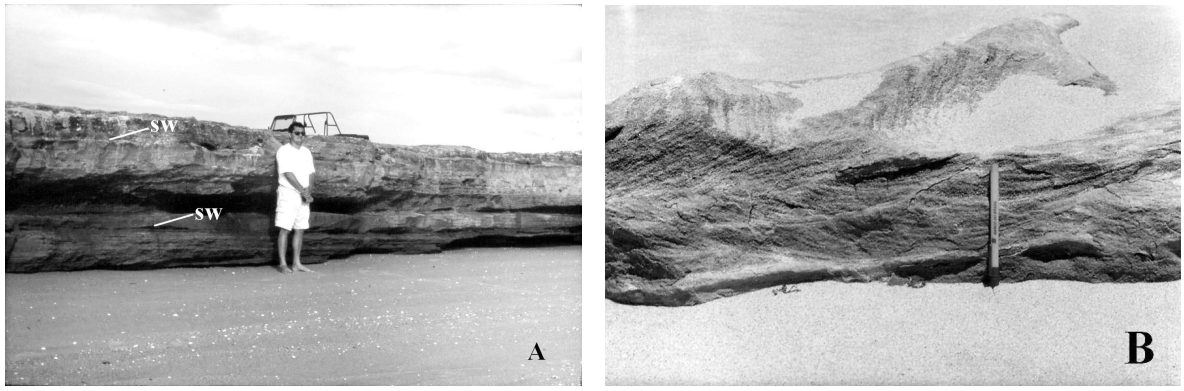

Figure 5.5 - Beachrocks and sedimentary structures in the foreshore and shoreface zones. (A) São Bento Beachrock showing swash-cross-stratification (sw) in the foreshore zone and (B) trough-cross-stratification in Cabelo Beachrock positioned in the upper part of shoreface zone.

Although some estimations exist bout sea level positions from beachrock facies (Bezerra *et al*. 1998), the exact mean sea level position cannot be determined due to the large thickness of the foreshore and shoreface deposits in beachrocks of meso and macrotidal coasts. In this case where the maximum Holocene mean sea level did not reach more than 1.5m above the present sea level (see chapter 4), an exact sea level indicator is required because the local spring tidal amplitude of 2.85m (DHN 1974) can disguise the indicator. According to Hopley (1986) only the uppermost level of beachrock cementation can be used as a reliable and precise sea level indicator. In this case, it represents the mean spring tide level. Thus it was attempted to define the uppermost cementation level of the beachrocks that

corresponds to the higher position of the foreshore deposit. Furthermore, the elevation of this uppermost level relative to the present maximum spring sea level was measured. Nevertheless the top of many beachrocks could not be defined as in many cases, both modern foreshore and backshore sediments (dunes) cover this top (Fig. 5.6).

In Figure 5.7 the topographic profile across the Guajiru Beachrock and Recuado Beachrock is shown, of which the latter is positioned entirely on land (Fig.5.8a). The profile shows that the top of the Recuado Beachrock, interpreted as its uppermost cementation level, is positioned at least 1m above the level of the top of the Guajiru beachrock, which corresponds to the present maximum spring sea level. Therefore it may be concluded that the Recuado Beachrock might represent a deposit of the Holocene highstand

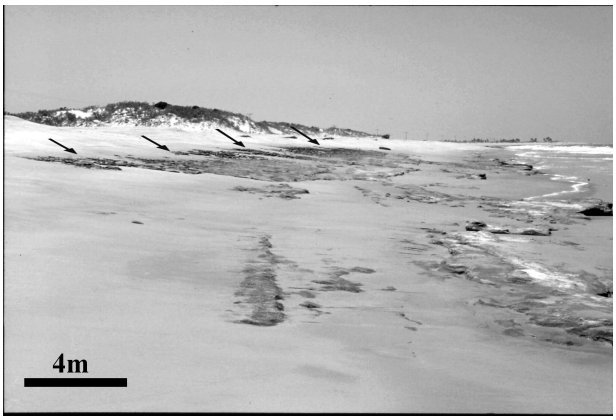

Figure 5.6 - Galinhos Beachrock 2 showing that the uppermost part (arrows in the figure) cannot be defined due to the cover by modern foreshore and backshore sediments.

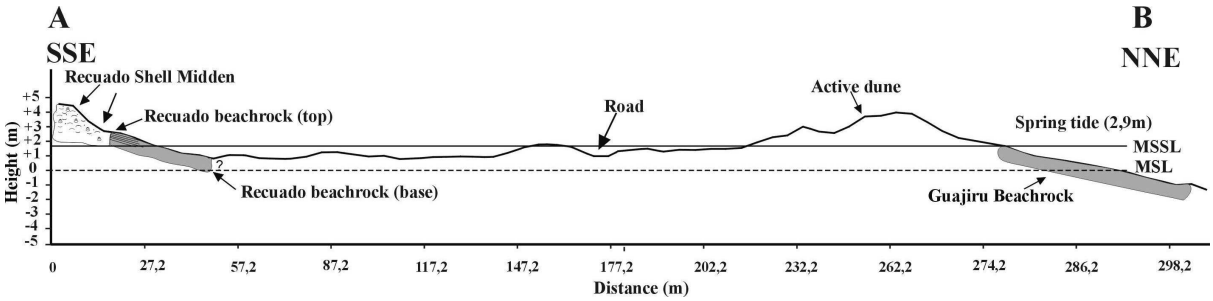

Figure 5.7 - Topographic profile normal to the Recuado and Guajiru Beachrocks showing that the top of the Recuado Beachrock is positioned at least 1m above the present maximum spring tide sea level and 2.6m above the present mean sea level. For location see Figure 5.2.

According Bezerra *et al*. (1998) the Recuado Beachrock was dated to 5450(+290/-390) cal yr BP matching with the age of the Holocene highstand proposed by some Brazilian sea level curves. These authors interpreted some shell accumulations as a marine terrace that were dated at 4070 +320/-280 cal yr BP and positioned somewhat parallel to the Recuado Beachrock. They concluded that this marine terrace is elevated at least 5m above the sea level predicted by the Touros Curve and could represent vertical Holocene tectonism. According to the field observations the shell accumulations (Fig. 5.8b) form separated small hills at an elevation between 3 and 5 m above modern mean sea level where rests of ceramics and anthropogenically-broken gastropod shells are commonly found.

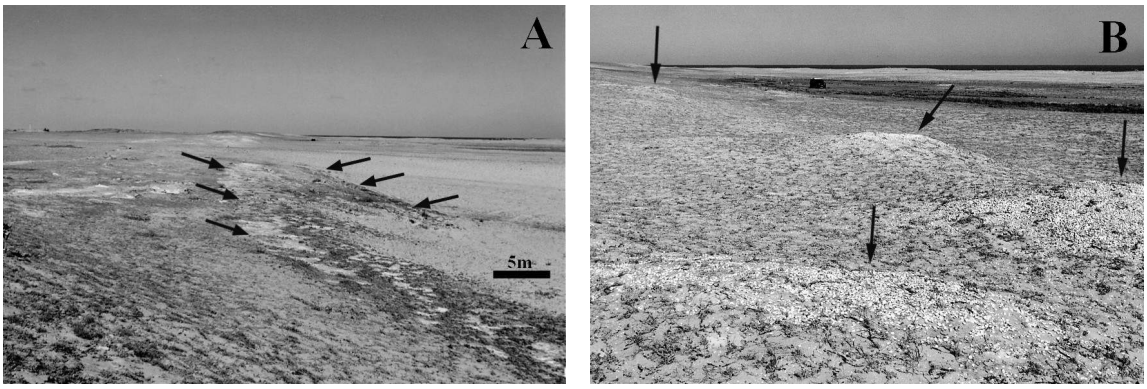

Figure 5.8 - (A) Recuado Beachrock and (B) shell-midden deposits. The arrows mark the various bodies.

Fairbridge (1976) and Martin *et al*. (1986) described the same characteristics for shell-middens (named Sambaquis) located on the southeastern coast of Brazil, although these deposits are much larger than those close to the Recuado Beachrock. The general geometry of marine terraces forms a regular wave-cut platform that does not match with such shell-middens.

5.4 - Radiocarbon dating

The AMS radiocarbon ages of the beachrocks were obtained from bivalve shells (Table Nr. 5.1). It is the first time that AMS radiocarbon dating on paleo sea level indicators has been undertaken in coastal studies on the Brazilian coast. A group of 13 well-preserved shells were selected upon which pre-treatment procedures were carried out. Additional 5 radiocarbon data gained from vibro-cores in the paleo-tidal flat of São Bento and Caiçara (Chapter 4) were used together with the data from the beachrocks.

The bivalve species found in were determined with reference to Maury (1934) and Campos e Silva *et al*. (1964). According to these authors the most common species, in order of abundance, present on the beach and in the beachrocks are *Donax striata, Divaricella quadrisulcata, Tivela mactroides, Anomalorcadia brasiliana, Anadara ovalis* and *Ostrea* sp. In this study *Lucina pectinata* was also found on the paleo- tidal flat of São Bento and Caiçara.

All radiocarbon ages presented here were calibrated using Dataset 2, 3 and 4 of CALIB rev4.3 (Stuiver *et al*. 1998) and corrected for isotopic fractionation based on the $^{13}C/^{12}C$ ratio measured simultaneously with the $^{14}C/^{12}C$ ratio by the AMS-system. There is no published information about reservoir age of marine or brackish water in the study area. Therefore no correction has been made for reservoir effects. The $\delta^{13}C$ values for the bivalve shells (Table Nr. 5.1) ranging from + 3.31‰ to –3.09‰show that the majority was typically from a transitional environment. The percent of marine carbonate in the shells used during the age calibrations was obtained from $\delta^{13}C$ values. The $\delta^{13}C$ values in fossils of original carbonate of bivalve shells vary mainly as a function of the environment where the shell lived (Keith and Parker 1965, Martin *et al*. 1986, Muhs and Kyser 1987, Krantz *et al* 1987, Hendry *et al*. 2001) and thus a relation between percent of marine carbonate and $\delta^{13}C$ can be proposed. Bivalve shells from freshwater yield $\delta^{13}C$ values varying from –9‰to –14‰(0% of marine carbonate), whereas those of marine origin show zero or positive values (100% of marine carbonate) (Keith and Parker 1964, Martin *et al*. 1986, Vita-Finzi 1992). Furthermore the freshwater carbonates might show a greater variability of $\delta^{13}C$ values which may be attributed to the presence of carbon dioxide produced through the oxidation of plant debris in

soil and by plant respiration (Faure 1986) and therefore do not necessarily indicate relation to the marine carbonate content.

Table 5.1 - AMS radiocarbon data of the beachrocks and vibro-cores samples

Laboratory number*	Sample	Elevation (m amssl)	Material (%MC)	$\delta^{13}C$ AMS (‰)	Conventional age [14C yr BP]	1σ[yr] # +/-	Calibrated age‡ [Cal yr BP]	1σ range† [Cal yr BP]
KIA 12334	Guajiru (Gua)	-0.2	Biv. shell (98%)	1.77±0.08	3150	30	2930	2960-2880
KIA 14751	Recuado Beachr. (RB)	+1	Biv. shell (83%)	-0,62 ± 0,07	5480	35	5910	5940-5900
KIA 14746	Recuado shell midden (RS)	+1.2	Biv. shell (71%)	-2,50 ± 0,08	5270	40	5730	5760-5680
KIA 12336	São Bento Beachr. (SB)	-2.5	Biv. shell (79%)	-1.31±0.11	6265	40	6790	6850-6740
KIA 14748	Cabelo Beachr.-a (C-a)	-1	Biv. shell (85%)	-0,35 ± 0,08	3990	30	4070	4090-3990
KIA 14755	Cabelo Beachr.-b (C-b)	-0.5	Biv. shell (95%)	1,26 ± 0,46	3795	35	3750, 3730	3810-3690
KIA 14744	Galos Beachr. 1 (Gl 1)	-2.8	Biv. shell (99%)	1,87± 0,09	4370	30	4510	4530-4440
KIA 14749	Galos Beachr. 2 (Gl2)	-0.7	Biv. shell (69%)	-2,84 ± 0,17	2595	40	2350	2390-2340
KIA 12338	Galinhos Beachr. 1 (G1)	-0.8	Biv. shell (80%)	-1,04± 0.20	3375	30	3330	3350-3300
KIA 14742	Galinhos Beachr. 2a (G2a)	0	Biv. Shell (100%)	3,31± 0,11	4485	35	4680, 4660	4770-4600
KIA 14747	Galinhos Beachr. 2b (G2b)	-0.2	Biv. shell (100%)	2,64 ± 0,09	2180	25	1780	1810-1730
KIA 14752	Galinhos Beachr.2c (G2c)	-0.8	Biv. shell (95%)	1,32 ± 0,05	2715	30	2400	2460-2350
KIA 14750	Galinhos Beachr.2d (G2d)	-1.6	Biv. shell (95%)	1,22 ± 0,07	3315	35	3200	3240-3140
Vibro-cores (Paleo-tidal flat close to São Bento – for location see Figure 4.2)								
KIA 13956	LCSBN (1a)	-2.8	Wood (0%)	-25,91 ± 0,14‰	6520	45	7430	7460-7420
KIA 13957	LCSBN (2b)	-2.8	Leaves (0%)	-26,33 ± 0,20‰	6125	40	6990	7090-6910
KIA 13958	LCSBN (2c)	-4.45	Bark (0%)	-27,19 ± 0,13‰	6035	35	6880; 6870; 6820 6810	6840-6760
KIA 14743	LCSBN (2a)	-1.8	Biv. shell (68%)	-3,08 ± 0,15‰	3575	30	3580	3630-3550
KIA 16093	LCSBN (2d)	-4.78	Biv. shell (68%)	-3,09 ± 0,41‰	6355	45	6950	7010-6890

* Leibniz Laboratory – Kiel, Germany
#1σ probability of conventional age
‡ Calibrated applying CALIB rev4.3 (Dataset 2, 3 and combination of 1 and 3): Stuiver *et al*., Radiocarbon 40: 1041-1083, 1998
†1σ enclosing 68,3% of area of probability distribution
AMSSL= above present maximum spring tide sea level
%MC = Percentage of Marine Carbon

The pre-treatment procedures were carried out on the shells to avoid contamination, which could lead to some unreliable radiocarbon ages. All shells were first mechanically cleaned under a binocular magnifying glass using a dentist drill. Afterwards they were examined by an electron scanning microscope (Fig. 5.9a and 5.9b) and X-ray diffraction. Only the samples that did not show signs of diagenetic alteration were chosen for ^{14}C-dating.

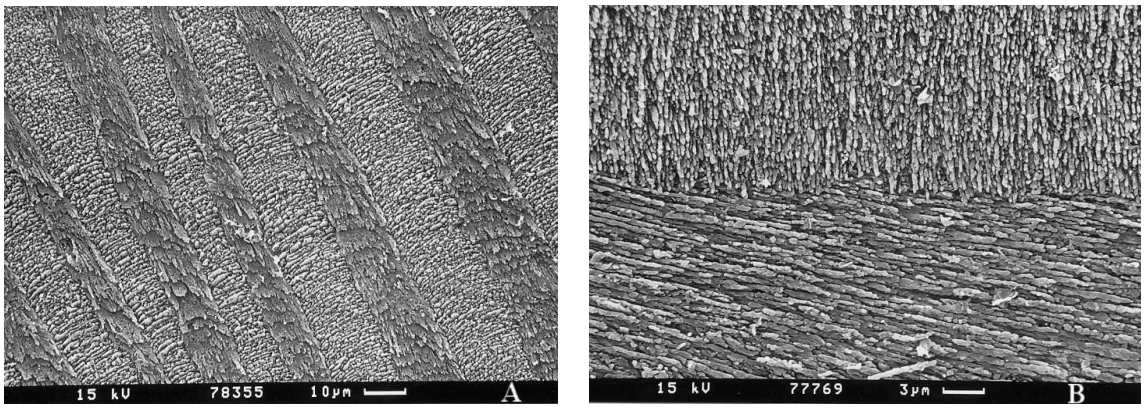

Figure 5.9 - Electron scanning micrographs of the shells showing needles of original aragonite forming crossed-lamellar structure: (a) Recuado Beachrock and (b) Cabelo Beachrock.

Obtained radiocarbon ages and their significances

The dating of beachrock from biogenic materials such as shells can give reliable ages when dated material is carefully chosen and cautious pre-treatment procedures are carried out. It is important to remember that the radiocarbon shell age is that at the organism death, thereafter it had been transported, deposited on a beach and subsequently cemented into the beachrock. The difference between the death of the organism and the cementation of the beachrock may be hundreds or even thousands years (Hopley 1986). Thus a careful choice of biogenic material is required. By choosing only well-preserved shells showing no signal of chemical and physical alteration, is it possible to reduce the difference between shell and cementation age because shell transportation in a high-energy environment, such as beaches, tends to promote chemical and physical alteration. Nevertheless the age yielded by the dating of a constituent organism can only be regarded as the maximum possible age for the beachrock cementation.

Guajiru Beachrock: One sample of bivalve shell located 0.2m below the MSSL in the upper foreshore deposit was dated at 2930 ±30 Cal yr BP. There is a good agreement between this age and that presented by Bezerra *et al*. (1998) for the same beachrock if the 2σ error suggested by these authors is considered. These authors dated this beachrock at 2759 +230/-110 Cal yr BP at 2σ. It is probable that the beachrock formation occurred approximately 2930±30Cal yr BP when the sea level position was possibly identical to the present.

Recuado Beachrock and Recuado Shell Midden: One sample of bivalve shell located at the uppermost part of the foreshore deposit and 1m above MSSL was dated at 5910±35 Cal yr BP. Two more radiocarbon ages for this beachrock are available. Caldas (1996) dated one bivalve shell from the uppermost part of Recuado Beachrock at 5455±200 Cal yr BP while Bezerra *et al*. (1998) obtained an age of 5450+290/-390 Cal yr BP for a bivalve shell positioned 3.9m above mean sea level. Silva (1991) obtained a conventional age of 5020±120 yr BP for cement of beachrock located on the Açu river delta and positioned at least 1m above the present high tide. The Recuado Beachrock certainly was formed during the Holocene highstand that according to some Brazilian sea level curves took place approximately 5200 yr BP. Therefore the age determined in this study is 450 years more than ages determined by the mentioned authors, and this might reflect several contributing factors. It may be possible that the shell's organism dated in this study died 450 years earlier than the organisms of the shells dated by previous authors, but all were deposited and cemented at the same age. Another reason for the age differences could be the different parameters used during the age calibration.

One sample of bivalve shell located at the base of the shell midden (1.2m above MSSL) and close to Recuado Beachrock was dated at 5730±40 Cal yr BP. Caldas (1996) and Bezerra *et al*. (1998) dated bivalve shells from the same deposit and obtained ages of 4130±280 Cal yr BP and 4070+320/-280 Cal yr BP, respectively. The age differences can be a result of the contamination of modern ^{14}C by secondary calcite in the bivalve shells that the above authors used.

São Bento Beachrock: One sample of bivalve shell (São Bento Beachrock, Table Nr. 5.1) located at 2.5m below MSSL (1m below mean sea level) in the upper shoreface deposit produced an age of 6790±40 Cal yr BP, which shows a good agreement at 2σ age extension for Bezerra's data for the same beachrock (Farol de Santo Alberto Beachrock of Bezerra *et al*. 1998). They dated this beachrock at 6460 +430/-390 Cal yr BP. It is probably that the São Bento Beachrock was formed during the last Holocene transgression (approximately 6700 Cal yr BP), when at this time the sea level was situated, interestingly, at the same position as the present.

Cabelo Beachrock: Two samples of bivalve shells from Cabelo Beachrock were dated. One sample (Cabelo beachrock-a, Table Nr. 5.1) positioned in the foreshore section at 1m below the MSSL gave an age of 4070±30 Cal yr BP, whereas the other Cabelo Beachrock-b, located at 0.5m below MSSL and also in the foreshore section, provided an age of 3750±35 Cal yr BP. This age difference suggests that the cementation process of the beachrock continued upward for at least 320 years.

Galos Beachrock 1: An age of 4510±30 Cal yr BP was obtained for a bivalve shell positioned at 2.8m below MSSL in the shoreface deposit.

Galos Beachrock 2: One sample of bivalve shell located at 0.7m below MSSL and in the foreshore deposit was dated at 2350±40 Cal yr BP. The difference between the Galos Beachrock 1 and 2 might demonstrate that each beachrock had been formed during different time although under same sea level conditions or the shells were transported and recemented.

Galinhos Beachrock 1: One sample of bivalve shell positioned at 0.8m below MSSL and in the foreshore deposit gave an age of 3330±30 Cal yr BP.

Galinhos Beachrock 2: Four samples of bivalve shells were dated from Galinhos Beachrock2. The sample Galinhos Beachrock 2a dated at 4680±35 and 4660±35 Cal yr BP was collected at the top (upper foreshore deposit and at MSSL) and in the extreme east of the beachrock closer to the Galos city (Fig. 5.2). The other 3 bivalve shells were sampled in front of Galinhos city (Galinhos Beachrock b, c and d). The samples Galinhos Beachrock 2b and 2c were taken at 0.2m and 0.8m below MSSL in the foreshore deposits, respectively. The ages obtained were 1780±25 Cal yr BP and 2400±30 Cal yr BP, respectively. The sample Galinhos Beachrock 2d was positioned at 1.6m below the MSSL in the foreshore deposit and gave age of 3200±35 Cal yr BP. This last sample suggests the maximum age at which the beachrock had started forming. The discordant age correlation between Galinhos Beachrock 2b, 2c and 2d may reflect a varied provenance of the material or vertical sequence of beachrock cementation; the latter being more probable. The sample Galinhos Beachrock 2a, contrary to the others certainly represents a reworked and recemented bivalve shell. Bezerra *et al*. (1998) obtained an age of 3430+240/-220 Cal yr BP for a bivalve shell collected at 1.1m above mean sea level.

It seems that Galinhos Beachrock 1 and 2 were formed during the same period.

Paleo tidal flat (São Bento and Caiçara): Three samples of organic matter and 2 of bivalve shells from vibro-cores of the paleo-tidal flat of São Bento and Caiçara were dated. The sample LCSBN-2a (bivalve shell in living position – Fig. 4.5) was collected on the surface of the paleo tidal flat which lies 1.8m below MSSL, and was dated at 3580±30 Cal yr BP. The other samples, LCSBN1a and LCSBN 2b, 2c and 2d (Table Nr. 5.1) present ages between 6800 to 7500 Cal yr BP and represent transgressive deposits.

5.5 - Holocene sea level history

Figure 5.10 shows the trend of the Holocene spring tide sea level (solid line in the Figure 5.10) based on lagoonal and beachrock ages. The use of the uppermost level of beachrock cementation as a reliable sea level indicator seems to be appropriate for a mesotidal coast where beachrocks are the most important coastal deposit. However difficulties exist in recognizing and defining the exact position of the uppermost level, as this level was almost always covered by current backshore and shoreface sand deposits. Despite these difficulties, it was possible to construct a transgressive Holocene maximum spring tide sea level curve showing a consistent trend. The regressive sequence of such a curve could not be determined due the difficulties mentioned above, but some conclusions can be reached.

According to the curve in Figure 5.10, the transgression passed the present mean sea level position 6500 Cal yr BP, as was predicted by other Brazilian sea level curves (Suguio *et al*. 1985, Peltier 1997 [Cited in Bezerra *et al*. 1998]), and reached its maximum approximately 5900-6000 Cal yr BP. The height of the maximum Holocene spring-tide sea level certainly did not extend 1.3m above the present one. Stated otherwise if the same tidal range is assumed for the Holocene period, the Holocene highstand was not higher than 1.2m above the modern as indicated by the Recuado Beachrock and Recuado shell midden. The age of this maximum is approximately 6000 Cal yr BP and it does not agree other Brazilian sea level curves, which indicate an age close to 5200 yr BP. Nevertheless there is no Holocene Brazilian sea level curve constructed with calibrated ages from paleo sea level indicators and perhaps this can explain the age differences, although the calibrated sea level curve from Peltier's model (1997 - cited in Bezerra *et al*. 1998) also predicts the Holocene highstand to occur approximately at 5200 Cal yr BP. The more appropriate explanation to this age differences is provided by the different parameters used during calibration of radiocarbon ages that change the ages either positive or negative in the time scale.

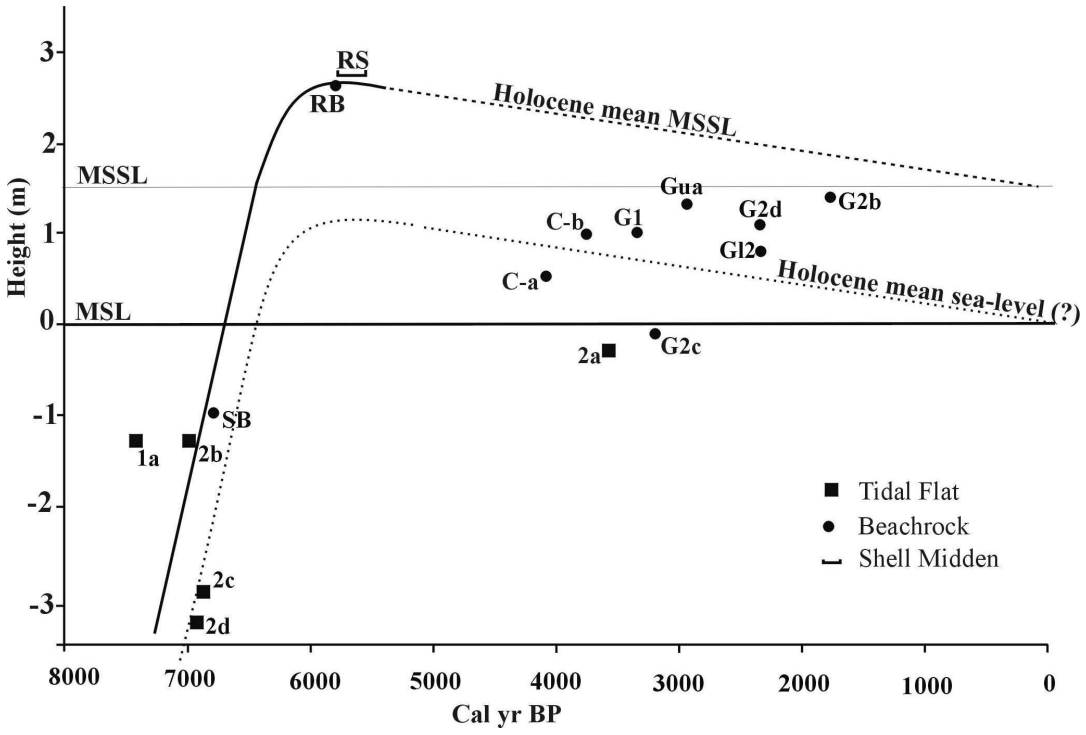

Figure 5.10 - Holocene sea level curves for the studied area. MSSL= present maximum spring tide sea level, MSL= present mean sea level. Sample codes: see Table Nr. 5.1.

The regressive sequence cannot be clearly reconstructed from the ages. An expected trend for both Holocene MSSL and Holocene mean sea level can be shown if no secondary oscillations have occurred and if the tidal regime during Holocene time was identical to the present. If the data from Figure 5.10 is compared with the proposed curves, it may be clear that the Holocene highstand was probably not higher than the present spring tide sea level and thus it may not necessarily be expected that many Holocene sea level coastal deposits will be positioned above the present MSL. In fact, only one part of one beachrock is positioned above the present MSL as well as the MSSL. Figure 5.7 shows that the presumed base of Recuado Beachrock coincides with the present mean sea level and only its upper foreshore part (former MSSL) is located above the current MSSL, which indicates that this beachrock could have been cemented during a Holocene sea level highstand. The beachrocks younger than 5000 Cal yr BP indicate that they were formed under sea level conditions similar to the present and secondary oscillations cannot be confirmed. Nevertheless the maximum elevation and the topography of the uppermost part of these beachrocks could not be determined and this perhaps explains the absence of ages around 5000 and 4000 Cal yr BP positioned above MSSL. Little vertical variation of Holocene sea level was also proposed by Mörner *et al*. (1999) for the coast between Belém and São Luis, where the sea level from 5200 to 4400 yr BP was very close to the present one. Our Holocene records support also the sea level changes presented here (see Chapter 4).

5.6 - Holocene sea level history: Diagenetic and chemical records

The chemical and diagenetic analyses of the beachrock cements allow for the modeling of their depositional environment and thus their correlation with the proposed Holocene sea level curve. Seventeen thin sections of the beachrocks were used in petrographycal studies and for further chemical and isotopic analyses.

5.6.1 - The beachrocks and their cements

All beachrocks of the studied area present microcrystalline-pelleted cement (micrite) (Figs. 5.11a and 5.11b) of high-magnesian calcite (HMC) and needles of aragonite forming a fringe (Figs. 5.11c and 5.11d), as the two most important carbonate cements. Figure 5.11 shows how these cements occur in the thin sections.

These cements precipitated in the beachrocks of the studied area indicate that they are typical of the marine phreatic zone (Longman 1980, Scoffin & Stoddart 1983, Coudry & Montaggioni 1986, James & Choquette 1990) and no signs of cements derived of freshwater vadose and freshwater phreatic zone (Bathurst 1971, Longman 1980, Coudray & Montaggioni 1986) has been recognized. Miketta (2001) had also demonstrated that the cements of the beachrocks located between São Bento and Galinhos have strictly been precipitated under marine influence with the exception of the cement of Galinhos Beachrock 2, which presents a slight tendency towards those precipitated through meteoric water. Nevertheless, this author concluded that it would not necessarily suggest aerial exposure of this beachrock during sea level oscillations. According to Miketta the present meteoric water flowing over the beachrock during low tide or its contact with ground water could induce these kinds of cement precipitations. Therefore secondary sea level oscillations that would result in a long aerial exposition of the beachrock (meteoric influence) cannot be considered.

Figures 5.11a and 5.11a show the cements found in the Galinhos Beachrock 1 and Recuado Beachrock. The three phases of typical marine cements for the São Bento beachrock (Micrite-Aragonite-Micrite [Fig.5.11c] and Aragonite-Aragonite-Micrite [Fig. 5.11d]) indicate three phases in which São Bento Beachrock had been subjected to the marine

phreatic zone. In fact, from Figure 5.10 (sample SB) it may be concluded that the first cement was already precipitated during the rise of the sea level.

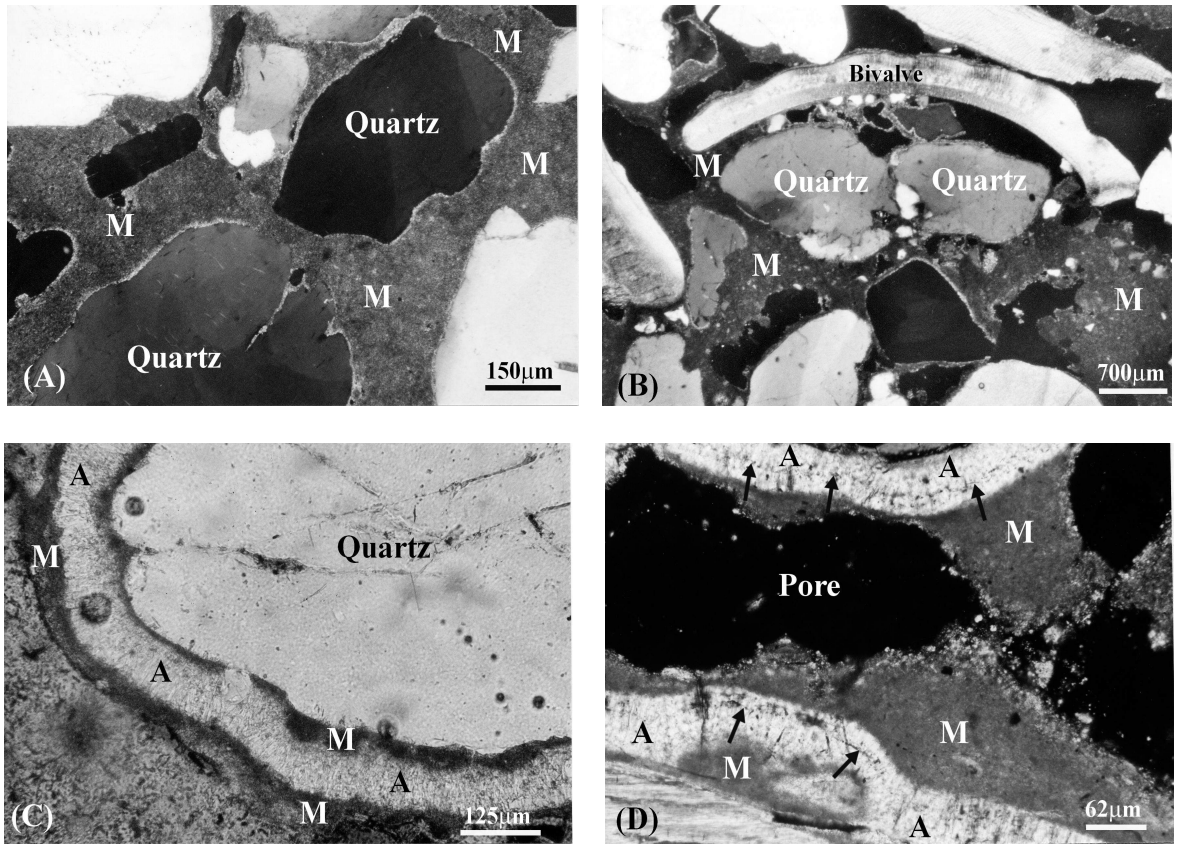

Figure 5.11 - The most common cements in the beachrocks of the studied area. (A) Microcrystalline mass of HMC (letter M) filling all spaces between the siliciclastic grains in the Galinhos Beachrock 1 (cross-polarized-light); (B) Microcrystalline mass of HMC (letter M) in the pores of Recuado Beachrock (cross-polarized light); (C) Two cements types in the São Bento Beachrock. The letter "M" represents the microcrystalline mass of HMC while "A" represents isopachous fringe of aragonite (plane-polarized light); (D) São Bento Beachrock (cross-polarized light) showing HMC filling the pore (letter M) and isopachous fringe of aragonite around grains. Observe that two phases of fringe of aragonite occur. The arrows indicate the limit between these phases.

Subsequently the São Bento Beachrock had been entirely under water when the second phase of the marine phreatic cement was precipitated. The third phase of precipitation under marine influence (HMC filling the pores) is currently taking place, since the beachrock was first located in the intertidal zone. All other beachrocks show only one phase of cement precipitation in the marine phreatic zone, which confirms the supposition that these beachrocks have been cemented solely within the intertidal zone of a sea level regime similar to the present.

5.6.1.1 - The cements and their chemistry

The chemical analyses of the cements (Table Nr. 5.2) indicate that all beachrocks have been cemented in the intertidal zone of the marine phreatic environment. The micrite cements

are magnesian-enriched calcite precipitates containing 13,16 to 14,89 mole‰$MgCO_3$ (Table Nr. 5.2) typically associated with the intertidal zone (Alexandersson 1972).

Table 5.2 – Mol‰ $MgCO_3$*, Sr (ppm)*, $\delta^{18}O$, $\delta^{13}C$ values of the beachrock cements.

Thin Section	Beachrock	Deposit	Cement	$MgCO_3$ (Mol%)	Sr (ppm)	$\delta^{13}C$ PDB	$\delta^{18}O$ PDB
SB5-A	São Bento	US	Micrite	13.16	0	3.07	-0.07
SB5-B	São Bento	MF	Aragonite fringe	--	12,600	2.93	0.21
BR-Rec	Recuado	UF	Micrite	14.89	0	-0.04	-1.37
Gali-Br2a	Galinhos-2	US	Micrite	14.26	0	2.64	0.45
Gali-Br2b	Galinhos-2	UF	Micrite	14.53	320	2.43	0.51
Gali-Br1	Galinhos-1	MS	Aragonite fringe	--	13,400	3.53	0.84
Gua-1	Guajiru	US	Aragonite fringe	--	10,500	3.44	0.33

* From electron microprobe.
MF= middle foreshore, US= upper shoreface, UF= upper foreshore, MS= middle shoreface.

The aragonite crystals commonly form isopachous rims around the grains or HMC (Fig. 5.11c and 5.11d) thus implying cementation in water-filled pores of a marine phreatic zone (e.g. Purser 1969, Moore 1971, Tietz & Müller 1971, Schröder 1973, Bathurst 1974 and Hanor 1978). Strontium is the major trace element in aragonite usually reaching from 7 to 10 parts per thousand (Kinsman 1969, Bathurst 1971, Friedman & Sanders 1978 and Tucker & Wright 1990). Values of 13,150 ppm have been reported by Strasser *et al*. (1989). The strontium contents in the aragonite cements of some studied beachrocks vary from 12,600 (São Bento Beachrock) to 10,500ppm (Guajiru Beachrock). The presence of aragonite with high strontium content indicates early diagenetic cements formed in shallow tropical seas (James & Ginsburg 1979, Veizer 1983, Coudray & Montaggioni 1986 and Morse & Mackenzie 1990) indicating that the Holocene beachrock cements in the studied coast have not experienced conditions of the meteoric environment.

5.6.1.2 - The cements: Carbon and oxygen isotopes

Milliman (1974), Margaritz *et al*. (1979), Veizer (1983) and Margaritz (1983) have shown that the variances in the stable isotopic composition of carbonate precipitates are a direct result of the different environments (for example fresh or marine) in which the precipitates were formed and altered. Particles and cements precipitated in marine environment have a mean $\delta^{13}C$ and $\delta^{18}O$ value close to zero, whereas those formed in a fresh-water environment become systematically more negative ($\delta^{13}C$=-5 to -15 and $\delta^{18}O$=-5 to -10). The negative values indicate post-depositional exchange of isotopes with meteoric waters. The $\delta^{13}C$ values in the beachrock cements range from -0.04‰to 3.53‰ $_{PDB,}$ whereas the $\delta^{18}O$ values vary from -1.37‰ to 0.84‰ $_{PDB}$ (Table Nr. 5.2). These values indicate cement precipitation of the beachrocks in a shallow, predominant marine environment with insignificant freshwater influx (Fig. 5.12).

The sample Br-Rec referent to the Recuado Beachrock micrite cement is the only one that does not plot in the shallow-water field. It can be observed in the Table Nr 5.2 that both $\delta^{13}C$ and $\delta^{18}O$ for Recuado Beachrock present values negative in comparison to the others. The depletion of $\delta^{13}C$ and $\delta^{18}O$ (sample BR-Rec) can be attributed to an influx of fresh-water, the effect of organic matter or secondary diagenetic alteration of marine cements in a meteoric environment. This last supposition can be rejected because the existence of HMC, easily transformed to low magnesian calcite during subaerial exposure (Bathurst 1971),

clearly demonstrates the presence of original intertidal cement. Furthermore the structure of the cements composed of micrite envelopes and isopachous fringe of aragonite, indicates precipitation under marine phreatic zone. The most appropriate explanation is the occurrence of both fresh-water influx and organic activity during the cementation of the Recuado Beachrock for the period of Holocene sea level highstand, when barrier-islands associated with mangroves and tidal channel existed (see Chapter 6 for more details).

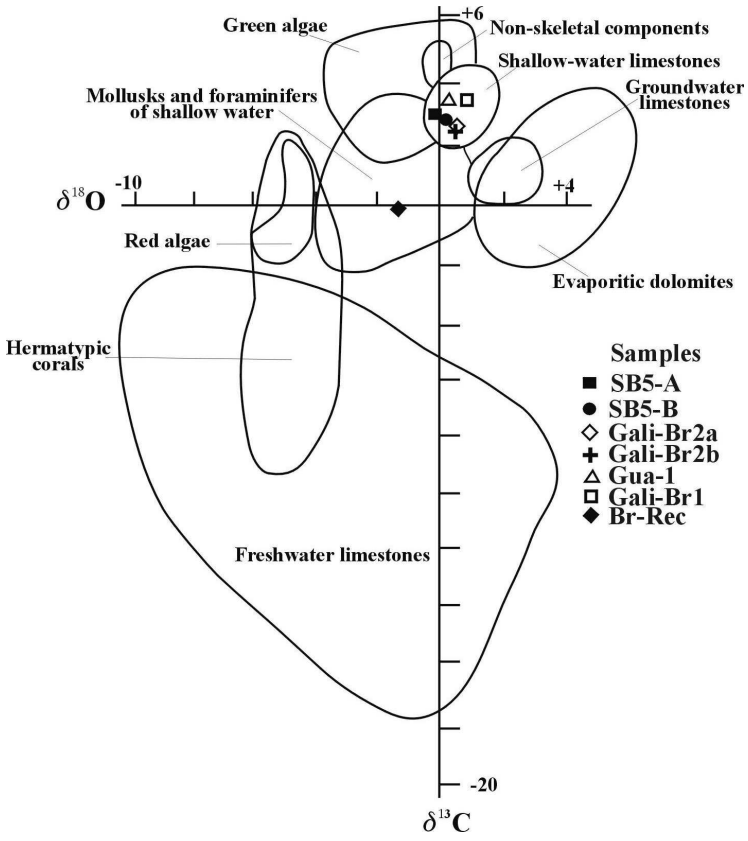

Figure 5.12 - Stable isotopic fields (PDB‰) for recent carbonate sediments and component particles (Milliman 1974). The black symbols represent the samples of beachrock cements from this study. See Table Nr. 5.2 for the analyses.

5.7 - Discussion, conclusions and perspectives

Sea level studies on the Brazilian coast have shown that during the last deglacial transgression the sea level passed the present position for the first time approximately 7000yr BP. Approximately 5200 yr BP the sea level reached a highstand at 3.5m above the current sea level and after which the level receded to the present level. Some secondary sea level oscillations have been suggested during the regressive phase. For the study area and surrounds there is only one sea level curve constructed from sea level indicators (Barreto *et al*. 2001) and another gained from glacio-hydro-isostatic model, named the "Touros Curve" by Bezerra *et al*. (1998). The first curve is somewhat similar to the Salvador curve with secondary oscillations whereas the second, gained from hydro-isostatic model, does not predict secondary oscillation.

In the study area, the determination of the uppermost part of the beachrock cementation and its relation with present sea level have shown to be a reliable sea level indicator. The determination of paleo-mean-sea-level from beachrock deposits in macro and mesotidal coasts is complicated because beachrock deposits can only hint at the former spring

tide level and the tidal amplitude. Therefore only the uppermost part of the beachrock can be used as a reliable sea level indicator.

In the study area the uppermost parts of the some Beachrocks were identified and both sampling and their elevation measurements in relation to the present sea level were carried out. Some ^{14}C dating from paleo tidal flat sediments were undertaken as well. The constructed sea level curve obtained from these data and its subsequent interpretations improved from chemical and diagenetic data has demonstrated that the mean sea level reached the present position along the northern coast approximately 6600 Cal yr BP as predicted by most sea level curves for the Brazilian coast (e.g. Suguio *et al*. 1985, Angulo & Lessa 1997). According to the beachrock geochronology the cementation of the São Bento Beachrock first took place during the sea level transgression when typical intertidal cements like HMC and needles of aragonite were precipitated in the pores of the ancient beach sediments. During the Holocene highstand that reached 1.2m above the present mean sea level, the São Bento Beachrock was drowned under typical marine phreatic control. During this stage the second cement (Aragonite fringe) on the São Bento Beachrock was precipitated.

The Recuado Beachrock was formed during the Holocene highstand. Its uppermost part of cementation represents at least the height of the maximum spring tide of the former sea level and thus can be used as a reliable sea level indicator. The elevation measurements show that this uppermost part is positioned 1.3m above the present spring tide level and if one considers that the tidal regime during the Holocene time has remained more or less identical, the mean sea level may be placed at approximately 1.5m below the uppermost part of the Recuado Beachrock. This suggests that Holocene highstand reached approximately 1.2m above the present level at 5910±35 Cal yr BP while at the same time the Holocene spring tide reached 1.3m above the modern one. Immediately above the highest beachrock lies lowermost part of the shell midden dated at 5730±40 Cal yr BP which is definitely above the tidal zone (Fairbridge 1976 and Martin *et al*. 1986).

These findings demonstrate that at least for the proposed Holocene highstand, substantial differences to other Brazilian records have been detected: the Salvador curve (Suguio *et al*. 1985 and Martin *et al*. 1985) suggests a highstand of approximately 5m whereas the Touros Curve (Peltier 1997 cited in Bezerra *et al*. 1998) predicts a Holocene highstand of approximately 2.2m above the present mean sea level. At least for the Salvador curve the highstand differences can be attributed to both regionally different tectonic uplift and subsidence trends in addition to the eustatic component in that region. The differences between the curve of this study and Peltier's glacio-hydro-isostatic model-curve for the Touros region (Bezerra *et al*. 1998) demonstrate that the sea level probably has experienced only eustatic changes. On the other hand, a Holocene highstand even corresponding to the modern sea level has been reported by Mörner *et al*. (1999) for the coast between São Luis and Belém (~600km NW).

The chemical and diagenetic data from the Recuado Beachrock demonstrate that it was cemented under typical marine control but with some fresh-water influx and organic activity. Such conditions can easily take place during the proposed evolution of the area when barrier-island systems associated with mangroves and tidal channels occurred.

The suggested Holocene local tectonics that, according to Caldas (1996) Caldas *et al*. (1997) and Bezerra *et al* (1998), produced local uplift and subsidence was not detectable. Most of the suggested Holocene tectonic events have been proposed indirectly from morphological and sedimentological observations. The dating of outcrops affected by tectonic structures will determine the age of such events.

The regressive Holocene sea level trend could be not determined from beachrocks younger than 5000 Cal yr BP because current foreshore and backshore deposits cover the uppermost level of cementation of the beachrocks. Nevertheless, it is suggested here that the elevation of the uppermost level of cementation can be recognized and measured through

digging a trench on the present upper foreshore zone. It has been suggested that the Cabelo Beachrock is the most indicative to show uppermost level of cementation above the present maximum spring tide level because it was cemented soon after the Holocene highstand (See Fig. 5.10) when the maximum spring sea level was yet higher than the present level. This is true if the Holocene sea level regression has been uniform up to nowadays and no secondary oscillations have taken place, as the diagenetic and chemical data have shown.

In comparison with the other Brazilian sea level curves for Holocene time, curve of this study presents almost the same trend, although the transgressive section with dated samples positioned below the current mean sea level, is better represented than in the other curves. To determine the exact position of the mean sea level from coastal sediments deposited under mesotidal regime is quite difficult. The difficulty increases when variation in sea level has not been large enough to deposit undoubted mean sea level indicators above the present spring tide level. Since the tidal range is greater than the observed Holocene sea level highstand (+1.2m), any small-scale higher frequency oscillation cannot be recognized. Only the uppermost part of the beachrock cementation and its height in relation to the current spring tide level has indicated that such deposit was cemented during sea level highstand. However it should be kept in mind that the upper levels of cementation were difficult do determine due to burial by current beach deposits. The continued observation of the beach-profile and the determination of the upper level of cementation will improve the regressive section of the sea level curve. The depositional model of the beachrock as a "frozen beach" and its direct comparison with modern beaches has permitted the positioning of shoreface-foreshore-backshore zonation with high precision. The careful distinction between both current mean sea level and current spring tide level, and their vertical relation to precise former sea level indicators in the area during minor sea level variations, may improve the database necessary for the construction of a sea level curve.

6 - Late Pleistocene and Holocene coastal evolution

6.1 - Introduction

The coastal evolution during the Holocene epoch for the studied area has here been determined from geochronological, geophysical, stratigraphic, chemical and petrographycal data as well from field observations. The comparison and analyses of all data collected in the studied area allows the separation of Holocene and Pleistocene deposits.

In the chapters 4 and 5, several elements of the Holocene coastal geology for the area have been already presented and discussed but older sedimentary deposits have not yet been introduced or discussed. The first section of this chapter will present data of deposits from the Pleistocene ages. The second part will deal with the integrated Holocene coastal evolution of the area based on the conclusions made in the chapters 4 and 5.

6.2 - Pleistocene deposits

On the studied coast some sedimentary outcrops located at the Ponta dos Três Irmãos and Ponta do Emissário, east of São Bento, build up coastal cliffs which are geomorphologically well distinct from those of Holocene ages. Correlated deposits have been described for the coast of Touros (Srivastava & Corsino 1984 and Testa & Bosence 1998). For the coast between São Bento do Norte and Ponta dos Três Irmãos (Fig. 6.1) Lima-Filho *et al*. (1995), Caldas (1996) were the first to describe and propose Pleistocene ages for these deposits based mainly on stratigraphical and geomorphological characteristics. Caldas *et al.* (2001) dated bivalve shells from Ponta do Emissário and close to Tibibau River (Fig. 6.1), and found ages between 30000 yr BP and 45000 yr BP. According to these authors such deposits could be older since these ages are close to the limit of the dating method used (AMS ^{14}C). More recently some authors have presented new geochronological data for these deposits (Barreto *et al*. 2002).

6.2.1 - Ponta dos Três Irmãos, Ponta do Emissário and Tubibau River deposits: Sedimentary characteristics

The sediments found in Ponta dos Três Irmãos (PTI), Ponta do Emissário (PE), close to Tubibau River and Santa Isabel Farm exhibit identical morphological, sedimentary and petrographycal characteristics. The PTI deposits (Fig. 6.1) are basically composed of sandstone that was deposited essentially in two coastal sub-environments: Foreshore and backshore zones (Fig. 6.2 and Fig. 6.3).

The foreshore deposits consist of grey sandstone with carbonate cements similar to the Holocene beachrocks. The grain size varies from fine to very coarse sand often associated with granules and pebbles. The dominant siliciclastic components are quartz with minor portions of limonite, feldspar, tourmaline, zircon, rock fragments, titanite and opaques. These siliciclastic components can reach up to 47% of the volume of the rock. The carbonate components are represented by bioclastics (red algae, green algae, bivalves, bryozoans, foraminifers and gastropods), which may reach up to 25% of the volume and carbonate cements forming up to 25% of the rock volume. The main sedimentary structure present in the foreshore deposits is swash-cross stratification indicating sedimentation in the intertidal zone. Therefore the foreshore deposits are interpreted as beachrocks.

The backshore deposit is made up of well-sorted medium to very fine sandstone. The dominant siliciclastic components are quartz and minor fractions of tourmaline, feldspar, titanite, zircon and opaques. The most common biodetrital components are red algae and

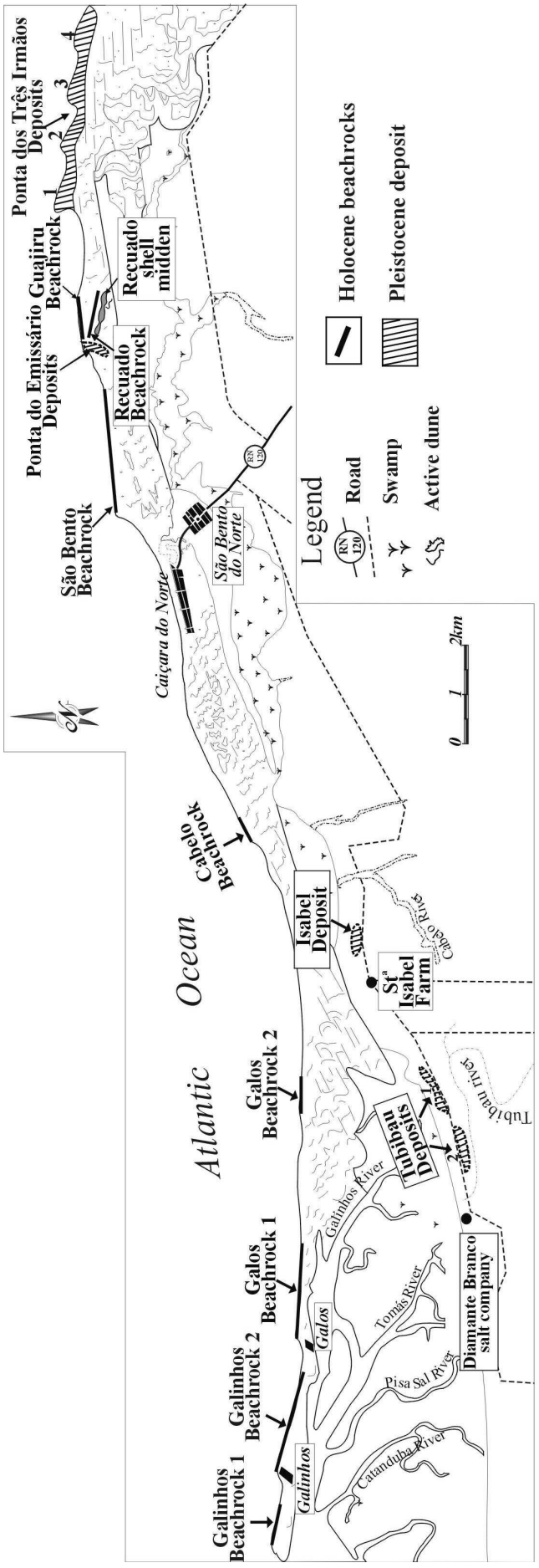

Figure 6.1 - Location of Holocene beachrocks and Pleistocene deposits on the studied area.

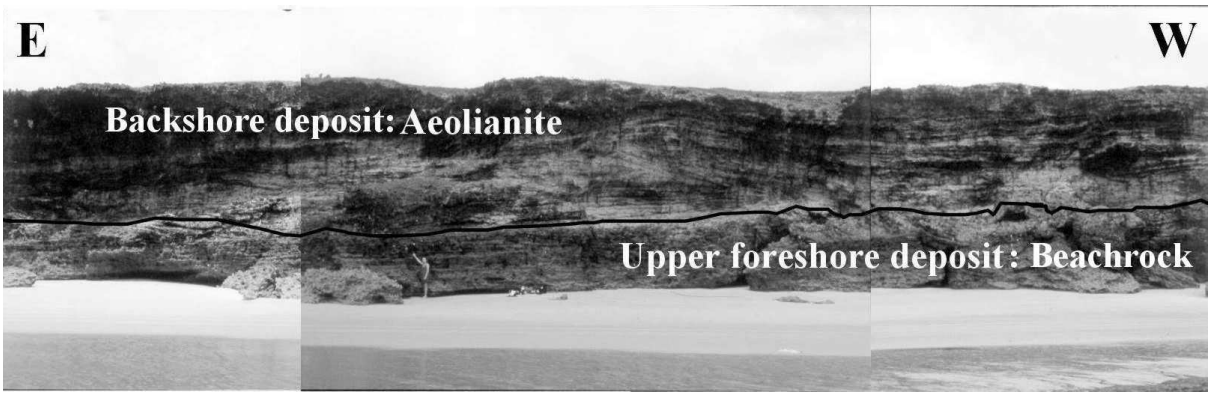

Figure 6.2 - Ponta dos Três Irmãos-4 sandstone. The black line limits the upper-foreshore deposit (beachrock) at the base that is capped by backshore deposit (aeolianite).

foraminifers reaching up to 15 % of the rock volume. The main sedimentary structure is trough-cross- beddings tangential to the base (Fig. 6.2 and 6.3). Solution pipes could be observed at the PTI and PE. Such pipes are commonly referred to the dissolution of roots but preserving their original structures (Miller & Manson 1994). These features allow for the interpretation as aeolianite.

The beachrocks at PTI and PE forming the lower part of the deposits presents different thicknesses varying from 1.8m at the site PTI-4 to 5.5m at PE site. The aeolianite of the upperpart shows similar thickness variations (6m at the site PTI-4 to 2m at the PTI-2 site). The contact between beachrock and aeolianite is marked by abrupt grain size difference. No erosive surface was observed.

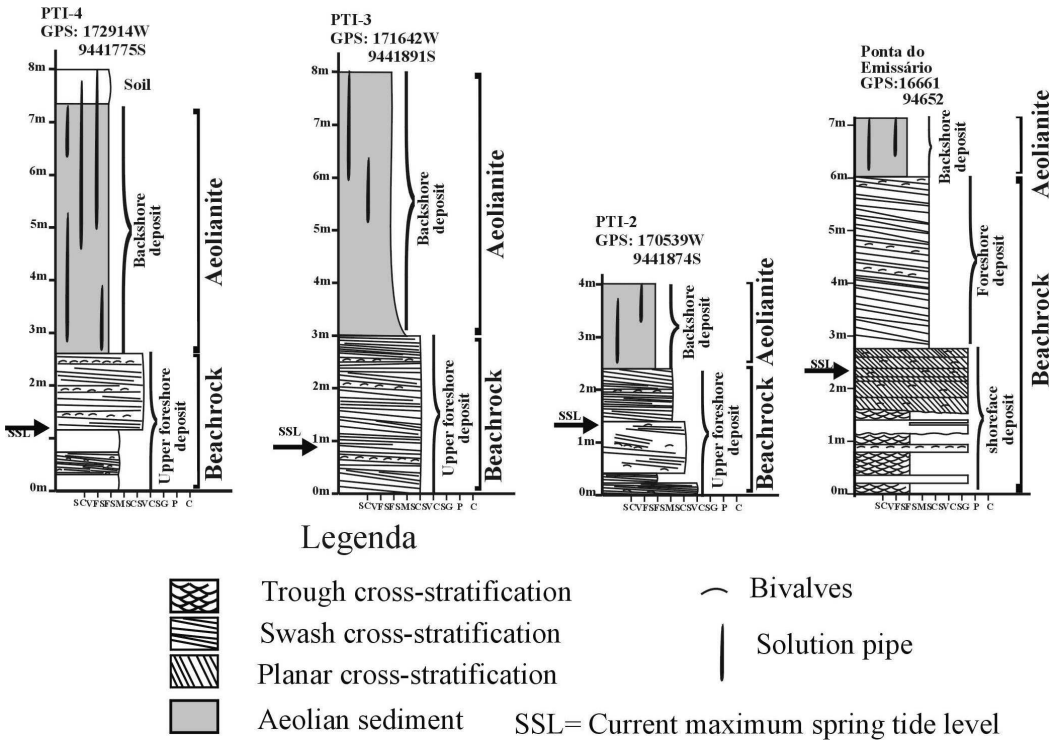

Figure 6.3 - Representative stratigraphic sections showing sedimentary structures and interpreted limits between the main beach zones of PTI and PE sandstones. Lithostratigraphic section of the Ponta do Emissário is according Lima-Filho (1995).

The PE, Isabel and Tubibau deposits can be correlated to those from PTI on the basis of sedimentary structures, petrography, stratigraphic relations and geomorphologic features. The PE deposit presents the same geometry and stratigraphic characteristics as the PTI sandstone although the beachrock is thicker (5.5m) and contains more bioclastics, consisting mostly of bivalve shells. The Isabel sandstone crops out as a small hill that is positioned approximately 10 meters above the present maximum spring-tide level. The petrographical and surface features of the quartz grains of the Isabel sandstone are similar to those from the upper part of PTI, thereby suggesting aeolian deposition. However this outcrop is a poor representative of this type of deposition as the various coastal deposits can not be separated. The Isabel aeolianite is made up of well-sorted medium to very fine subrounded siliciclastic grains being cemented by carbonate.

The Tubibau deposits are formed by calcarenites with many bioclasts (bivalve shells). Swash-cross stratification can be found in some part of the outcrops. Nevertheless, these deposits have been entirely removed from their original position for salt bed construction and thus interpretation of sedimentary structures as well as the original heights of outcrops becomes difficult. Despite these problems, the petrographycal analyses have shown that such deposits present the same characteristics observed for the beachrocks of PTI. The presence of bioclasts, siliciclastic components and secondary carbonate cements originating from those typical of intertidal origin reveal a depositional environment between foreshore and shoreface zone.

Measurements of dip direction of foresets in the aeolianite preserved in the cliffs parallel to the beach line indicate that they were deposited by winds blowing mainly from an east-northeast direction as suggested by the steeper slopes westward (paleo-slip face). The present wind pattern, which has built up coastal dunes, shows similar orientations at this point of the coast.

The stratigraphical correlations between beachrock that is covered by aeolian sediments allow for the interpretation of an environmental change from highstand to regressive deposits.

The scanning electron microscope analyses of the surface features of the quartz grains of both beachrock and aeolianite from PTI (Fig. 6.3) improved the environmental interpretations of these deposits substantially. The quartz surface features "illustrate" the mechanical and chemical action during and after grain transportation through water and wind Krinsley & Doornkamp 1973, Al-Saleh & Khalaf 1982, Mycielska-Dowgiallo & Woronko 1998, Newsome & Ladd 1999). Nine samples were collected from the aeolianite and beachrocks of the study area. These samples consist of three sand samples stemming from the aeolianite of the PTI and one sample from the Isabel aeolianite. The final five samples were taken from the beachrocks of PTI.

Figure 6.4 shows the main surface features observed on the quartz grains. Each type of sediment (aeolian or subaqueous) is characterized by an abundance of certain surface features.

The quartz grains from *aeolianites* are mainly well rounded (Fig. 6.4a and 6.4b) and present silica precipitation as an important feature (Fig. 6.4b). Mechanical pits scattered all over the grain surface occur (Fig. 6.4a) when silica precipitation is not predominant. Krinslay & Doornkamp (1973), Higgs (1979) and Al-Saleh & Khalaf (1982) have demonstrated that such surface characteristics are abundant on aeolian grain sediments.

The quartz grains from beachrock deposits show triangular pits and oriented etch pits as the most important surface features (Fig. 6.4c and 6.4d). The triangular pits (etched V-indentations from Krinsley & Doornkamp 1973) and oriented etch pits are associated with silica precipitation of grain sediments of marine environment (Higgs 1979). Krinslay & Doornkamp (1973) also described such features of grains which have been immersed in seawater.

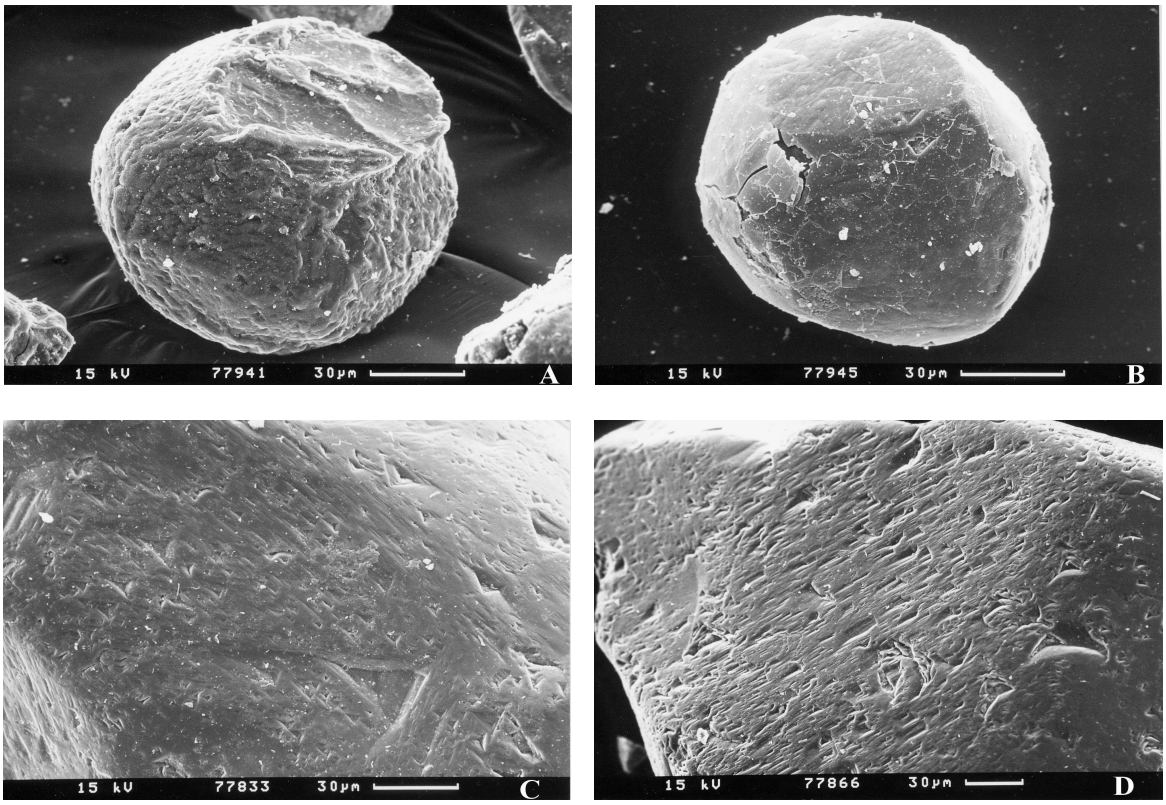

Figure 6.4 - Surface features of quartz grains from aeolianite and beachrock of PTI. (a) Very well rounded aeolian grain from the middle part of the aeolianite at PTI-4 with several depressions produced by mechanical impacts during grain transport, (b) very well rounded quartz grain from top of the aeolianite at PTI-3 smoothed due to the solution-precipitation phenomena. Note the hole cracks on the left side of the grain that is the beginning of chemical weathering, (c) oriented V-shaped pits produced by silica precipitation in subaqueous environment on grain from upper part of the beachrock of PTI-3 and (d) a grain showing parallel etch pits from beachrock of PTI-4.

6.2.2 - Ponta dos Três Irmãos, Ponta do Emissário and Tubibau River deposits: Diagenetic, chemical and isotopic characteristics of their cements

As many authors have shown, the compositional and morphological characteristics of individual cements in such coastal deposits depend upon environmental conditions (Bathurst 1971, Bathurst 1974, Longman 1980, Coudray & Montaggioni 1986). Thus the carbonate cements found in the coastal deposits of the study area can show how such deposits have been positioned in relation to the sea level (marine or continental influence) after their deposition and cementation. As seen in the last section, the compositional and sedimentary features of the deposits present at the PTI, PE, Tubibau and Isabel Farm have allowed to interpret most of them as typical beach deposits. In such environment the carbonate cementation presents some particular characteristics and compositions (see chapter 5) that indicate the rock position in relation to the sea level. Such cements, which are typically marine, are quite unstable under the influence of meteoric waters where high magnesian calcite (HMC) is transformed to low magnesian calcite (LMC) (Tucker & Wright 1990). According to Friedman & Sanders (1978) HMC can change into LMC within a time span of 7000 to 10000 years. The most carbonate cements found actually in PTI, PE, Tubibau and Isabel deposits

can be related to those originating in freshwater phreatic environments (Longman 1980), as will be discussed below.

Ponta dos Três Irmãos Sandstones: The beachrocks are characterized by open to semi-closed interparticle pore spaces and semi-preserved skeletal grain mineralogy (Fig.6.5a and 6.5b). LMC forms elongated blades (EB in Fig. 6.5a) and radiaxial fibrous calcite (white arrow in Fig. 6.5b). These two types of cements are the most important usually forming thick rims that cover all grains. Probably LMC forming microcrystalline cement (micrite) has been found overlaying the radiaxial fibrous calcite (black arrow in Fig. 6.5b). Such sample was collected from beachrock, 0.3m above present spring tide and its cement might demonstrate a new generation of precipitation under marine or meteoric influence. Such cement texture is common to those related to marine HMC and could represent a new precipitation during the Holocene highstand. Nevertheless chemical and isotopic analyses should be undertaken to know precisely if this cement really has a marine origin.

LMC forming blocky calcite occurs in both beachrock and aeolian sediments although it is more frequent in the aeolianites of the PTI (Fig 6.5c and 6.5d) and Isabel aeolianite. The blocky calcite tends to fill all pore spaces between the grains forming a mosaic texture (Fig. 6.5d). Such cementation is also characteristic of the active zone of a freshwater phreatic environment.

Ponta do Emissário Sandstone: The beachrock and aeolianite of Ponta do Emissário present almost the same cement characteristics as those described for PTI, although two phases of marine precipitations and their alteration thereafter in a freshwater phreatic environment has been identified for the beachrock section. The cements are LMC forming stubby blades (black arrow in Fig. 6.5e) as the first generation and elongated blades (white arrow in Fig. 6.5e) as the second generation. Such kinds of cements seem to be the product of unstable original marine cements such as aragonite needles and HMC in the freshwater environment (Scoffin 1987). Overgrowths of LMC blades have filled the sandstone pores producing a blocky calcite pattern (Fig. 6.5e). Pendant or gravitational LMC cement typical of freshwater origin has been found in the beachrock section of PE sandstone (Fig. 6.5f). In the same figure, the two cement generations can be observed. Stubby blades form the first generation of freshwater cement but elongated blades the second one. The forward gravitational growing of the elongated blades to the pore center formed the pendant pattern (Fig. 6.5f).

The geometry and contact relations between the two cement types observed in PE sandstone reveal that they were precipitated during two events in which they had been under marine conditions. Such events could be related to eustatic sea level oscillation and/or vertical tectonic movements affecting the Pleistocene coastal deposits and permitting their immersion in seawater. Although it is quite difficult to answer only from cement patterns which process, if not both, is more probably, some suppositions can be made.

If all Pleistocene deposits have the same age possibly corresponding to the penultimate transgression and if they had all been under the same marine influence, the cementation pattern on the grains should be identical at least in all the foreshore sections of the beachrocks. It is observed that the sedimentary characteristics of the Pleistocene deposits are identical and that they together form one same regressive sequence. If this is true, the tectonic alternative seems to be more appropriate to explain the second generation of marine cement. Many authors have suggested that neotectonic events have affected the coastal deposits of this area (Bezerra *et al*. 1998, Caldas 1996, Caldas *et al*. 1997, Silva 1991, Vital *et al*. 2002b and Vital *et al*., in review). However the age of the neotectonic event(s) remains theme of discussion (see Radiocarbon dating, section 6.2.3).

Tubibau deposits: The Tubibau beachrock show blocky calcite as the most important carbonate cement (Figs. 6.5g and 6.5h). The primary porosity reaches an average of 10% of the rock volume while those beachrocks of PTI and PE present values varying from 17% to

35%. Both Tubibau-1 and Tubibau-2 beachrocks show large quantities of bioclastic fossils. The bioclastic fossils are mostly represented by bivalve shells that are totally recrystallized to LMC (white arrow in Fig. 6.5h). Original calcite bivalve shells (*Ostrea* sp.) apparently occur without any signs of recrystallization (black arrow in Fig. 6.5h).

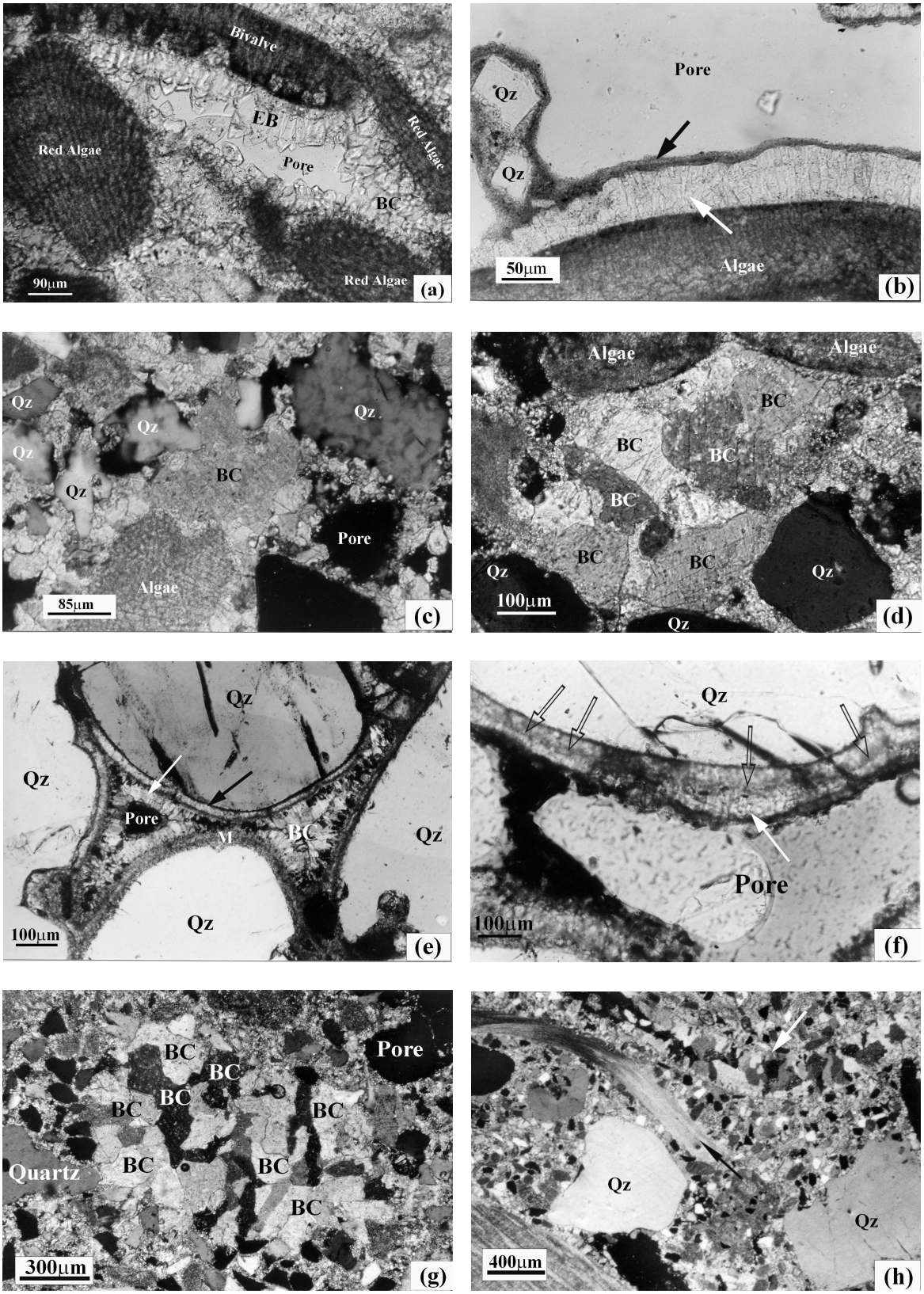

Figure 6.5 - (On previous page): Carbonate cements and their diagenetic features: (a) LMC forming elongated blade rim (EB) on a bivalve shell and blocky calcite (BC) filling the pore space in the beachrock of PTI-4 (plane-polarized light); (b) LMC forming radiaxial fibrous calcite rim (white arrow) that is overlaid with probably HMC as indicated by the black arrow in beachrock of PTI-3 (plane-polarized light); (c) LMC as blocky calcite (BC) filling almost entirely the pore space between quartz (Qz) grains in the beachrock of PTI-2 (cross-polarized light); (d) LMC forming blocky calcite filling former pore space of beachrock of PTI-3 (cross-polarized light); (e) Two generations of LMC forming stubby blade rim (black arrow) and elongated blades (white arrow) that grow forward to the pore forming blocky calcite (BC) from beachrock sediments of PE . Microcrystalline cement probably of LMC (M) occurs as well as the first generation (cross-polarized light); (f) Two generation of LMC cements forming stubby blade as the first generation and the second as pendant cements (white arrow) of beachrock deposit of PE. The transparent arrows indicate the contact between the two cement generations (plane-polarized light); (g) LMC forming blocky cement (BC) in a former pore space of the Tubibau-1 beachrock. Note that the BC has filled almost entirely the pore space (cross-polarized light); (h) Tubibau-2 beachrock showing original aragonite bivalve shell totally transformed in LMC (white arrow). The black arrow indicates an *Ostrea* calcite shell apparently preserved (cross-polarized light).

The high abundance of LMC filling almost all pores in Tubibau beachrock contrasts with those LMC from PTI and PE where the primary porosity is still well preserved.

The chemical composition and stable isotopic values for the Pleistocene and Holocene carbonate cements are listed in Table Nr. 6.1.

Table 6.1 - Chemical and isotopic values of the Holocene and Pleistocene deposit cements

Thin Section	Outcrop	Cement Type	*$MgCO_3$ (Mol%)	*Sr (ppm)	$\delta^{13}C$ PDB	$\delta^{18}O$ PDB
HOLOCENE						
SB5-A	São Bento Beachrock	Micrite	13.16	0	3.07	-0.07
SB5-B	São Bento Beachrock	Aragonite fringe	NV	12,600	2.93	0.21
BR-Rec	Recuado Beachrock	Micrite	14.89	0	-0.04	-1.37
Gali-Br2a	Galinhos-2 Beachrock	Micrite	14.26	0	2.64	0.45
Gali-Br2b	Galinhos-2 Beachrock	Micrite	14.53	320	2.43	0.51
Gali-Br1	Galinhos-1 Beachrock	Aragonite fringe	NV	13,400	3.53	0.84
Gua-1	Guajiru Beachrock	Aragonite fringe	NV	10,500	3.44	0.33
PLEISTOCENE						
PE-1	Ponta do Emissário BR	Blade-1	2.56	830	-7.64	-3.91
PE-2	Ponta do Emissário BR	Blade-2	3.48	260	-6.16	-4.25
PTI-2a	Ponta dos Três Irmãos-2	Blocky	0.6	600	-6.49	-3.82
PTI-2b	Ponta dos Três Irmãos-2	Blocky	0.49	900	-7.07	-3.36
PTI-3a	Ponta dos Três Irmãos-3	Blade and Blocky	2.02	800	-7.3	-4.48
PTI-4a	Ponta dos Três Irmãos-4	Blade	0.05	200	-6.28	-3.1
TUB-1a	Tubibau-1	Blocky	0.7	400	-10.35	-3.95
TUB-1b	Tubibau-1	Blocky	0.82	800	-10.13	-4.34
TUB-2a	Tubibau-2	Blocky	0.16	540	-9.63	-3.79
TUB-2b	Tubibau-2	Blocky	0.32	0	-10.03	-4.59

NV= No value; BR= Beachrock
*From electron microprobe.

The chemical and isotopic signatures for carbonate cements of Holocene age are listed as well as the comparison with those of the Pleistocene age. From the chemical and isotopic signatures the deposits of different ages can be easily separated. While the Holocene cements

present characteristics typical of marine origin, the Pleistocene cements demonstrate typical transformations under freshwater influence. The Pleistocene carbonate cements are magnesium-poor calcite precipitates (LMC) containing 3.48 to 0.05 Mol % of $MgCO_3$ (Table Nr. 6.1). The strontium contents of carbonate is usually high in aragonite originally from a marine environment, and low in a freshwater environment. The values of Sr content in this study between 0 to 900 ppm would indicate the latter case, however the supposition is maintained that carbonate cement was originally marine.

The isotopic values for the Pleistocene cements also indicate a post-depositional exchange with meteoric waters (Table Nr. 6.1). The $\delta^{13}C$ in the Pleistocene cements varies between -6.28 and -10.03 (related to the universal PDB standard), whereas the $\delta^{18}O$ varies between -3.1 and -4.59. From Table Nr. 6.1 it is evident that the ^{18}O and ^{13}C concentrations in the Pleistocene deposits are low, when compared to those of the Holocene deposits. The depletion of ^{13}C implies alteration in a relatively open system in which soil-CO_2 derived from oxidation of organic matter and depleted in ^{13}C is produced in the vadose zone. The $\delta^{18}O$ signature of the sedimentary carbonates is controlled among other factors, by the temperature of the repositioning of replacement carbonates, the $^{18}O/^{16}O$ ratio of the water from which the carbonates precipitate, the original $\delta^{18}O$ values of the skeletal grains, and the water/rock ratio (Morse & Mackenzie 1990). The Figure 6.6 shows the $\delta^{13}C$ *vs.* $\delta^{18}O$ diagram of Milliman (1974) together with the samples of this study.

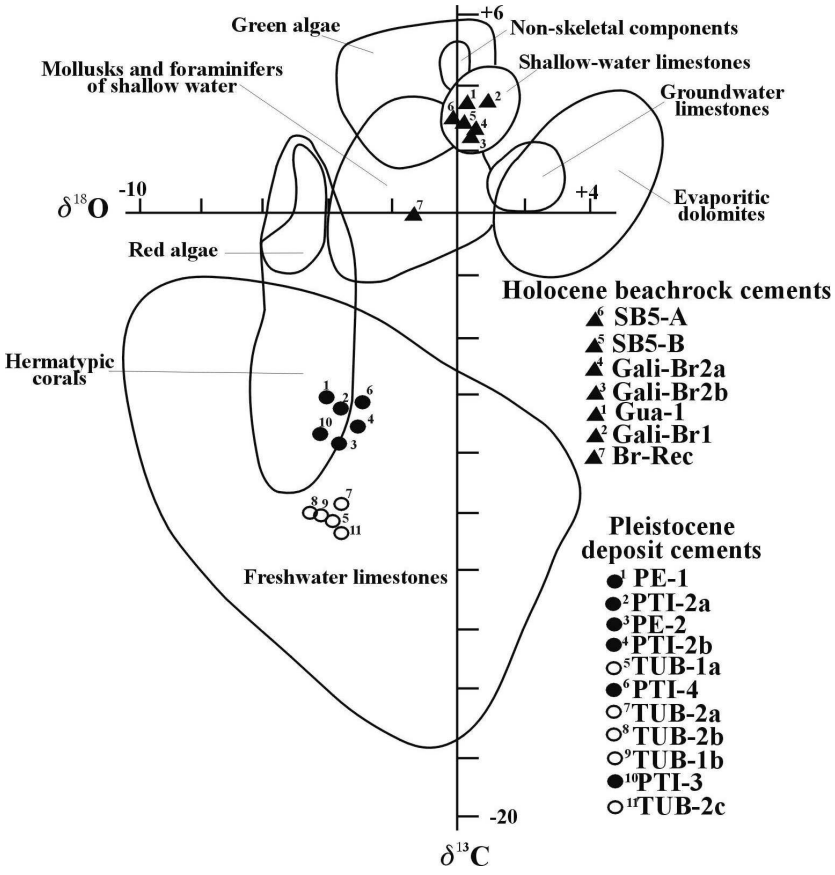

Figure 6.6 - Oxygen-and-carbon-isotope plot (PDB‰) for Holocene and Pleistocene deposit cements. The diagram structure and carbonate sediment fields were obtained from Milliman (1974). See Table Nr. 6.1 for isotopic values.

The diagram illustrates that the Holocene cements plot in the shallow water limestones, with exception of sample 7, whereas those Pleistocene cements form two groups

within of freshwater limestone field. The cements from PE and PTI deposits form the group marked by black dots whereas open circles represent the cements obtained from Tubibau deposits. The separation between these two groups reflects the chemical changes of the precipitated solution during the cementation process. Such chemical changes certainly reproduce the different outcrop positions after cementation relative to the sea and groundwater levels as well as proximity to dense vegetation. An explanation for the high depletion of $\delta^{13}C$ in Tubibau beachrock could be the dense vegetation combined with a thin soil layer that has buried such beachrock. This would result in a high rate of organic matter decomposition causing the depletion of $\delta^{13}C$ in the freshwaters within the pores. Another explanation could be that the Pleistocene deposits located eastward are younger than those positioned westward. Thus, the Tubibau beachrock could have been subjected for a longer time period to diagenesis and chemical alterations. Nevertheless this last supposition can only be answered with an age determination of these deposits.

6.2.3 - Radiocarbon dating

Radiocarbon datings were carried out on shelly material from PE and Tubibau deposits. The careful pretreatment was necessary due to the scarcity of carbonate material, which has not been recrystallized. Figure 6.7 demonstrates that the recrystallization process, marked by the transformation from aragonite to calcite, occurs preferentially as a front migrating inward from the outer valve surface (Fig. 6.7a). An aragonite band seems to still be preserved in the bivalve shell (Fig. 6.7a) Note the thickness of the calcite band on the half of the shell when contrasted with that located on the inner half. This probably suggests that the recrystallization process has taken place mainly due to the meteoric water percolation in the outcrop since the bivalve shells were deposited, with the valve outer surface positioned upwards.

X-ray diffraction of the two bands reveals that the white portion is uncontaminated aragonite and the grey band is secondary calcite. In Figure 6.7b it can be seen that the aragonite crystal preserves the cross-lamellar structure typical for aragonite bivalve shells whereas the calcite occurs as a block crystal. The isotopic composition of both carbonates was measured. The sampled sites are marked by black dots on the bivalve shell in Figure 6.7a. The $\delta^{13}C$ and $\delta^{18}O$ signatures of the aragonite minerals show undoubtedly that they are uncontaminated with secondary calcite and they can be correlated with those of mollusks and foraminifers of shallow water (Fig. 6.8) whereas the calcite mineral can be associated with those of a freshwater environment (Milliman 1974). After the pretreatment of the bivalve shells they were sampled for both aragonite and secondary calcite, for dating using the AMS ^{14}C system that requires at least 1 mg carbon to allow a precise measurement. The results are shown in the Table Nr. 6.2.

For the Tubibau beachrocks only *Ostrea*, which is a bivalve shell composed mineralogically of calcite was dated.

The obtained ages for aragonite, secondary and primary calcite show values ranging between 34540 + 510/-480 yr BP and 45560 +1950/-1570 yr BP. For PE sandstone original aragonite exhibited ages varying from 39530 +1000/-890 (Sample PE-8) to 44760 + 1810/-1480 (Sample PE-1) whereas secondary calcite with greater negative values for $\delta^{13}C$ produced ages varying from 37110 +720/-660 (Sample PE-3) to 45560 +1950/-1570 (Sample PE-6). Ostrea shells from Tubibau deposits were dated at 37940 +860/-780 yr BP (Sample Tubibau-1), 40930 +1260/-1090 yr BP (Tubibau-2a) and 42 060 +1470/-1240 yr BP (Sample Tubibau-2b). All data demonstrate that the real ages for both original and secondary mineralogy are probably beyond the limit of radiocarbon dating. This conclusion is based on the fact that for these ages the sea level estimated from isotopic data was positioned 70-80m

below the modern level (Hanebuth *et al*. 2002, Chappell *et al*. 1996 and Rohling *et al*. 1998). That is to say the coastline 40000 years ago in the study area was located some 20 km seaward from the current coastline. Thus one cannot expect beach deposits with 40000 years age to be found on the modern coastline. Therefore the deposits discussed above could be correlated with those of the penultimate transgression (Martin *et al.* 1993) or older.

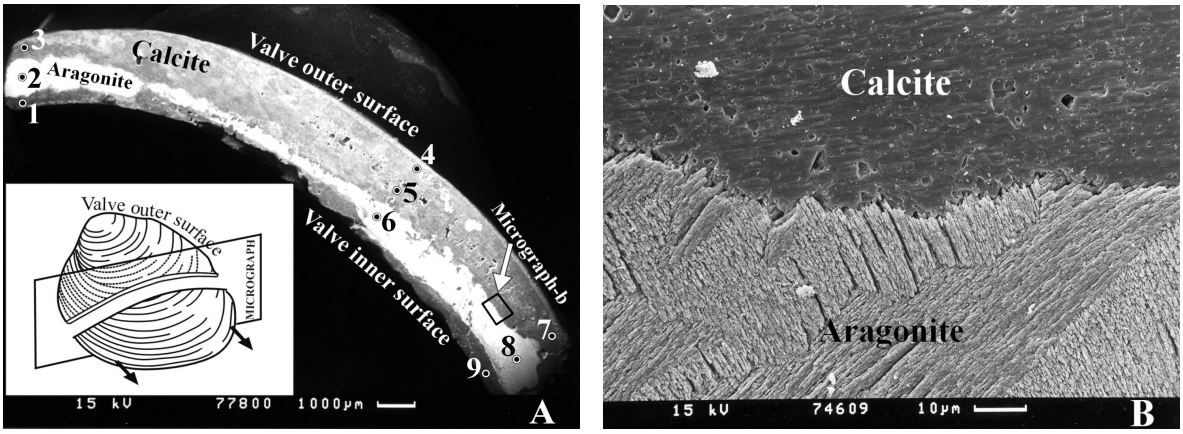

Figure 6.7 - Micrographs of a partially recrystallized bivalve shell from PE sandstone. (a) Micrograph normal to the maximum growth axis of the clam showing a thicker band of secondary calcite in the valve outer side and a thinner white band composed of original aragonite. The dots refer to the sampled sites for isotopic analyses; (b) detail of the contact between original aragonite, showing crossed-lamellar structure, and secondary calcite in the shell.

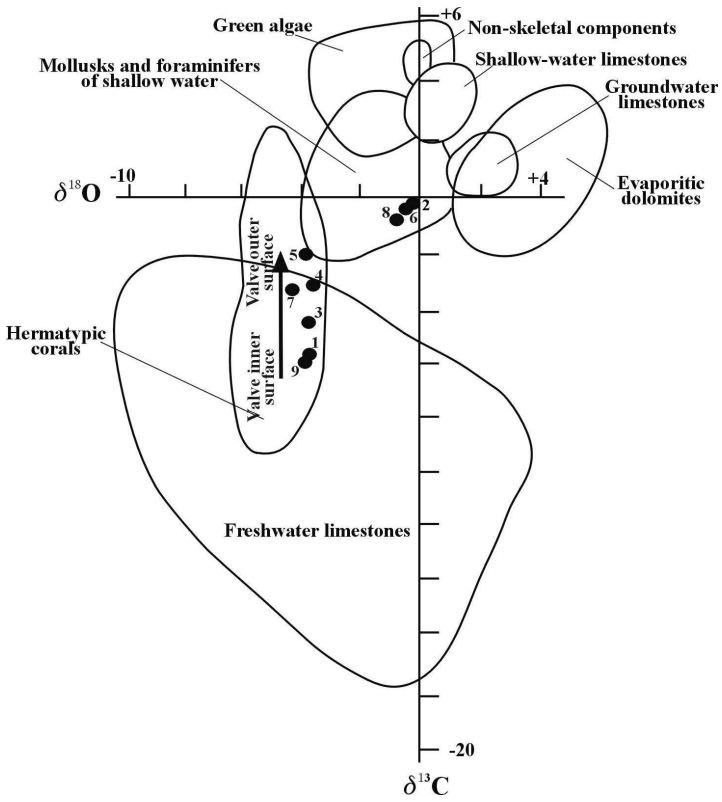

Figure 6.8 - Oxygen-and-carbon-isotopic plot (PDB‰) for aragonite and calcite present in the bivalve shell viewed in the Figure 6.7a. Diagram and carbonate sediment fields were obtained from Milliman (1974).

Contamination with old ^{14}C in secondary calcite is not considered because the reactions involving carbonate exchange are restricted to the meteoric aqueous phase (see fig. 6.7a). Thus the carbonates are originated during the aragonite-calcite transformation *in situ* (dissolution of aragonite bioclasts and original marine cements). One would expect older ages for the original aragonite and younger ages for the secondary calcite due the contamination with modern ^{14}C (atmosphere), but all ages are similar. Bowman (1990) has shown that a contamination of 10% of modern ^{14}C in a sample at 40000 years old carbonate would result in a radiocarbon age of 18010 years (-21990 younger than original age). Although it cannot be determined to which extent the sample of this study have been contaminated with modern ^{14}C, it may be assumed that the ages of secondary calcite contaminated with "modern" carbon are still beyond the dating limit. The ages obtained for the samples PE-3 and PE-5 represent much younger depositional ages. However extreme contamination by modern ^{14}C and repeated contamination by younger ^{14}C (possibly more than 10%) may have altered the age to such an extent that approximately 90000 years are eliminated since the possible deposition during the penultimate transgression.

Table 6.2 – AMS radiocarbon data of the Pleistocene deposits

Laboratory Number*	Sample	Height (m assl)	X-ray ES	$\delta^{13}C$ AMS (‰)	Age [^{14}C yr BP]	[yr BP] +/-
KIA 11731	PE-1	-0.3	PA	0.14±0.1	44760	1810/1480
KIA11733	PE-2	-0.4	SC	-4.96±0.34	43670	1580/1320
KIA11734	PE-3	-0.2	SC	-7.0±0.6	37110	720/660
KIA11735	PE-4	6.1	PA	1.48±0.08	43370	1490/1260
KIA11737	PE-5	0.3	SC	-5.53±0.18	34540	510/480
KIA12337	PE-6	-0.7	SC	-5.16±0.08	45560	1950/1570
KIA14745	Tubibau-1	0.5(?)	PC	0.39±0.07	37940	860/780
KIA14753	Tubibau-2a	0.7(?)	PC	-0.71±0.11	40930	1260/1090
KIA14754	Tubibau-2b	0.7(?)	PC	-0.12±0.1	42060	1470/1240
KIA16091	PE-7	6.0	PA	0.78±0.15	39530	1000/890
KIA16092	PE-8	5.8	SC	-5.23±0.18	40520	1170/1020

* Leibniz Laboratory – Kiel, Germany
m assl= meter above spring tide sea level
ES= electron microscopy; PA= primary aragonite; SC= secondary calcite; PA= primary calcite

The ages for Tubibau beachrocks also seem to be beyond the limit of radiocarbon dating. The *Ostrea* shells are originally composed of primary calcite and do not show any signal of contamination with modern carbon. The $\delta^{13}C$ values (Table Nr. 6.2) are typical for an organism living in marine shallow water. The age differences between samples of the same horizons (e.g. Tubibau 2a and 2b) may reflect the use of inappropriate background material during the dating (Nadeau *et al*. 2001) or even postdepositional reworking.

As demonstrated, the depositional age of the Pleistocene deposits could not be determined using the radiocarbon dating method. Therefore, U-Th techniques were employed in the attempt to date the Pleistocene bioclasts.

6.2.4 - U-Th dating

Six samples of *Ostrea* shells were chosen for U-Th dating. Through observations of thin section of the bioclasts, detailed inspection with electronic microscopy and investigations of the magnesium content from microprobe analysis, the most suitable shelly material for U-Th dating was identified. Since all aragonite shells showed signs of recrystallization, only *Ostrea* that are composed of calcite, were selected for U-Th dating. The magnesium (Mg) and

strontium (Sr) content in the selected O*strea* shells (Table Nr. 6.3) correspond to the reference ranges cited by Milliman (1974), who compiled the chemical analyses of selected pelecypod shells. The Mg content measured in the *Ostrea* shells of the area varies from 0.25 to 1.4% whereas the Sr content varies from 0.01 to 0.081%. With the exception of *Ostrea*-2 all other elemental content varied within the reference value limits, suggesting the absence of recrystallization. Analyses of the *Ostrea* under the electron scanning microscopic do not show any signal of recrystallization, although in calcite shells this is quite difficult to recognize. Moreover the structural arrangement of the calcite crystal forming regular foliated structures may conceal allogenic constituents.

Table Nr. 6.4 presents the radiometric data obtained in the *Ostrea* shells. All shells from the Tubibau 1 (TU-1) beachrock were selected from the same horizon, which is positioned at 0.7m above the present spring-tide level. Two shells were collected from PE beachrock at 0.4m above and 0.2m below the present spring-tide level. The samples U5024 and U5031 are from the same shell. The $^{230}Th/^{234}U$ ages were calculated using the equation of Kaufman & Broecker (1965).

Table 6.3 - Microprobe analyses of Pleistocene *Ostrea*

	Mineral	Percent	
		Mg	Sr
Ostrea-1	Calcite	0.31	0.031
Ostrea-2	Calcite	1.4	0.081
Ostrea-3	Calcite	0.25	0.042
Ostrea-4	Calcite	0.36	0.090
Ostrea-a	Calcite	0.19	0.010
Ostrea-b	Calcite	0.57	0.050

The need of radiometric ages reaching more than 50,000 years in coastal studies has increased with the discovery and description of Pleistocene coastal deposits related to the penultimate, or older, sea level cycles. The U-Th methods have yielded the requisite ages for coastal deposits raging from 5,000 to 300,000 years, but several studies have also demonstrated their invalidity for molluscs (Szabo & Rosholt 1969, Kaufman *et al*. 1971, Szabo & Wedder 1971, Sherwood *et al*. 1994 and McLaren & Rowe 1996). Some authors, nevertheless, have found consistent U-Th ages from molluscs for Holocene and Pleistocene coastal deposits (Ivanovich *et al*. 1983 and Giresse *et al*. 2000). The key assumption in the age determination is that the shells have remained in a closed system with respect to these elements after the death of the mollusc. Various criteria have been proposed to validate and evaluate carbonate samples (Veeh & Burnett 1982). Among these criteria: a) there should be no evidence of recrystallization and/or deposition of void filling cement; b) the U content in the sample should not differ significantly from that in a contemporary equivalent and c) the $^{234}U/^{238}U$ ratio should be consistent with the $^{230}Th/^{234}U$ ratio of the sample (that is to say the ratio should show a systematic decrease with age). Furthermore the $^{234}U/^{238}U$ activity ratios in the dated marine shells should be close to 1.14±0.01, the accepted value for oceanic waters (Kaufman *et al*. 1971). If this ratio is greater than 1.14, assimilation and uptake of uranium isotopes at least partly from sources other than oceanic waters has taken place (Veeh & Burnett 1982).

The obtained U-Th data for bivalve shells (Table Nr. 6.4) show that the various samples collected in one horizon have different ages. For Tubibau 1 the ages range from 54.1 to 134.8kyr whereas for PE sandstone the ages vary from 73.2 to 97.6 kyr. The samples numbered U5024 and U5031 are two sub-samples from one *Ostrea* and they exhibited different ages. In general the data reveal that the shells have behaved as geochemically open system. Therefore all age must be considered suspect. Two samples, U5025 and U 5026, yielded a $^{234}U/^{238}U$ activity ratio close to the ocean waters and result in ages corresponding to

the penultimate sea level highstand (isotope substage 5e, Chappel *et al*. 1996 and Hearty *et al*. 1999) but more data is needed to confirm this age-interval.

Table 6.4 – Uranium series disequilibrium data obtained from bivalve shells

Laboratory Number	Sample (location)	Height (m assl)	^{238}U (dpm/g)	Activity ratios		Apparent age (kyr)
				$^{234}U/^{238}U$	$^{230}Th/^{234}U$	
U5025	*Ostrea*-1 (TU-1)	0.7(?)	0,46±0,001	1,13±0,01	0.72±0.008	134.8±4
U5030	*Ostrea*-2 (TU-1)	0.7(?)	0,19±0,001	1,18±0,01	0.55±0.01	85.7±2
U5027	*Ostrea*-3 (TU-1)	0.7(?)	0,15±0,001	1,20±0,03	0.40±0.011	54.1±2
U5026	*Ostrea*-4 (TU-1)	0.7(?)	0,34±0,001	1,13±0,01	0.69±0.009	122.2±4
U5028	*Ostrea*-a (PE)	0.4	0,20±0,001	1,18±0,01	0.50±0.007	73.2±2
U5024	*Ostrea*-b (PE)	-0.2	0,20±0,001	1,16±0,01	0.54±0.008	82.1±2
U5031	*Ostrea*-b (PE)	-0.2	0,21±0,001	1,16±0,01	0.60±0.011	97.6±3

TU-1 = Tubibau beachrock 1, PE = Ponta do Emissário beachrock.
assl = above current spring tide sea level
dpm/g = decay unit per minutes per gram

Although no secondary diagenetic alteration has been identified in the bivalve shell with transformations of original shell mineralogy, the results indicate that shells are likely to exchange uranium with the environment. Similar observations were described by Szabo & Wedder (1971) for mollusk shells without visible alteration from California.

Recently Barreto *et al*. 2002 dated the aeolianites of the PTI, via thermoluminescence (TL) at 117-110 kyr and linked them to those located 1000km further south along the coast and suggested an uplift of 12m for the PTI deposits. Although the authors did not discuss the significance of the TL ages, it is believed that the beach deposits represent the last Pleistocene sea level highstand. When correlated to the isotopic substage 5e (120 kyr) the sea level can be positioned approximately 6 m higher than the present level (Chapell *et at*. 1996 and Shackleton 1987). Nevertheless the depositional age could be even higher, which would then correspond to an earlier Quaternary sea level highstand. Thus more dating with use of different techniques should help to position the depositional age precisely in time.

The fact that such coastal deposits (aeolianite and beachrocks) form cliffs reaching 20 m in height and thus occurring 10-12m above the sea level predicted for 120 kyr ago in this area (Barreto *et al*. 2002), does not necessarily mean a later uplift of 10-12m. The aeolianites are not a direct sea level indicator. Only the height of the contact between aeolianite and beachrock can be used as a relative sea level indicator if no erosional surface is present. In this case the top of the beachrock (upper foreshore) represent the former spring-tide sea level.

In the cross sections of the cliffs at PTI and PE no erosional surface between aeolianite and beachrock was recognized (Fig. 6.3). Therefore the top of the beachrock should represent the former spring-tide sea level. If one considers that the sea level 120kyr ago was approximately 6m higher than the current level (Chapell *et at*. 1996 and Shackleton 1987) one would expect beach deposits to occur some kilometers inland from the present coastline. This is not the case. Another interesting fact is that at PTI the contacts between aeolianites and beachrock (upper foreshore) lay between 1.4m and 2.1m above the present maximum spring-tide level whereas at PE this contact is positioned 3.5m above the present maximum spring-tide sea level (Fig. 6.3).

The different heights of the contact between aeolianite and beachrock relative to the present spring-tide level indicate different rates of tectonic uplift over the whole area. The beachrock facies was deposited under sea level conditions similar to the modern because a

spring-tide level positioned 3.5m above the present spring tide would set down beach sand some kilometers inland from the current coastline. The recognition of two phases of marine cement precipitation and its later alteration in freshwater environment for PE beachrock suggests that such deposit was subjected twice to the marine influence via tectonics. The absence of visible tectonic structures in the outcrops hinders the interpretation of the tectonic kinematic patterns responsible for the uplift. The Carnaubais fault that occurs on the eastern limit of the Potiguar rift may play an important role in the tectonic coastal history of this area. With the help of shallow seismic profiles (GPR), such structures affecting coastal outcrops can be evidenced and so enable an appropriated tectonic regime of tension to be proposed.

6.3 - Holocene coastal evolution

The start of Holocene coastal evolution for the study area may be recognized as the point when the sea flooded the inner shelf and subsequently reached, for the first time, the position of the current sea level 7000 yr BP. The progressive flooding of the inner shelf produced landward retreat of ancient coastlines, which is marked by parallel sets of aligned underwater outcrops related to ancient beachrocks. During the inner shelf flooding the ancient deposits were reworked and redeposited by the inner shelf currents which had started to develop. The coast had previously been built as a consequence of penultimate sea level highstand approximately 120000 yr BP, after which followed a regression to the last glacial maximum. Together with vertical tectonic movements, this provided a complicated framework for the subsequent Holocene coastal evolution of the area. The occurrence of seafloor highs and lows on the inner shelf that have conditioned the main underwater currents may reflect such vertical tectonics. The actual coastline roughly follows that evidenced for the penultimate transgression due the similar sea level highstands.

During the Holocene transgression large amounts of inner shelf sediments had been transported landward producing transgressive barriers. When such barrier-islands are positioned close to the actual coastline, shallow lagoons and tidal flats are formed on the landside being connected to the open sea by tidal channels and/or tidal inlets.

The boomer profiles taken along the main tidal channel parallel to the Galinhos' Spit (Fig. 6.9) show internal sedimentary structures and deposit geometry that can be correlated to those of already filled paleo-channels. Acquisition of subsurface stratigraphic information on Galinhos spit with GPR identified washover, paleo-channel, shoreface and lagoonal deposits

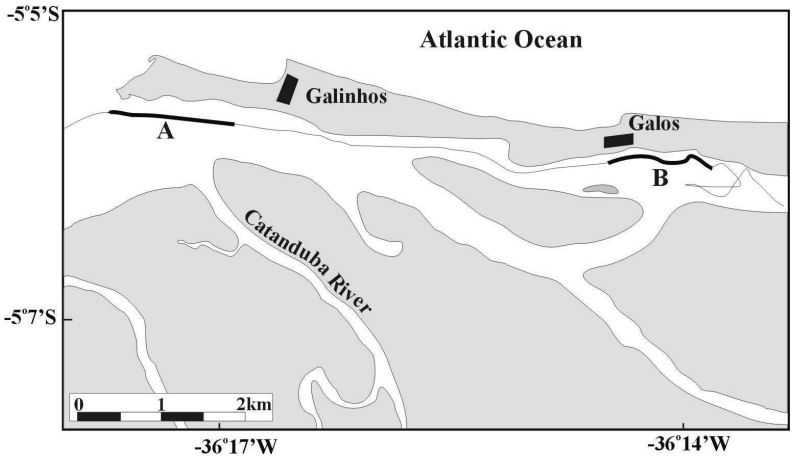

Figure 6.9 - Location of the examined boomer profiles (adapted from Rotzoll 2001). The thin line represents the entire profile whereas the thicker lines symbolize the sections showed in the Figures 6.10 and 6.11.

confirming the existence of former barrier-island (Xavier *et al*. 2001, Lima *et al*. (2002a).

Figure 6.10 shows boomer profile "A" demarcated in Figure 6.9. At least three channels (C1, C2 and C3) can be identified from this boomer profile. The filled channel C3, positioned eastwards, presents reflectors dipping from east to west over a distance of about 135m. Further to the west the same reflector becomes horizontal after which the dip direction changes to east. The channel C2 is well shown by the reflectors. It is 150m wide and 1.5m deep. This buried channel may probably represent the extension of the Catanduba River (Fig. 6.9) to the open sea when the spit of Galinhos was a barrier-island system. Another smaller channel seems to occur at the end of the spit (C1). It shows an asymmetrical shape and it may represent the active channel present at this position.

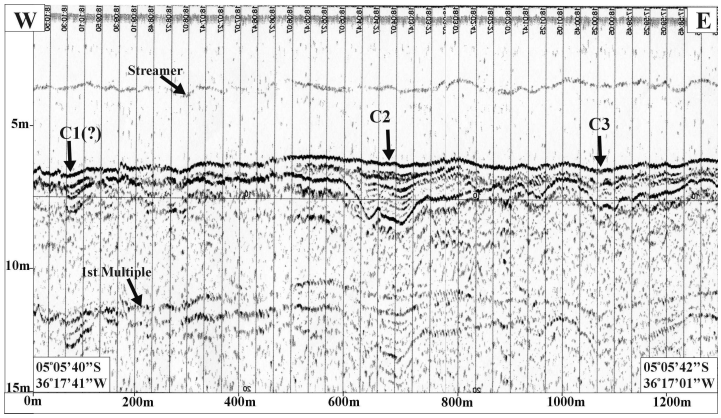

Figure 6.10 - Section "A" showing filled former channels (as indicated by arrows) positioned normal to the spit of Galinhos. For location see Figure 6.9.

Figure 6.11 shows the boomer profile "B", the position of which is illustrated in Figure 6.9. In this section at least two possible paleo-channels can be identified from the reflectors. The buried channel C2 presents reflectors dipping mainly from east to west. The sediment thickness reaches 1.5m and the paleo-channel width is approximately 165m.The reflectors at the base of the buried channel C1 dip from west to east over a distance of 175m. The deeper part of the paleo-channel reaches 2.9m below the higher surface. Some reflectors dipping to the west seem to represent sedimentary structures such as cross bedding. Nevertheless the reflectors are indistinct and further interpretation cannot be undertaken.

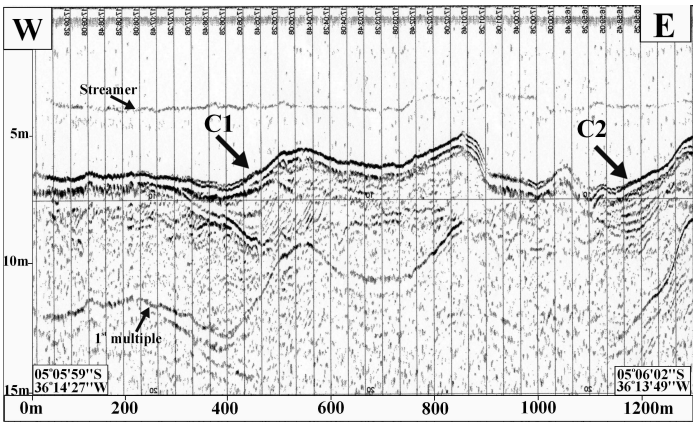

Figure 6.11 - Section "B" showing two filled former channels (a rrows in the figure) that were positioned perpendicular to the current spit of Galinhos. For location see figure 6.9.

The occurrence of such paleo-channels in the spit of Galinhos demonstrates that this spit has not prograded and built up continually from east to west as its shape suggests. Such paleo-channels have originated during the maximum of the last transgression when the mean sea level was 1.2m above its present position (Fig. 6.12). At this time the presence of transgressive barriers had induced the occurrence of larger lagoonal areas and water volumes from Ponta dos Três Irmãos to Galinhos. The tidal channels landward of the barrier-island were wider due to the large water volume of the sea level highstand moving the shoreline further inland. The tidal flat of São Bento had the same tidal channel system as in Galinhos. During Holocene highstand Recuado beachrock was cemented (Fig. 6.12). It seems that the Recuado beachrock was formed from a beach of a transgressive barrier because lagoonal sediments can be found on the landward side of this beachrock (Fig. 6.12). The same origin can be also proposed for São Bento beachrock, which during the maximum of the Holocene transgression had been submersed and the second phase of marine cementation was precipitated. Although the age control of the beach ridges close to São Bento and Caiçara is still missing, it is believed that the ridge positioned furtherest inland must represent a transgressive barrier (Fig. 6.12). The presence of lagoonal deposits supports this scenario. The Holocene highstand was 1.2m above the present mean sea level as indicated by the Recuado Beachrock and the transgressive sand ridge São Bento (see Chapter 4, Fig. 4.2).

The formation of longshore currents occurring along the coastline started to intensify since the sea level stabilized in its current position. The build up of coastal dunes probably set up of the Holocene highstand and was increased later during sea level regression as the beach face subjected to the wind action from east and northeast became wider. The combination of sea level drop, coastal currents and the build up of coastal dunes has fundamental importance on the later evolution of the coastline (Fig. 6.13): Approximately 3600 yr BP when the sea level was receding, regressive sand ridges on the coast of São Bento and Caiçara were deposited. Also the tidal inlets became narrower due to both longshore transport (downdrift migration of the barrier) and dune advance (Fig. 6.13). The sedimentation in the lagoon of São Bento was cyclic and ceased shortly after 3600 yr BP. The high content of evaporite minerals in different sediment sections of the paleo-lagoon confirms this supposition. Both dune advance and longshore transport of sediments should have played an important role in the cyclic sedimentation in the lagoon. The connections between the lagoon and the open sea were probably closed several times by the dune advance and sedimentation induced by longshore transport (downdrift migration of the barrier). The availability of sediments in the eastern part of the area seems to have been higher than in the western part. The satellite image in Figure 3.1 (Chapter 3) explains this phenomenon, indicating that the sediment load in the eastern portion of the inner shelf is much higher than in the western portion. Moreover the wind approach, which has been responsible for coastal dunes build up, moves sediment from east to west, which is almost the direction of the coastline. The transported sand is thus deposited in the beach zone. In contrast, the wind acting on the barrier-island of Galinhos is in average southwestward directed producing dune advance landward (Figs. 6.13 and 6.14). This pattern leads to a sediment lack for this area in comparison with the eastern portion. This may explain the absence of regressive sand ridges in the region of Galinhos. While the sedimentation in the lagoons located eastward ceased, sedimentation in lagoons in the west is continuing. At present only tidal channels are open, but shallow lagoons are converted to saltworks and shrimp farming for the major part. The vibrocore records in the lagoon system of Galinhos and their datings confirm the high rate of sedimentation. The permanent marine inflow and outflow in the tidal system of Galinhos and Galos has permitted such a high rate of sedimentation. Although it cannot be said exactly when the tidal inlets of the barrier-island system of Galos and Galinhos were totally closed, it is supposed that this should have occurred sometime before the cementation of the beachrocks located in this area, as they lie perpendicular to the ancient tidal inlets. As the ages of the beachrocks located on

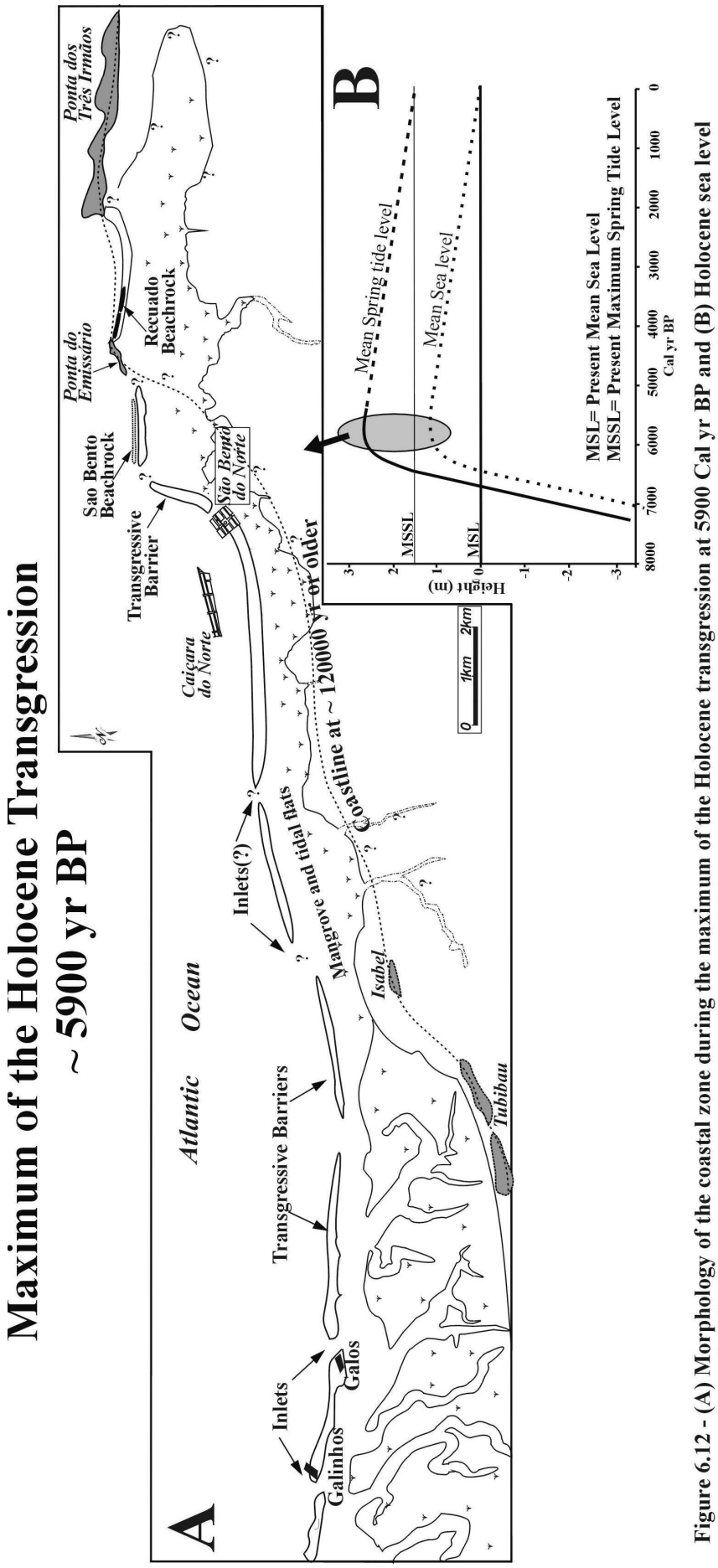

Figure 6.12 - (A) Morphology of the coastal zone during the maximum of the Holocene transgression at 5900 Cal yr BP and (B) Holocene sea level curve for the area.

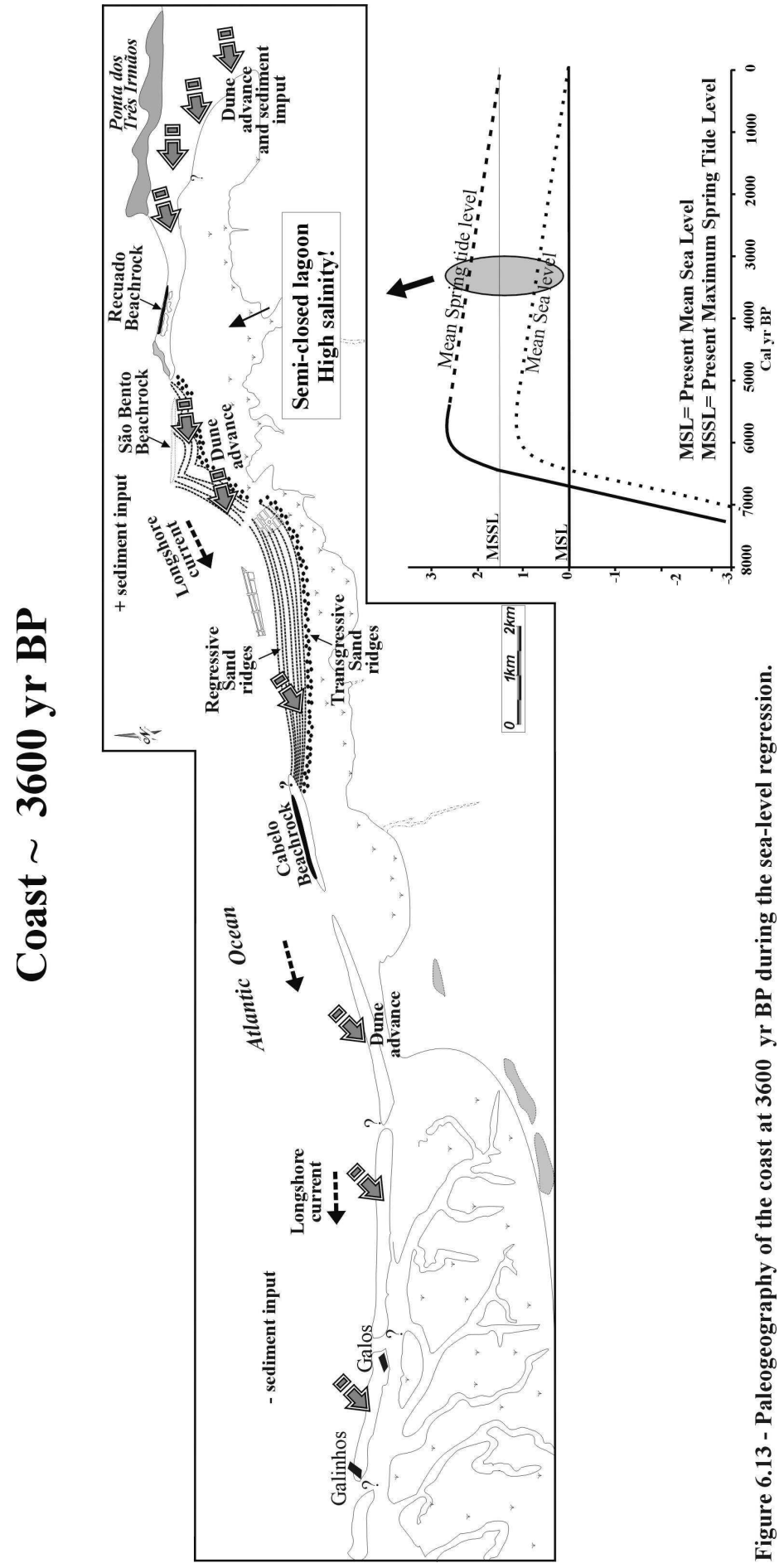

Figure 6.13 - Paleogeography of the coast at 3600 yr BP during the sea-level regression.

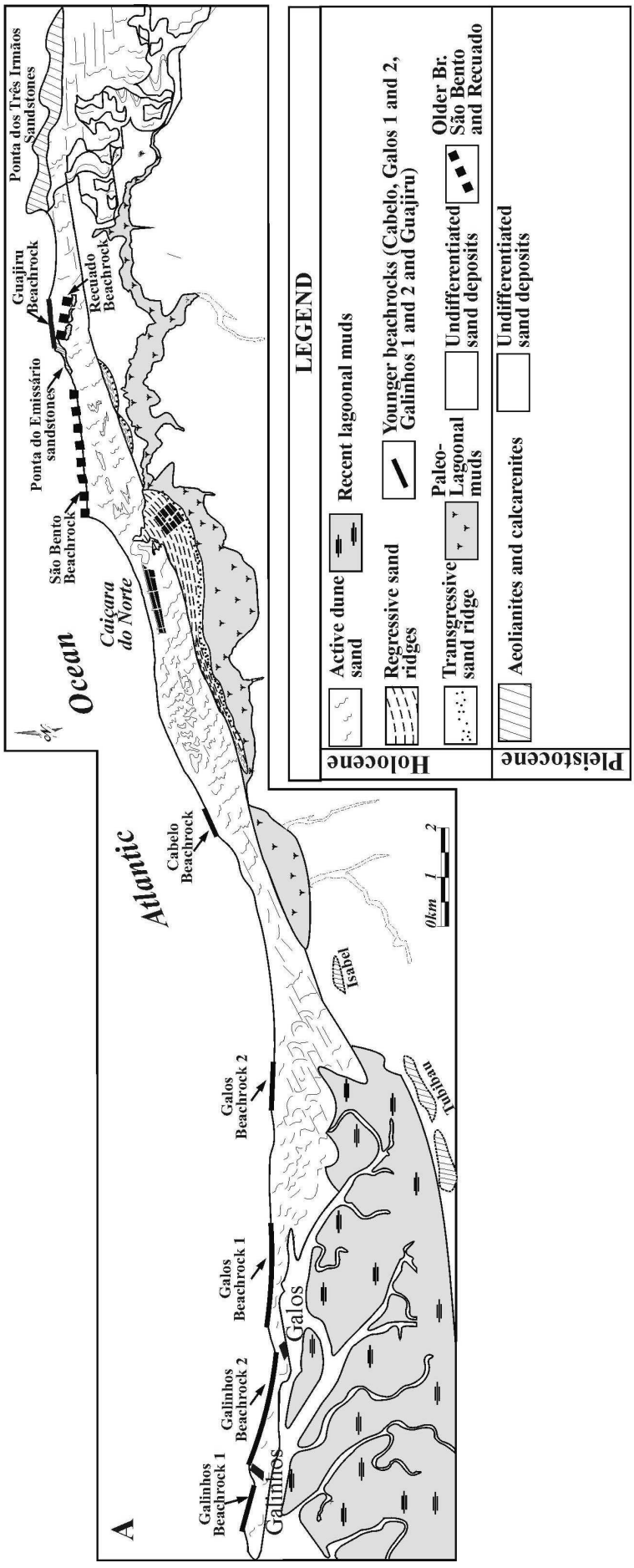

Figure 6.14 - Geology and morphology for the coast between Ponta dos Três Irmãos and Galinhos.

the spit of Galinhos range from 1780 Cal yr BP to 3330 Cal yr BP, the closure of the first tidal inlets should have occurred shortly before 3300 yr BP. Once the tidal inlets were closed, the rapid build up of coastal dunes along the spit and the continuation of sedimentation due to the longshore currents (downdrift migration of the barrier) impeded the reactivation of such connections between the lagoon and the open sea. Such inlets may also have been closed at different times during the regressive phase.

The current coastal morphology (Fig. 6.14) demonstrates that at the time when the paleo-lagoon close to São Bento and Caiçara became extinct, no connection with the open sea existed whereas the lagoon located landward of Galinhos and Galos until today has active tidal channels. The dune advance in the eastern part has closed all connections between the paleo-lagoon and open sea although the paleo-lagoon surface lies almost at the same level as that of the current mean sea level. In the west, landward dune migration has buried lagoonal mud but the tidal channel system remained active due to the existence of the tidal inlet located to the extreme west of the area. The reason why this connection has not been terminated might be the strong ebb flow that impedes the downdrift migration of the spit (Fig. 6.15). All sediment being transported by the longshore drift and ebb outflow has been by-passed to west and the connection between lagoon and open sea has remained open (Fig. 6.15). Lima *et al* (2002b) and Rotzoll (2001) showed that the spit morphology has changed since 1954, but general a trend is not conspicuous. The spit will not migrate further westward to close the channel as long current relation between ebb flow and longshore drift remains active. Such equilibrium relation may be disturbed, for example if ebb-induced flow is not strong enough to maintain sediment transport. The current deterioration of the tidal channels with the increasing use of the lagoonal system for salt-works and shrimp farms might disturb the velocity and power of the ebb flow.

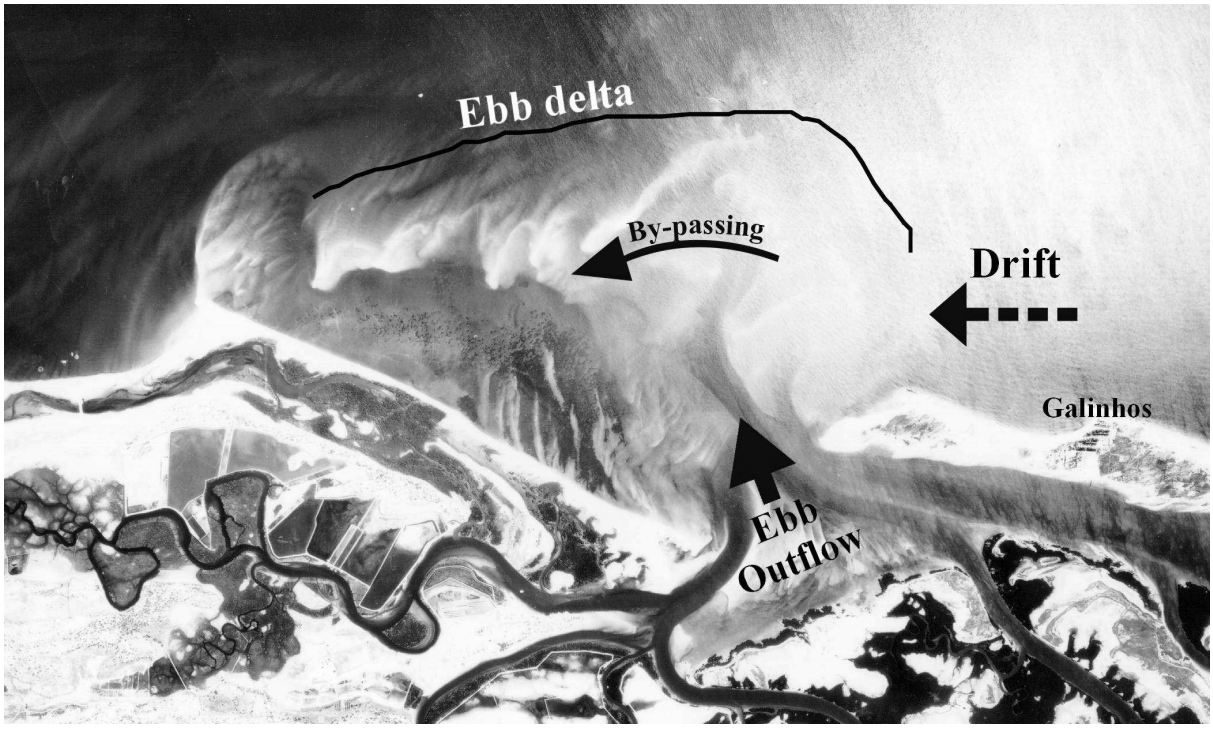

Figure 6.15 - Aerial photograph of 1988 during ebb tide. Note that sediments transported by both ebb outflow and longshore drift, are being deposited westward. The strong ebb jet outflow impedes the growth to westward of the spit.

7 - Conclusions and perspectives

- The inner shelf of the area presents two main zones of sedimentation: a) the eastern part is formed mainly by subaqueous dunes, which have been subjected to the southeastern branch of the North Brazilian Current and (b) the western part that is composed principally of subaqueous sand ridges and seems to be controlled mainly by a northeastern component of the North Brazilian Current. Lithified sediments occur in the two main zones forming lines parallel to the current coast. These deposits, probably beachrock lines, are relicts of the sea level transgressions and regressions that have flooded and exposed the inner shelf during the late Quaternary. The continuation of the research on the inner shelf will improve the understanding of its build up and related flooding history during the late Quaternary.
- The last phase of the deglacial transgression and subsequent regression, littoral drift and dune build up and migration have controlled the Holocene sedimentation of the coast. In the São Bento area lagoonal deposits beyond the modern coastline dated at 7000 Cal yr BP, 3m below the modern sea level, mark such transgression whereas younger sand ridges indicate the regression of the sea. In the Galinhos' area the transgressive phase apparently did not allow for sea level indicators to be preserved whereas the regressive phase may be indicated by the closure of tidal inlets and set up of the spit. High content of evaporite minerals in the lagoonal muds of the paleo-tidal flat of São Bento and the low rate of sedimentation when compared with that of the lagoonal system of Galinhos since the last transgression indicates cyclic marine ingressions and semi-closed lagoon environment for this area. The periodic advance of dune fields closing tidal inlets seems to be the main factor controlling the cyclic marine ingressions. The last marine ingression in the lagoon of São Bento occurred at 3580 Cal yr BP.
- The lagoonal system of Galinhos and Galos has been active since the last transgression permitting a high rate of sedimentation. The increase in human activities through the extension of the saltworks and shrimp farms may disturb the equilibrium conditions in the ebb jet outflow of the tidal system of Galinhos culminating in westward advance of the Galinhos' spit and closure of the unique link between tidal system and open ocean.
- The relative rise compared to the modern mean sea level in the area began approximately at 6400 Cal yr BP, reached the highstand 1.2m above the current level at 5900 Cal yr BP and probably fell to its present position thereafter. Deposits located at a high position within the transgressive and regressive sequences as well as beachrock data confirm this sea level history. The dating of the regressive sequence (beach ridges) and determination of the uppermost level of cementation of the Cabelo beachrock among others will improve the sea level curve of the area.
- Isotopic, chemical and diagenetic data of the Holocene beachrock cements agree with the proposed sea level history. The cements present isotopic and chemical signatures typical of marine origin and thus secondary sea level oscillations, which would allow the alteration of primary marine cements and their precipitation in a meteoric environment, could not have taken place during sea level drop. Vertical tectonics that, according some authors, have caused coastal emergence and submergence during Holocene time cannot be evidenced from geochronological, chemical, diagenetic, isotopic and topographic profiles.
- Only integrated sedimentological, diagenetic, isotopic and age control approaches for beachrocks deposited under mesotidal regime provide reliable data to position former sea levels and thus to propose a model of coastal evolution.

- A group of deposits almost parallel to the current coastline present cements with chemical, isotopic and diagenetic signatures different to those of the Holocene age. Sedimentary and stratigraphic characteristics demonstrate that such deposits compose a regressive sequence. These deposits are composed of aeolianites on the top and foreshore and shoreface deposits at the base (beachrock). Radiocarbon ages of bioclasts found in the beachrocks give average age of approximately of 42000 yr, whereas U-Th ages could not be considered reliable due the open system in the bivalve shells. The deposits are at least 120000 yr old, which corresponds to the penultimate transgression which occurred along the Brazilian coast. Further dating by different radiometric methods in such deposits could indicate their most appropriate age of deposition.
- Two diagenetic cementation stages described for the carbonate cements in the Pleistocene deposits of the Ponta do Emissário suggest that such sandstone might have been exposed at least twice to marine conditions. Such marine influences may not be due to the variation in the eustacy of the sea level during Pleistocene time, because correlated sandstone positioned beside the Ponta do Emissário sandstone present just one stage of cementation. Differential subsidence and/or uplift occurring after sediment deposition (120000 years ago?) might have positioned such deposit under marine influence. Moreover altitudes of the contact between beachrocks and aeolianite that do not show erosional contact present differences up to 3.0m suggesting differential vertical movements. Nevertheless, the absence of visible faults affecting such deposits hinders a better understanding of the tectonic pattern that affected such outcrops. The use of Ground Penetrating Radar on the Pleistocene deposits could decipher such tectonic structures.
- The beachrock lines on the studied coast have worked as a natural protector against coastal erosion. On areas where beachrocks do not occur, serious problems of coastal erosion have taken place (e.g. Caiçara village).
- As future research on the studied area it is suggested that:
  1) Sea bottom morphology and subsurface structures mapped by side-scan sonar and reflexive-seismic surveys in order to follow sea level variations during the Holocene and also during older transgressions on the inner shelf.
  2) The submerged beachrocks and/or other lithified sediments on the shelf must be dated to follow the earlier phases of the deglacial sea level rise and maybe even older Quaternary transgressions on the shelf.
  3) Continuation of the stratigraphic and environmental investigations of the paleo-lagoons that occur along of the north coast of Rio Grande do Norte and systematical studies including a complete coverage by cores in such areas, should give information about spatial geometry of the paleo-lagoonal deposits and thus the Holocene and late Pleistocene evolutionary history of the coast will be better understood.
  4) The definition of the reservoir ocean age for the area as well as of the terrigenous "pollution" in the (paleo) lagoons will improve the carbonate age calibration for marine samples.

Admiralty, 1996. Admiralty Tide Tables: The Atlantic. Admiralty Hydrography Department. The Hydrographer of the Navy, Southampton.

Al-Saleh, S. and Khalaf, F.I., 1982. Surface textures of quartz grains from various recent sedimentary environments in Kuwait. *Journal of Sedimentary Petrology*, 52(1): 215-225.

Alexandersson, T., 1972. Mediterranean Beachrock cementation: Marine precipitation of Mg-Calcite. In: Stanley, D. J. (Editor), The Mediterranean Sea: A Natural Sedimentation Laboratory. Dowden Hutchison & Ross, Pennsylvania, pp. 203-223.

Angulo, R. J. and Lessa, G. C., 1997. The Brazilian sea-level curves: a critical review with emphasis on the curves from Paranaguá and Cananéia regions. *Marine Geology*, 140: 141-166.

Angulo, R.J., Gianini, P.C.F., Suguio, K. and Passenda, L.C.R., 1999. Relative sea-level changes in the last 5500 years in southern Brazil (Laguna-Imbituba region, Santa Catarina State) based on vermitid ^{14} C ages. *Marine Geology*, 159: 323-339.

Araripe, P.T. and Feijó, F.J., 1994. Bacia Potiguar. *Revista de Geociências da Petrobrás*. 8(1):127-141.

Arz, H.W., Pätzold, J. and Wefer, G., 1999. Climatic changes during the last deglaciation recorded in sediment cores from the northeastern Brazilian Continental Margin. *Geo-Marine Letters*, 19: 209-218.

Ashley, G.M., 1990. Classification of larger-scale subaqueous bedforms: A new look at an old problem. *Journal of Sedimentary Petrology*, 60(1): 160-172.

Asmus, H.E. and Guazelli, W., 1981. Descrição sumária das estruturas da margem continental brasileira e das áreas oceânicas e continentais adjacentes. In: PETROBRAS. *Estruturas e tectonismo da margem continental brasileira e suas implicações nos processos sedimentares e na avaliação do potencial dos recursos minerais*. Rio de Janeiro, CENPES/DIMEP, pp.187-269.

Badyukov, D.D., 1986. Ancient shorelines as indicators of sea level. *Journal of Coastal Research*, 2(2):147-157.

Barreto, A. M. F., Bezerra, F.H.R., Suguio, K., 2000a. Variações do nível relatico do mar durante o Holoceno no Rio Grande do Norte, Brasil. In: *XVIII Simpósio de Geologia do Nordeste*, *Vol. 16* (Ed. by S. B. Geologia), Sociedade Brasileira de Geologia, Recife. pp. 15

Barreto, A.M.F., Suguio, K., Bezerra, F.H.R. 2001. Comparação das curvas de variação do nível relativo do mar no Holoceno do litoral norte-riograndense entre si e com outras curvas do Brasil. In: *VIII Congresso da ABEQUA - Mudanças globais e o Quaternário*, Associação Brasileira de Estudo do Quaternário, Imbé. pp. 106-108.

Barreto, A. M. F., Bezerra, F. H. R., Suguio, K., Tatumi, S. H. 2000b. Algumas evidências de níveis marinhos Pleistocênicos no litoral do Rio Grande do Norte, Brasil. In: *XVIII Simpósio de Geologia do Nordeste*, Vol. 16 (Ed. by S. B. Geologia), Sociedade Brasileira de Geologia, Recife. pp. 16.

Barreto, A.M.F., Bezerra, F.H.R., Suguio, K., Tatumi, S.H., Yee, M., Paiva, R.P. and Munita, C.S., 2002. Late Pleistocene marine terrace deposits in northeastern Brazil: sea-level changes and tectonic implications. *Palaeogeography, Palaeoclimatology, Palaeoecology*, 179: 57-69.

Bathurst, R.G.C., 1971. Carbonate sediments and their diagenesis. Developments in Sedimentology, 12. Elsevier Sciences, Amsterdam, 658 pp.

Bathurst, R.G.C., 1974. Marine diagenesis of shallow water calcium carbonate sediments. *Annual Review of Earth and Planetary Sciences*, 2:257-274.

Bertani, R.T., Costa, I.G., and Matos, R.M.D., 1990. Evolução tectono-sedimentar, estilo estrutural e habitat do petróleo na Bacia Potiguar. In: Raja Cabaglia, G.P., Milani, E.J. (eds), Origem e evolução das bacias sedimentares. Rio de Janeiro, PETROBRAS. pp. 291-391.

Bezerra, F.H.R., Lima-Filho, F.P., Amaral, R.F., Caldas, L.H.O. and Costa-Neto, L.X., 1998. Holocene coastal tectonics in NE Brazil. In: I. Stewart, C. Vita-Finzi (eds) Coastal Tectonics. Geological Society, London, 146: 279-293.

Bezerra, F.H.R., Vita-Finzi, C. and Filho, F.P.L., 2000. The use of marine shells for radiocarbon dating of coastal deposits. *Revista Brasileira de Geociências*, 30(1): 211-213.

Bigarella J.J., 1975. Reef sandstones from Northeastern Brazil (a survey on sedimentary structures). In: I *Simp. Intern. Sobre o Quarternário*, Vol 47 (Ed. by Associação Brasileira da Ciência). Curitiba-Porto Alegre, pp. 395-410.

Bowman, S., 1990. Interpreting the Past Radiocarbon Dating. British Museum Press. 64pp.

Caldas, L.H.O., 1996. Geologia costeira da região de São Bento do Norte e Caiçara, Litoral Norte Potiguar. Graduation, Universidade Federal do Rio Grande do Norte, Natal, 83 pp.

Caldas, L.H.O., Medeiros, W.E., Dantas, E.P. and Jardim-de-Sá, E.F. 1997. Caracterização geológica e geofísica de uma estrutura na borda leste do Gráben de Umbuzeiro, Bacia Potiguar/RN e implicações neotectônicas. Congresso Internacional da Sociedade Brasileira de Geofísica, Rio de Janeiro, 2:885-888.

Caldas, L.H.O., Stattegger, K. and Vital, H., 2001. The north coastal zone of the Rio Grande do Norte State, NE Brazil; and its associated continental shelf: An overview. In: *2001 Margins Meeting, Vol. 14* (Ed. by S. Roth and A. Rüggerberg), Deutsche Geologische Gesellschaft, Hannover. pp. 37.

Campos e Silva, A., Silva, D.D. and Vasconcelos, M.D.T., 1964. Informações sobre a malacofauna dos beach rocks de Touros e São Bento do Norte, Rio Grande do Norte. *Arquivos do Instituto de Antropologia*, 1, 79-89.

Cestaro, L.A., 1994. Os elementos do clima de Galinhos, RN, como recursos naturais à disposição do Homem. *Cadernos Norte-rio-grandense de Temas Geográficos*, 8(1): 13-28.

Chappell, J., Omura, A., Esat, T., McCulloch, M., Pandofi, J., Ota, Y. and Bard, B., 1996. Reconciliation of late Quaternary sea levels derived from coral terrraces at Huon Peninsula with deep-sea oxygen isotope records. *Earth and Planetary Science Letters*, 141: 227-236.

Cooper, J.A.G., 1991. Beachrock formation in low latitudes: implications for coastal evolutionary models. *Marine Geology*, 98:145-154.

Costa-Neto, L. X. D. 1997. Evolucão geológica-geomorfológica recente da plataforma continental interna ao Largo do Delta do Rio Acu, Macau-RN. Master Thesis, Universidade Federal Fluminense, Niterói, 214 pp.

Coudray, J. and Montaggioni, L., 1986. The diagenetic products of marine carbonate as sea-level indicators. In: O.v.d. Plassche (Editor), Sea-level research: a manual for the collection and evaluation of data. Geo Books, Norwich, pp. 311-360.

Cremonine, O., Goulart, J.P.M. and Soares, U.M., 1996. O Rifte Potiguar: Novos dados e implicações tectônicas, 4º Simpósio sobre o Cretácio do Brasil, UNESP-Campus de Rio Claro/SP, pp. 89-93

Delibrias, C. and Laborel, J. 1969. Recent variations of the sea level along the Brazilian coast. *Quaternaria* 14:45-49.

DHN. 1974. Carta náutica 700 - Brasil costa norte de Fortaleza a PTI. Marinha do Brasil, Diretoria de Hidrografia e Navegação - DHN, Rio de Janeiro. 2nd Edition.

Dominguez, J.M.L., Martin, L. and Bittencourt, A.C.S.P., 1987. Sea Level history and Quaternary evolution of river mouth associated beach-ridge plains along the east-southeast Brazilian coast: a summary. In: D. Nummedal, O.H. Pilkey and J.D. Howard (Editors), Sea Level fluctuation and coastal evolution. Society of Economic Paleontologist and Mineralogist special publication, pp. 115-127.

Dominguez, J. M. L., Bittencourt, A. C. D. S. P. and Martin, L., 1992. Controls on Quaternary coastal evolution of the east-northeastern coast of Brazil: roles of sea-level history, trade winds and climate. *Sedimentary Geology*, 80, pp. 213-232.

Edwards, R.L., Chen, J.H. and Wasserburg, G.J., 1986. ^{238}U- ^{234}U- ^{230}Th systematics and the precise measurement of the time over the past 500,000 years. *Earth and Planetary Science Letters*, 81:175-192.

Einig, C. 2000. Sediment dynamics of the Galinhos Spit (NE-Brazil). Master Thesis, Christian-Albrechts Universität, Kiel, 106 pp.

Erlenkeuser, H. and Wefer, G., 1981. Seasonal growth of bivalves from Bermuda recorded in their O-18 profiles. Proceedings of the Fourth International Coral Reef Symposium, Manila, pp. 643-648.

Fairbridge, R.W., 1976. Shellfish-eating Preceramic indians in Brazil. *Science*, 191: 353-359.

Faure, G., 1986. Principles of isotope geology. John Wiley & Sons, New York, 464 pp.

Figueiredo, A.G., 1980. Response of water column to strong wind forcing, Southern Brazilian inner shelf: implications for sand ridge formation. *Marine Geology*, 35:367-376.

Fonseca, V.P., 1996. Estudo morfo-tectônico da área do baixo curso do Rio Açu (Açu-Macau), Rio Grande do Norte. Master Thesis, Unversidade Federal de Minas Gerais, Belo Horizonte, 109 pp.

Fonseca, V. P. 1997. Compartimentação litorânea entre Ponta do Mel e Ponta dos Três Irmãos, Litoral Norte do Rio Grande do Norte. In: *XVII Simpósio de Geologia do Nordeste, Vol. 15* (Ed. by S. B. Geologia), pp. 374-378. Sociedade Brasileira de Geologia, Fortaleza.

Fortes, F., 1987. Mapa geológico da Bacia Potiguar (1:1000.000), PETROBRAS/DEBAR/DINTER/SEBAP, Natal, Internal Report, 125 pp.

Françolin, J.B.L. and Szatmari, P., 1987. Mecanismos de rifteamento da porção oriental da margem norte brasileira. *Revista Brasileira de Geociências*, 17(2): 196-207.

Friedman, G.M. and Sanders, J.E., 1978. Principles of Sedimentology. John Wiley & Sons, New York. Pp. 144-179.

Giresse, P., Barusseau, J.-P., Causse, C. and Diouf, B., 2000. Successions of sea-level changes during the Pleistocene in Mauritania and Senegal distinguished by sedimentary facies study and U/Th dating. *Marine Geology*, 170: 123-139.

Gorini, M.A., Dias, G.T.M., Mello, S.L.M., Espíndola, C.R.S., Gallea, C.G., Dellapiazza, H. and Castro, J.R.J.C., 1982. Estudos ambientais para implantação de gasoduto na área de Guamaré (RN). In: *XXXII Congresso Brasileiro de Geologia*, *Vol. 4* (Ed. by S. B. Geologia), pp. 1531-1539. Sociedade Brasileira de Geologia, Salvador.

Hanebuth, T.J.J., Stattegger, K. and Saito, Y., 2002. The stratigraphic architecture of the central Sunda Shelf (SE Asia) recorded by shallow-seismic surveying. *Geo-Marine Letters*, 22:86-94.

Hanor, J.S., 1978. Precipitation of beachrock cements: mixing of marine and meteoric waters vs. CO_2 degassing. *Journal of Sedimentary Petrology*, 48:489-502.

Hearty, P.J., Kindle, P., Cheng, H.L. and Edwards, R.L., 1999. A +20m middle Pleistocene sea-level highstand (Bermuda and Bahamas) due to a partial collapse of Antarctic ice. *Geology*, 27(4): 375-378.

Hendry, J.P., Perkins, W.T. and Bane, T., 2001. Short-term environmental change in a Jurassic lagoon deduced from geochemical trends in aragonite bivalve shells. *Geological Society of America Bulletin*, 113(6): 790-798.

Higgs, R., 1979. Quartz-grain surface features of Mesozoic-Cenozoic sands from the Labrador and Western Greenland continental margins. *Journal of Sedimentary Petrology*, 49(2):599-610.

Hopley, D., 1986. Beachrock as a sea-level indicator. In: O.v.d. Plassche (Editor), Sea level research: A manual for collection and evaluation of data. Geo books, Norwich, pp. 157-173.

Hustedt, S. 2000. Aeolian morphodynamics in the region of Sao Bento do Norte on the NE-coast of Brazil. Master Thesis, Christian Albrechts University, Kiel, 63 pp.

Isla, F.I., 1989. Holocene sea-level fluctuation in the southern hemisphere. *Quaternary Science Reviews*, 8:359-368.

Ivanovich, M., Vita-Finzi, C. and Henning, G.J., 1983. Uranium-series dating of molluscs from uplifted Holocene beachs in the Persian Golf. *Nature*, 302(31): 408-410.

James, N.P. and Choquette, P.W., 1990. Limestones - The sea-floor diagenetic environment. In: I.A. Mcreath and D.W. Morrow (Editors), Diagenesis. Geoscience Canada, Ottawa, pp. 13-34.

James, N.P. and Ginsburg, R.N., 1979. The seaward margins of Belize barrrier and atoll reefs. International Association of Sedimentology, Special pulblication, 3, 197pp.

Jardim de Sá, E. F., 1984. Evolução proterozóica da Província Borborema. In: *XI Simpósio de Geologia do Nordeste*, (Ed. by S. B. Geologia), pp. 271-297. Sociedade Brasileira de Geologia, Recife.

Jones, E.J.W., 1999. Marine Geophysics. John Wiley & Sons, Chichester, 466 pp.

Kaufman, A. and Broecker, W. S., 1965. Comparison of 230Th and 14C ages for carbonate material from Lake Lahontan and Bonneville. *Journal of Geophysics Research*, 70:4039-4054.

Kaufman, A., Broecker, W.S., Ku, T.L. and Thurber, D.L., 1971. The status of U-series method of mollusk dating. *Geochimica et Cosmochimica Acta*, 35: 1155-1183.

Keith, M.L. and Parker, R.H., 1965. Local variation of ^{13}C e ^{18}O content of mollusk shells and the relatively minor temperature effect in marginal marine environments. *Marine Geology*, 3: 115-129.

Kindler, P. and Bain, R.J., 1993. Submerged Upper Holocene beachrock on San Salvador Island, Bahamas: Implications for a recent sea-level history. *Geologische Rundschau*, 82: 241-247.

Kinsman, D.J.J., 1969. Interpretation of Sr (Super +2) concentrations in carbonate minerals and rocks. *Journal of Sedimentary Petrology*, 39(2): 486-508.

Knoppers, B., Ekau, W. and Figueiredo, A. G., 1999. The coast and shelf of east and northeast Brazil and material transport. *Geo-Marine Letters*, 19:171-178.

Krantz, D.E., Williams, D.F. and Jones, D.S., 1987. Ecological and paleoenvironmental information using stable isotope profiles from living and fossil molluscs. *Palaeogeography, Palaeoclimatology, Palaeoecology*, 58: 249-266.

Krinsley, D.H. and Doornkamp, J.C., 1973. Atlas of quartz sand surface textures. Cambridge University Press, Cambridge, 91 pp.

Lessa, G.C., Angulo, R.J., Giannini, P.C. and Araújo, A.D., 2000. Stratigraphy and Holocene evolution of a regressive barrier in south Brazil. *Marine Geology*, 165: 87-108.

Lima, Z.M.C., Andrade, P.R.O., Xavier, P., Vital, H., Amaro, V.E. and Medeiros, W.E. 2002a. Sand spit from NE Brazil: High-resolution Quaternary analogs for reservoir models. AAPG Annual Meeting. pp. 1-7.

Lima, Z.M.C., Alvez, A.L., Amaro, V.E. and Vital, H. 2002b. Evolução da linha de costa do esporão de Galinhos (NE Brasil) utilizando fotografias aéreas e imagens Landsat TM. *Pesquisas*. (in press).

Lima-Filho, F.P., Córdoba, V.C. Caldas, L.H.O., Pereira, M.M.V., Fonseca, VP., Nogueira, A.M.B. and Bezerra, F.H.R., 1995. Considerações sobre a geologia costeira de São Bento do Norte e Caiçara, RN: evidências de indicadores do nível relativo do mar. Simpósio de Processos Sedimentares e Meio Ambiente, Recife-Brasil 1, 150-152.

Lima Filho, M. D., Magnólia, A. and Manso, V. A., 2000. Níveis marinhos elevados do estado de Pernambuco: Uma questão revisitada. In: *XVIII Simpósio de Geologia do Nordeste, Vol. 16* (Ed. by S. B. Geologia), pp. 32. Sociedade Brasileira de Geologia, Recife.

Longman, M. W., 1980. Carbonate diagenetic texture from nearsurface diagenetic environments. *The American Association of Petroleum Geologists Bulletin*, 64(4):461-487.

Magaritz, M., Gavish, E., Bakler, N. and Kafri, U., 1979. Carbon and oxygen isotope composition indicators of cementation environment in recent, Holocene, and Pleistocene sediments along the coast of Israel. *Journal of Sedimentary Petrology*, 49(2): 401-412.

Margaritz, M., 1983. Carbon and oxygen isotope composition of recent and ancient coated grains. In: T.M. Peryt (Editor), Coated grains. Springer Verlag, Berlin, pp. 27-37.

Martin, L., Suguio, K. and Flexor, J.M., 1986. Shell middens as source for additional information in Holocene Shoreline and sea-level reconstruction: examples from the coast of Brazil. In: O.v.d. Plassche (Editor), Sea-level research: a manual for the collection and evaluation of data. Geo Books, Norwich, pp. 618.

Martin, L., Suguio, K. and Flexor, J. -M., 1993. As flutuações de nível do mar durante o Quaternário superior e a evolução geológica de "deltas" Brasileiros. *Boletim do IG-USP*, 15, 1-186.

Martins, L.R. and Coutinho, P.N., 1981. The Brazilian continental margin. *Earth-Science Reviews*, 17: 87-107.

Matos, R. M. D., 1992. Deep seismic profiling, basin geometry and tectonic evolution of intracontinental rift basin in Brazil. Doctor of Philosophy, Cornell University. 275pp.

Matos, R. M. D., 1994. The Northeastern Brazilian Rift System. *Tectonics*, 11(4):767-790.

Maury, C.J., 1934. Fossil invertebrata from northeastern Brazil. *American Museum of Natural History*, Bulletin, LXVII, 123-179.

Mayer, E., 1974. Estratigrafia preliminar da Plataforma Continental da Bacia Potiguar-RN. PETROBRAS, Natal, Internal Report.

McBride, R.A. and Moslow, T.F., 1991. Origin, evolution and distribution of shoreface sand ridges, Atlantic inner shelf, U.S.A. *Marine Geology*, 97: 57-85.

McLaren, S.J. and Rowe, P.J., 1996. The reliability of uranium-series millusc dates from the Western Mediterranean Basin. *Quaternary Science Reviews*, 15: 709-717.

Metcalf, W.G. and Stalcup, M.C., 1967. Origin of the Atlantic Undercurrent. *Journal of Geophysical Research*, 72: 4959-4975.

Miketta, P., 2001. Großkartierung des Hochdynamischen Küsteabschinittes zwischen Caicara und Galinhos, NE Brasilien. Diplom Arbeit Thesis, Universität Kiel, Kiel, 73 pp.

Miller, W.R. and Manson, T.R., 1994. Erosional features of coastal beachrock and aeolianite outcrops in Natal and Zululand, South África. *Journal of Coastal Research*, 10(2):374-394.

Milliman, J.D., 1974. Marine Carbonates. Part I: Recent sedimentary carbonates. Springer Verlag, Berlin, 379 pp.

Ministério do Exército, 1985. Carta topográfica. Folha Jandaíra SB.24-X-D-III, MI-899. 1:100000. Departamento de Engenharia e Comunicação. Diretoria de serviço geográfico.

Ministério do Exército 1983. Carta topográfica. Folha Pureza . Folha SB.25-V-C-I. MI-900. 1:100000. Departamento de engenharia e comunicações. Diretoria de serviço geográfico

Ministério do Meio Ambiente 1996. Macrodiagnóstico da zona costeira do Brasil na escala da união. MMA, Brasília, pp. 280.

Mook, W.G. and Plassche, V., 1986. Radiocarbon dating. In: O.v.d. Plassche (Editor), Sea level research: a manual for the collection and evaluation of data. Geo Books, Norwich, pp. 618.

Moore, C.H. Jr., 1971. Beachrocks cements, Grand Cayman Island, B.W.I. In: O.P. Bricker (Editor), *Carbonate Cements*. The Johns Hopkins university Studies in Geology 19, 9-12.

Morais, M.C.C., 1998. Terras Potiguares. Dinâmica Editora, Natal, 305 pp.

Moreira, M. M., 1994. Geodinâmica das seqüências sedimentares Cenozóicas e neotectônicas da região litorânea do município de Touros-RN. Graduation, Universidade Federal do Rio Grande do Norte, Natal, 97pp.

Mörner, N. A., Rosseti, D. and Toledo, P. 1999. Sea-level changes in NE Brazil, regional eustasy and local tectonics. In: *The non-steady state of the inner shelf and shorelines: coastal change on the time scale of decadesto millennia in the late Quaternary. Vol. PDF version of abstracts with programs, inaugural meeting of ICP Project 437 - Costal environmental change during sea level highstands.* (Ed. by C. H. Fletcher and J. V. Matthews), pp. 112. University of Hawaii, Honolulu-Hawaii.

Morse, J.W. and Mackenzie, F.T., 1990. Geochemistry of Sedimentary Carbonates. Developments in Sedimentology 48. Elsevier Sciences, Amsterdam, 707 pp.

Muhs, D.R. and Kyser, T.K., 1987. Stable isotope composition of fossil mollusks from southern California: Evidence for a cool last interglacial ocean. *Geology*, 15: 119-122.

Mycielska-Dowgiallo, E. and Woronko, B., 1998. Analiza obtoczenia i zmatowienia powierzchni ziarn kwarcowych frakcji piaszczystej i jej wartosc interpretacyjna. *Przeglad Geologiczny*, 46(12): 1275-1281.

Nadeau, M-J., Schleicher, M., Grootes, P.M., Erlenkeuser, H., Gottang, A., Mous, D.J.W., Sarntheim, M., and Willkomm, H., 1997. The Leibniz-Labor AMS facility at the Christian-Albrechts University, Kiel, Germany. *Nuclear Instruments and Methods in Physics Research*, 123: 22-30.

Nadeau, M-J., Grootes, P.M., Voelker, A., Bruhn, F. and Duhr, A., 2001. Carbonate ^{14}C Background: Does it have multiple personalities? *Radiocarbon*, 43(2a):169-176.

NATRONTEC/ECOPLAN. 1995. Fabricação de barrilha e implantação de emissário submarino - Estudo de impacto ambiental: Diagnóstico, análise de impactos e programa de gestão ambiental, ECOPLAN, Natal. 186pp.

Neves, C. A. O., 1987. Análise regional do trinômio geração-migração-acumulação de hidrocarbonetos na Seqüência Continental Eocretácica da Bacia Potiguar emersa, NE Brazil. Master Thesis, Universidade Federal de Minas Gerais.

Newsome, D. and Ladd, P., 1999. The use of quartz grain microtextures in the study of the origin of sand terrains in West Australia. *Catena*, 35: 1-17.

Nimer, E., 1989. Climatologia do Brasil. IBGE, Rio de Janeiro, 422 pp**.**

Nogueira, A. M. B., Costa-Neto, L. X., Lima, M. S., Oliveira, M. I. M., Silvan, F. C., Fernandes, C. A. N. 1990. Evolução geo-ambiental da faixa costeira entre a Ponta do Calcanhar e Ponta dos Marcos - RN. In: *XXXVI Congresso Brasileiro de Geologia*, *Vol. 2* (Ed. by S. B. Geologia), Sociedade Brasileira de Geologia, Natal, pp. 784-795.

Oliveira, M. I. M. D., Bagnoli, E., Farias, C. C., Nogueira, Â. M. B. and Santiago, M., 1990. Considerações sobre a geometria, petrografia, sedimentologia, diagênese e idade dos beachrocks do Rio Grande do Norte. In: *XXXVI Congresso Brasileiro de Geologia*, *Vol. 2*. Sociedade Brasileira de Geologia, Natal, pp. 621-634.

Omoto, K., 2001. Radiocarbon ages of beach rocks and late Holocene sea-level changes in the southern part of the Nansei Island, Southwest of Japan. *Radiocarbon*, 43(2B):887-898.

Paschelke, F., 2000. Sedimentological and environmental survey of the channel system near Galinhos, Rio Grande do Norte, Brazil. Master Thesis, Christian-Albrechts, Kiel, 114 pp.

Peltier, W.R., 1988. Lithospheric thickness, Antartic deglaciation history, and ocean basin discretization effects in a global model of postglacial sea level changes: A summary of some sources of nonuniqueness. *Quaternary Research*, 29:93-112.

Pirazzoli, P.A., 1991. World atlas of Holocene sea-level changes. Oceanography Series, 58. Elsevier, Amsterdan, 300 pp.

Ponte, F. C., Dauzacker, M. U. and Porto, R., 1978. Origem e acumulações de petróleo nas bacias sedimentares brasileiras. In: *I Congresso Brasileiro do Petróleo*. IBP, Rio de Janeiro, pp. 121-146.

Purser, B.H., 1969. Synsedimentary marine lithification of Middle Jurassic limestones in the Paris basin. *Sedimentology*, 12:205-230.

Ramsay, P.J., 1995. 9000 years of sea-level changes along the Southern African Coastline. *Quaternary International*, 31: 71-75.

Ramsay, P. J. and Cooper, J. A. G., 2002. Late Quaternary sea-level changes in South Africa. *Quaternary Research*, 57:82-90

Reineck, H.E. and Singh, I.B., 1973. Depositional Sedimentary Environments. Spring Verlag, Berlin, 439 pp.

Richardson, P.L. and Walsh, D., 1986. Mapping climatological seasonal variations of surface currents in the Tropical Atlantic using ship drifts. *Journal of Geophysical Research*, 91: 10537-10550.

Riedel, K., 2000. Untersuchugen zur Küstendynamik und Küstenentwiklung bei Sao Bento. Master Thesis, Christian-Albrechts Universität, Kiel, 55pp.

Röber, V., 2001. Structure and dynamics of the inner shelf north of Galinhos, Rio Grande do Norte (NE-Brazil). Master Thesis, Christian-Albrechts Universität, Kiel, 95 pp.

Rock-Color Chart Committee. 1984. Rock Color Chart, Geol. Soc. of America, USA.

Rohling, E.J., Feton, M., Jorissen, F.J., Bertrand, P., Ganssen, G. and Caules, J.P., 1998. Magnitudes of sea-level lowstands of the past 500.000 years. *Nature*, 394: 162-165.

Rotzoll, K., 2001. Structure and dynamics of the tidal channel system near Galinhos, Rio Grande do Norte (NE-Brazil). Master Thesis, Christian-Albrechts Universität, Kiel, 79 p.

Schleicher, M., Gootes, P.M., Nadeau, M.-J. and Scoon, A., 1998. The carbonate 14C background and its components at the Leibniz AMS facility. *Radiocarbon*, 40(1): 85-93.

Schröder, J. H., 1973. Submarine and vadose cements in Pleistocene Bermuda reef rock. *Sedimentary Geology*, 10:179-204.

Scoffin, T.P., 1987. An Introduction to Carbonates Sediments and Rocks. Blackie, Glasgow. 274pp.

Scoffin, T.P. and Stoddart, D.R., 1983. Beachrocks and intertidal cements. In: A.S. Goudie and K. Pye (Editors), Chemical sediments and geomorphology. Academic Press, London, pp. 401-425.

Shackleton, N.J., 1987. Oxygen isotopes, ice volume and sea level. *Quaternary Science Reviews*, 6: 183-190.

Sherwood, J., Barbetti, M., Ditchburn, R., Kimber, R.W.L., McCabe, W., Murray-Wallace, C.V., Prescott, J.R. and Whitehead, N., 1994. A comparative study of Quaternary techniques applied to sedimentary deposits in Southwest Vitoria, Australia. *Quaternary Science Reviews*, 13: 95-110.

Silva, C. G., 1991. Holocene stratigraphy and evolution of the Açu river delta, Rio Grande do Norte state, Northeastern Brazil. Doctor of Philosophy, Duke University, Durham, 400 p.

Silveira, I.M., 2002. Estudo evolutivo das condições ambientais da região costeira do município de Guamaré-RN. Master thesis. PPGG-UFRN. 172p.

Silveira, I.C.A., Miranda, L.B.d. and Brown, W.S., 1994. On the origins of the North Brazil Current. *Journal of Geophysical Research*, 99(C11): 22501-22512.

Snedden, J.W. and Bergman, K.M., 1999. Isolated shallow marine sand bodies: deposits for all interpretations. In: K.M. Bergman and J.W. Snedden (Editors), Isolated shallow marine sand bodies: Sequence stratigraphic analysis and sedimentologic interpretation. SEPM Special Publication. SEPM Society for Sedimentary Geology, Tulsa, pp. 1-11.

Snedden, J.W. & Dalrymple, R.W., 1999. Modern shelf sand ridges: From historical perspective to a unified hydrodynamic and evolutionary model. In: K.M. Bergman and J.W. Snedden (Editors), Isolated shallow marine sand bodies: Sequence stratigraphic analysis and sedimentologic interpretation. SEPM Special Publication. SEPM Society for Sedimentary Geology, Tulsa, pp. 12-28.

Snedden, J.W., Kreisa, R.D., Tillman, R.W., Culver, S.J. and Schweller, W.J., 1999. An expanded model for modern shelf sand ridges genesis and evolution on the New Jersey Atlantic shelf. In: K.M. Bergman and J.W. Snedden (Editors), Isolated shallow marine sand bodies: Sequence stratigraphic analysis and sedimentologic interpretation. SEPM Special Publications. SEPM Society for Sedimentary Geology, Tulsa, pp. 147-163.

Souza, S. M. D., 1982. Atualização da litoestratigrafia da Bacia Potiguar. In: *XXXII Congresso Brasileiro de Geologia, Vol. 5*, Sociedade Brasileira de Geologia, Salvador, pp. 2392-2406.

Srivastava, N. K. and Corsino, A. R., 1984. Os carbonatos de Touros: Petrografia e estratigrafia. In: *XI Simpósio de Geologia do Nordeste*, Sociedade Brasileira de Geologia, Natal, pp. 165-176.

Stoddart, D.R. and Cann, J.R., 1965. Nature and origin of beach rocks. *Journal of Sedimentary Petrology*, 35: 243-273.

Stramma, L., Ikeda, Y. and Peterson, R.G., 1990. Geostrophic transport in the Brazil Current region north of 20^{o}S. *Deep-Sea Research*, 37(12): 1875-1886.

Strasser, A., Davaud, E. and Jedoui, Y., 1989. Carbonate cements in Holocene beachrock: example from Bahiret el Biban, Southeastern Tunisia. *Sedimentary Geology*, 62: 89-100.

Stuiver, M. and Reimer, P.J., 1993. Extended ^{14}C database and revised CALIB radiocarbon calibration program. *Radiocarbon*, 35: 215-230.

Stuiver, M., Reimer, P.J., Bard, E., Beck, J.W., Burr, G.S., Hughen, K.A., Kromer, B., McCormac, G., Van der Pflicht, J., and Spurk, M., 1998. INTECAL98 Radiocarbon age calibration, 24,000-0 cal BP. *Radiocarbon*, 40:1041-1083.

Suguio, K., Martin, L. and Flexor, J. -M., 1980. Sea level fluctuations during the past 6000 years along the coast of the State of Sao Paulo, Brazil. In: Earth rheology, isostasy and eustasy (Ed. by N. A. Mörner), John Wiley & Sons, pp. 471-486.

Suguio, K., Martin, L., Bittencourt, A. C. S. P., Dominguez, J. M. L., Flexor, J. M. and Azevedo, A. E. G., 1985. Flutuações do nível relativo do mar durante o Quaternário Superior ao longo do litoral Brasileiro e suas implicações na sedimentação costeira. *Revista Brasileira de Geociências*, 15, 273-286.

Suguio, K., Barreto, A. M. F., Bezerra, F. H. D. R., 2001. Formações Barra de Tabatinga e Touros: Evidências de paleoníveis do mar Pleistocênicos da costa Norte-riograndense. In: *VIII Congresso da ABEQUA - Mudanças Globais e o Quaternário*, Associação Brasileira de Estudos do Quaternário, Imbé, pp. 108-109.

Summerhayes, C.P., Coutinho, P.N., França, A.M.C. and Ellis, J.P., 1975. Upper continental margin sedimentation off Brazil - Salvador to Fortaleza Northeastern Brazil. *Contribuitions to Sedimentology*, 4: 44-78.

Szabo, B.J. and Rosholt, J.N., 1969. Uranium-series dating of Pleistocene molluscan shell from Southern California - An open system model. *Journal of Geophysical Research*, 74(12): 3253-3260.

Szabo, B.J. and Wedder, J.G., 1971. Uranium-series dating of some Pleistocene marine deposits in Southern California. *Earth and Planetary Science Letters*, 11: 230-290.

Swift, D.J.P., 1975. Tidal sand ridges and shoals-retreat massifs. *Marine Geology*, 18: 105-134.

Swift, D.J.P. and Field, M.E., 1981. Evolution of a clastic sand ridge field: Maryland sector. North American inner shelf. *Sedimentology*, 28:461-482.

Tabosa, W. F., 2000. Dinâmica costeira da Região de São Bento do Norte e Caiçara do Norte - RN. Graduation, Universidade Federal do Rio Grande do Norte, Natal, 76 pp.

Testa, V. and Bosence, D. W. J., 1998. Carbonate-siliciclastic sedimentation on high-energy, ocean-facing, tropical ramp, NE Brazil. In: Carbonate Ramps, *Vol. 149* (Ed. by V. P. Wright and T. P. Burchette), Geological Society of London, London, pp. 55-71.

Testa, V. and Bosence, D. W. J., 1999. Physical and biological controls on the formation of carbonate and siliciclastic bedforms on the north-east Brazilian shelf. *Sedimentology*, 46(2): 279-301.

Tietz, G. and Müller, G., 1971. High-magnesian calcite and aragonite cementation in recent beachrocks, Fuerteventura, Canary Islands, Spain. In: O.P. Bricker (Editor), *Carbonate Cements*. Johns Hopkins University Studies in Geology, 19, pp. 4-5.

Tintelnot, M., 1996. Holocene and Late Pleistocene climate changes and sea-level fluctuations in tropical northeastern Brazil - evidence from marine clay mineral records, Jahrestagung der DTTG. DTTG, Freiberg, pp. 72-88.

Tucker, M.E., 1988. Techniques in sedimentology. Blackwell Scientific. London, 394 pp.

Tucker, M.E. and Wright, V.P. 1990. Carbonate Sedimentology. Blackwell Scientific. London, 482pp.

Tucker, M.E., 1996. Sedimentary rocks in the field. John Wiley & Sons. Chichester, 153 pp.

Van Andel, T. H. and Laborel, J., 1964. Recent high relative sea level stand near Recife, Brazil. *Science*, 145:580-581.

Veeh, H.H. and Burnett, W.C. 1982. Carbonate and phosphate sediments. In: Ivanovich, M. and Harmon, R.S. (Editors), Uranium series disequilibrium: Applications to environmental problems, Claredon Press, Oxford. Pp. 459-480

Veizer, J., 1983. Trace elements and isotopes in sedimentary carbonates. In: Carbonates: Mineralogy and chemistry, *Reviews in Mineralogy*, 11 (Ed. by R. J. Reeder), Mineral Soc. America, Book Crafters, Chelsea, pp.265-300.

Vianna, M. L. and Solewicz, R., 1988. Feições fisiográficas submarinas da plataforma continental do RN visíveis por imagens de satélite. In: Simpósio de Sensoriamento Remoto, *Vol. 3*, Natal, pp. 581-587.

Vianna, M.L., Cabral, A.P. and Gherardi, D.M., 1993. TM-Landsat imagery to the study of the impact of global climate change on a tropical environment during the last deglaciation. *International Journal of Remote Sensing*, 14: 2971-2983.

Vita-Finzi, C. 1992. Shells, isotopes, and tectonics. *Israeli Journal of Sciences*, 41:1-8.

Vital, H.; Amaro, V.E., Tabosa, W.F., Guedes, I.M.G., Stattegger, K., Caldas, L.H.O. 2002a. Pattern of sediment distribution in tectonic setentrional coast of Rio Grande do Norte state, Northeastern Brazil. *EOS Transactions*, 83(4):17.

Vital, H., Stattegger, K., Amaro, V., Schwarzer, K., Frazano, E. P., Silveira, I. M. and Caldas, L. H. O. 2002b. Interactions of sea level and tectonics on large scale bedforms preserved on a tropical shelf: The Rio Grande do Norte shelf, northeastern Brazil In: Second Conference of the IGCP464, Cananéia.

Vital, H., Stattegger, K., Tabosa, W.F. and Riedel, K., in review. Why does erosion occur on the northern coast of Rio Grande do Norte State, NE Brazil?: The Caiçara example. In: Klein, A. (Ed). Brazilian sand beaches. *Journal of Coastal Research*. Special issue, 35.

Vollbrecht, R. and Meischner, D., 1993. Sea level and diagenesis: a case study on Pleistocene beaches, Whalebone Bay, Bermuda. *Geologische Rundschau*, 82:248-262.

Xavier, P.N., Lima, Z.M.C., Andrade, P.R.O., Oliveira Jr, J.G., Medeiros, W.E. and Vital, H. 2001. GPR image of the Galinhos península. NE Brazil: The register of geologic evolution from a paleo-channel to a sand spit. GPR in sediments at the Geological Society and UCL. London.

Woodroffe, C.D. and Grime, D., 1999. Storm impact and evolution of a mangrove-fringed chenier plain, Shoal Bay, Darwin, Australia. *Marine Geology*, 159: 303-321.